Investigation of the Propensity for Self-Association of the N-Terminal Domain of Annexin A2 in the Presence of Anionic Lipids

A Major Qualifying Project Report:

Submitted to the Faculty of
WORCESTER POLYTECHNIC INSTITUTE

In partial fulfillment of the requirements for the
Degree of Bachelor of Science
In Biochemistry

By

Abigail Cornwell

Project Advisor:

Professor Arne Gericke

Date: April 24, 2017
Approved: April 25, 2017

TABLE OF CONTENTS

ACKNOWLEDGMENTS

I'd like to thank Dr. Arne Gericke for allowing me to work in his lab throughout much of my undergraduate career. His advice and the projects I was given, taught me most of the skills required to complete this project. He also enabled me to travel to Germany to learn the skills necessary to work with annexins. Throughout this project he has provided me with the tools to succeed while allowing me to learn trial and error skills. As a result, I have become a more independent scientist. His helpful advice has taught me so many things that have helped me to become a much better analytical thinker.

I would like to thank Dr. Volker Gerke David Grill, Anna Livia Linard-Matos, Rathan Nammalwar, Nina, Sophia, Andy and all of the other scientists at the ZMBE UWW for welcoming me into their lab, providing me with protocols, DNA, and the knowledge and skills to complete this research. Vielen Dank!

In the Gericke lab group, I would like to thank Dr. Alonso Ross for providing assistance, support, and encouragement throughout this project and most of my undergraduate career. I'd also like to thank Anne-Marie Bryant for always being happy and willing to assist me and give me advice. I would particularly like to thank her for helping me with sequencing, primer design, freezing samples in liquid nitrogen, and with my Western Blots. I'd like to thank Brittany Neumann for teaching me to use the Fluorimeter for the FRET assays and for teaching me to analyze my data using Origin. I would also like to thank her for helping me with lipid extrusion and the DLS. I would like to than Vanessa Pinderi for helping me with my phosphate assays and lipid preparation.

In the Scarlatta group, I would like to thank Ashima for teaching me about FCS-FLIM. I would like to thank Osama and the other members of the Scarlatta group for always being generous and sharing equipment and supplies when I needed it. I would also like to thank Dr. John Leszyk from the University of Massachusetts Medical School for analyzing my ANXA2 WT Coomassie gel band using mass spectrometry. Lastly, I would like to thank Julia (Arguello lab) and the other members of the Arguello group for allowing me to use their miniprep kit and their Nanodrop.

ABSTRACT

Annexin A2 (ANXA2), a calcium-dependent membrane binding protein shown to promote membrane domain formation, is implicated in many cellular processes. In order to determine if ANXA2 promotes domain formation by self-associating with the N-terminal domain of adjacent ANXA2 proteins upon binding anionic phospholipids, Forster Resonance Energy Transfer (FRET) assays were performed using ANXA2 proteins fluorescently labeled at the singular, exposed N-terminal cysteine residue. No FRET transfer was observed, suggesting that under these experimental conditions the N-terminal domains do not interact.

TABLE OF FIGURES

TABLE OF TABLES

CHAPTER 1—INTRODUCTION

Annexins are a family of structurally conserved peripheral membrane proteins which bind anionic phospholipids in a calcium-dependent manner. These proteins have a structurally conserved C-terminal core domain and an N-terminal domain which is unique to each annexin protein (Ayala-Sanmartin, Zibouche, Illien, Vincent, & Gallay, 2008). Annexins are implicated in human health and disease and affect a diverse array of cellular processes; particularly related to membrane functions. Annexin A2 (ANXA2) is regarded as the annexin protein most extensively investigated regarding human health and disease" (Hajjar, 2015).

The ANXA2 gene is comprised of 13 exons on chromosome 15q21 (Hedhli et al., 2012). Over time, ANXA2 has been referred to as calpactin I heavy chain (CAL1H), annexin II, chromobindin 8, lipocortin II, and placental anticoagulation protein IV (Saxena, Lai, Chao, Jeng, & Lai, 2012). ANXA2 is present in endothelial cells, monocytes, macrophages and many cancer cells (Bharadwaj, Bydoun, Holloway, & Waisman, 2013). In cancer cells, ANXA2 and its binding partners, such as S100A10, have been shown to promote metastasis by remodeling actin and regulating the cytoskeleton (Lokman, Ween, Oehler, & Ricciardelli, 2011). As a mediator of the plasminogen activator system, ANXA2 plays a role in regulating thrombolysis, fibrinolysis, and wound healing (Lokman et al., 2011). Additionally, ANXA2 mediates endocytosis, exocytosis, lipid raft formation, and lipid and calcium signaling.

The physiological importance of the calcium-dependent phospholipid and membrane binding of ANXA2 in these cellular processes is currently being elucidated (Gerke & Moss, 2002). Modifying the calcium concentration, pH level, or the anionic phospholipid composition has been shown to alter ANXA2 interactions with anionic phospholipids both *in vitro* and *in vivo*. Alterations in ANXA2 organization at the plasma membrane under differing reaction conditions indicates that under specific conditions ANXA2 may undergo a conformational or physiological change; which could explain its diverse role within the human body.

The N-terminal domain is likely the region of ANXA2 most effected by a conformational or physiological change because it has been shown to regulate the function of ANXA2 by altering calcium affinities at protein-interaction sites in the core domain (Gerke, Creutz, & Moss, 2005). Many researchers have characterized the core domain of different annexins, but there are still a lot of questions regarding the role of the N-terminal domain of annexins in cellular processes;

particularly in the calcium-dependent membrane bridging of annexins (Ayala-Sanmartin et al., 2008).

ANXA2 has a single exposed cysteine residue on its N-terminal residue which can be fluorescently labeled and studied using techniques such as fluorescence resonance energy transfer (FRET) or fluorescence lifetime imaging microscopy (FLIM). FLIM can more accurately measure nanosecond FRET events between two fluorescently labeled proteins within a cell than traditional FRET because it measures the fluorescence lifetime of the donor independent of the local concentrations of donor and acceptor fluorophores (Becker et al., 2004).

Previous studies of annexin proteins using FRET and other fluorescence techniques have revealed the ways different types of annexins interact with anionic phospholipids. FRET is used to identify the extent of the interaction between two proteins, which surfaces they use to make contact, and the spatial location of two proteins in relation to each other. The residues near the N-terminal end are unique to each annexin protein, therefore different annexins interact with anionic phospholipids differently.

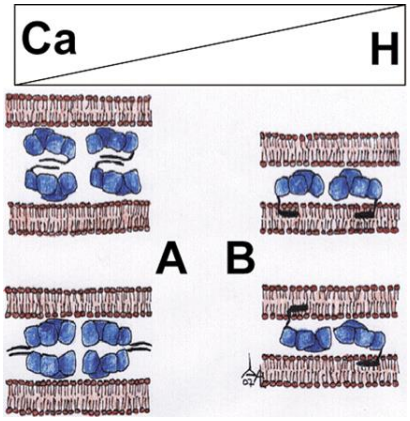

***Figure 1.1**: (A, left) the proposed model for membrane bridging of ANXA2 in a calcium-dependent manner, (B, right) the proposed model for membrane bridging of ANXA2 in a proton-dependent manner. (Zibouche, Vincent, Illien, Gallay, & Ayala-Sanmartin, 2008)*

In 2008, Zibouche et al. found a direct interaction between the N-terminal domain of ANXA2 and POPS/POPC vesicles without large structural changes in the core domain. They also discovered interactions between the N-terminal domains of adjacent ANXA2 proteins that were not in contact with the membrane as well as alterations in ANXA2 organization as a result of high Ca^{2+} concentration (Fig. 1.1). In 2008, Ayala-San-Martin et al. (2008) further supported these findings. Interestingly, Ayala-San-Martin et al. found that regardless of the lipid composition used (POPC,

POPS, PE, and cholesterol), neighboring ANXA2 N-terminal domains interacted in the presence of lipids and calcium, but not in the absence of lipids, or in solutions with lipid lacking calcium. In contradiction to these findings, Patel et al. (2005) found that in the presence of POPC/POPS phospholipids (0.1mM) and calcium chloride (0.5mM) at pH 7.4, ANXA2 does not self-associate at the N-terminal residue. In some experiments, they observed a small change in the acceptor of ANXA2 upon membrane binding which they believe was due to chance interactions of a donor and acceptor.

These studies did not look at the effect of phosphatidylinositol-4,5-diphosphate ($PI_{(4,5)}P_2$) on self-association. In the presence of $PI_{(4,5)}P_2$ANXA2 has been shown to link adjacent GUVs and to induce membrane indentations (Drücker, Pejic, Galla, & Gerke, 2013). A study performed by Illien et al. (2012), characterized the role of calcium in causing ANXA2 to aggregate membranes containing $PI_{(4,5)}P_2$or PS in the presence and absence of cholesterol. $PI_{(4,5)}P_2$-containing membranes required higher calcium ion concentrations than POPS-containing membranes to cause half maximal membrane bridging by ANXA2, suggesting that in the presence of $PI(4,5)P_2$, ANXA2 may experience structural changes of the N-terminal residue or the calcium-binding sites on the core domain.

In this paper, FRET was used to determine whether the N-terminal residues of lateral ANXA2 self-associate in the presence and absence of 100nm vesicles comprised of varying concentrations of $PI_{(4,5)}P_2$, POPC, and POPS. The singular exposed cysteine residue on the N-terminal domain of ANXA2 was labeled with AlexaFluor C5 Maleimide 488 (donor) fluorescent dye and AlexaFluor C5 Maleimide 568 (acceptor) fluorescent dye, then lipid or $CaCl_2$ titrations were performed.

This research was intended to provide a platform for future ANXA2 characterization studies as well as to complement existing data regarding the interactions of the N-terminal residue of ANXA2. Additionally, this research should expand current understanding regarding membrane domain formation by peripherally associated proteins.

CHAPTER 2—BACKGROUND

This background begins by providing a brief summary of the important role the plasma membrane plays in cellular processes (Section 2.1). In Section 2.2, the role of membrane domains and membrane proteins, particularly peripheral membrane proteins, in mediating cellular processes through lipid-protein and protein-protein interactions is discussed. Section 2.3 and 2.4 elaborates on the properties and role of annexins, a family of physiologically relevant peripheral membrane proteins. In Section 2.5, annexin A2, the most studied annexin regarding human health and disease, and the focus of this research paper, is described. Finally, in Section 2.6, the use of fluorescence microscopy techniques, such as Fluorescence Resonance Energy Transfer (FRET) and Fluorescence Lifetime Imaging Microscopy (FLIM), in protein-interaction studies is described.

2.1 Membrane Domains

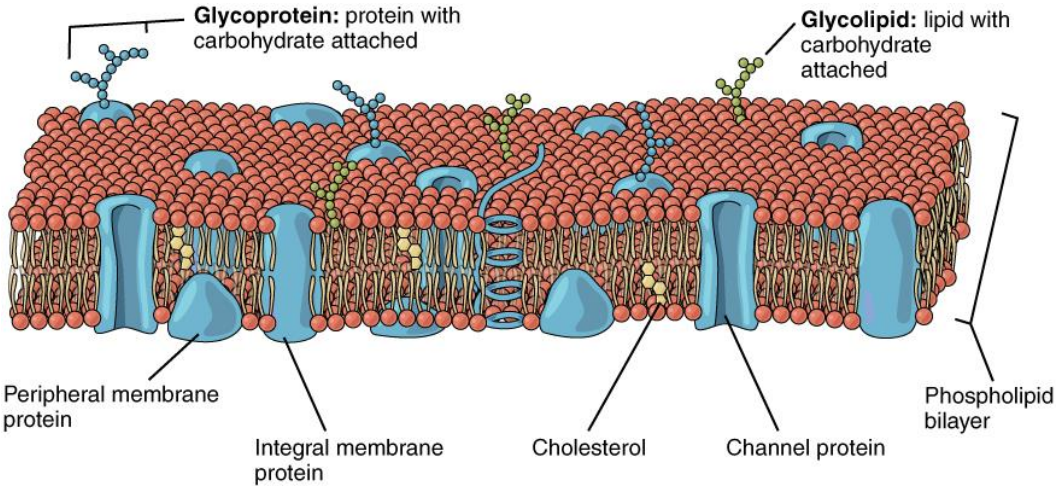

***Figure 2.1**: Model of the plasma membrane (https://en.wikipedia.org/wiki/Biological_membrane)*

According to the fluid mosaic model developed by Singer and Nicholson, the plasma membrane forms a phospholipid bilayer which acts as a sea in which various proteins and carbohydrates float around (Fig. 2.1). The plasma membrane provides protection from the extracellular environment and it plays an important role in conveying cellular signals, transporting water and nutrients into cells, and exporting waste products outside of cells (Maxfield, 2002). Its role in signaling and transport is reliant on the formation of small, localized regions of membrane which contain lipid compositions and properties that differ from the surrounding bilayer, commonly known as membrane domains or lipid rafts. There are numerous types of membrane domains which serve diverse roles, characterized using techniques; such as, fluorescence microscopy, electron microscopy, fluorescence resonance energy transfer, and single-molecule tracking. Due to the

small size and dynamic nature of domains they are difficult to study and many questions remain regarding how they form and are maintained (McIntosh, 2015).

2.2 Role of Peripheral Membrane Proteins

The roles of proteins in modifying, maintaining, and forming lipid rafts/membrane domains is central to uncovering the roles of membrane domains and the signaling processes they facilitate. Proteins are needed to produce signals that elicit an intracellular or extracellular response. A review by Rossy et al. (2014) concluded that proteins serve an essential role in regulating membrane organization by exploiting a lipid's biophysical properties, such as its charge, thereby stimulating organization (Rossy, Ma, & Gaus, 2014). The nature of the domain is characterized by its chemical composition and physical properties as well as the features of the proteins and other macromolecules it interacts with (Jacobson, Mouritsen, & Anderson, 2007). Studying how peripheral membrane proteins interact with membrane domains can uncover the role a specific membrane domain serves in mediating the function of a given protein and vice versa (Rossy et al., 2014).

When peripheral membrane proteins interact with the plasma membrane they can alter lipid composition in three ways resulting in (Luckey, 2014):

(1) A homogeneous lipid mixture: causes no lipid reorganization
(2) De-mixing according to the law of mass action: Redistribute lipids with no preferential interaction
(3) Total de-mixing: concentration of specific lipids in a domain that binds protein

In turn, lipids can alter the folding, structure, and organization of membrane and amphitrophic proteins which influences protein function and interactions with the membrane. Lipids can function in metabolic signaling and they play a role in the post-translational modification of some proteins. Lipids have varied chemical makeups and can work cooperatively with neighboring lipids of differing types to influence cellular processes (Bogdanov, Mileykovskaya, & Dowhan, 2008).

Protein-lipid interactions are necessary because membrane proteins oftentimes require lipids for activity or to bind to or insert itself into the plasma membrane (Luckey, 2014). Protein recruitment to the membrane and the activation of signaling cascades oftentimes result from protein binding to a specific class of lipid (Loura, Prieto, & Fernandes, 2010). Adjacent membrane lipids that do

not bind proteins can also interact with peripheral membrane proteins, modulating these interactions (Glomset, 1999). When proteins bind membrane surfaces this can facilitate further changes in the structure and function of the protein. Groups of proteins that concurrently bind to a membrane surface can also interact with each other creating a complex network of membrane-related events (Glomset, 1999).

2.3 Annexins

Annexins are an ancient, conserved family of peripheral membrane proteins which are useful to study because they are widely expressed in plants and animals. These proteins are soluble and hydrophilic (Gerke & Moss, 2002). Humans have twelve types of annexin proteins which all serve different, but related, functions in the body. Structurally, annexins have four or eight super helical repeats which form right-handed binding sites for calcium ions. Annexins also have a carboxyl core domain which is shaped like a concave disk and an amino, N-terminal, domain connected at the concave portion of the disc facing the cytosol (Fig. 2.3), (Gerke et al., 2005).

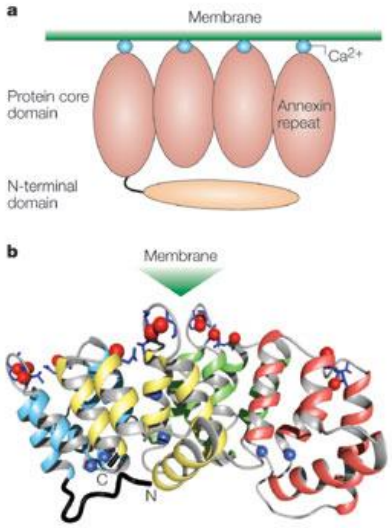

Annexins: linking Ca^{2+} signalling to membrane dynamics
Volker Gerke, Carl E. Creutz & Stephen E. Moss
Nature Reviews Molecular Cell Biology **6**, 449-461 (June 2005)

***Figure 2.2**: Structure of ANXA2 bound to the membrane (top), and the ribbon diagram of ANXA2 (bottom)*

2.3.1 Core Domain

The core domain reversibly binds calcium and anionic phospholipids. Structurally, the core domain has four homologous domains which each contain five α-helices (A-E). The AB and DE domains are connected by loops that form an endonexin fold, which is considered the signature amino acid sequence of annexins (Lizarbe, Barrasa, Olmo, Gavilanes, & Turnay, 2013),

(Bharadwaj et al., 2013). The lipid and calcium binding sites protrude from the convex side of the core domain facing the plasma membrane (Drücker, Pejic, Grill, Galla, & Gerke, 2014). In the presence of calcium, the ANXA2 core domain can connect two membrane surfaces and aggregate lipid vesicles (Drücker et al., 2014).

2.3.2 N-terminal Domain

Annexins also have unique N-terminal interaction domains which contain sites for post-translational modification and protein-protein interactions (Valapala & Vishwanatha, 2011) The N-terminal domain influences the stability and function of annexins and it is capable of binding cytosolic protein ligands, such as those of the S100 family (Valapala & Vishwanatha, 2011). The N-terminal domain also regulates the specific function of individual annexins. The N-terminal domain of different annexins vary in length and sequence (Lizarbe et al., 2013). It is believed that shorter amino terminal domains of smaller annexin proteins can alter calcium-dependent binding of phospholipids by stabilizing or weakening different conformational changes of annexins (Gerke & Moss, 2002). Annexin A2 (ANXA2) has a medium-sized N-terminal domain containing 30 amino acids as well as sites for phosphorylation and proteolysis (Liu, 1999).

2.4 Physiological Relevance of Annexins

Over the years, many researchers have conducted experiments in order to elucidate the biochemical properties and the subcellular localization of annexins (Rescher & Gerke, 2004). These experiments highlighted the physiological relevance of annexins, which are involved in many important cellular processes. For example, annexins are implicated in membrane transport (including ion transport, endocytosis and exocytosis), immune functions, redox regulation, cell-cell adhesion, cellular signaling, and the regulation of membrane cytoskeleton contacts (Drücker et al., 2014), (Bharadwaj et al., 2013). Figure 2.3, shows the various roles annexins are believed to play inside and outside of cells (Lizarbe et al., 2013). These cellular processes have important implications in human health and disease. Annexins are used as early markers for apoptosis and are overexpressed in certain tumor cells (Luckey, 2014). The term “annexinopathy” was coined in 1999 to recognize the role annexins play in human pathophysiology as they mediate diverse, interconnected cellular functions (Hajjar, 2015).

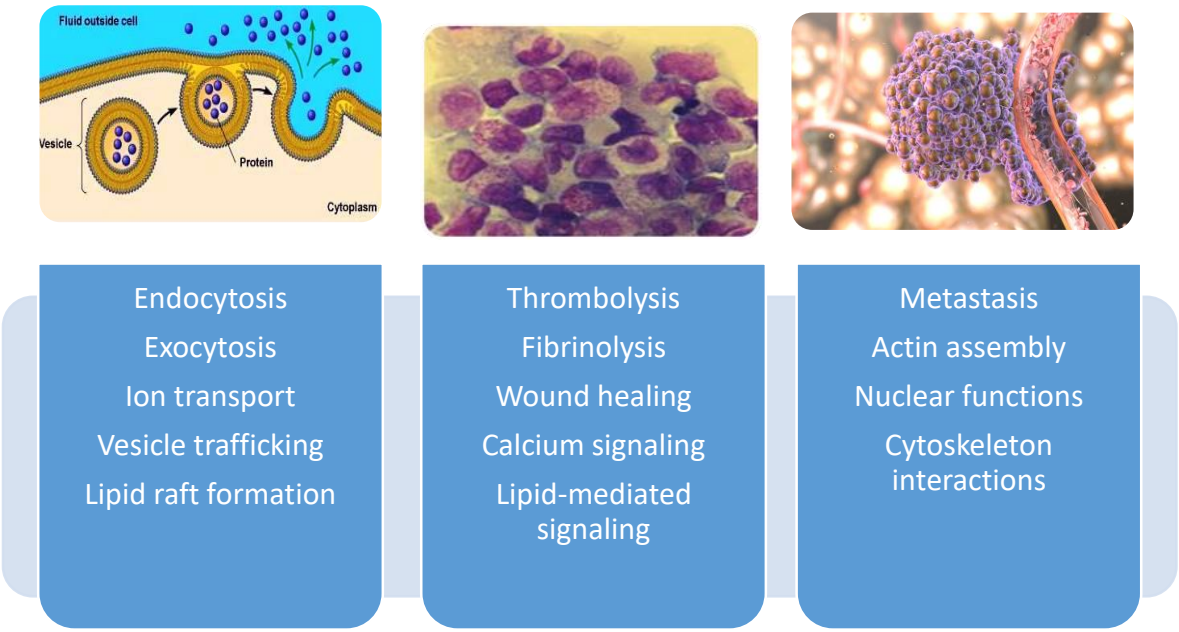

Figure 2.3: Function of annexin proteins in cells (Lizarbe et al., 2013), (Hajjar, 2015), (Luckey, 2014).

2.5 Physiological Relevance of Annexin A2

According to Dr. Hajjar, Weill Cornell Medical College, "Annexin A2 (ANXA2) is arguably the most extensively investigated annexin regarding health and disease" (Hajjar, 2015). ANXA2 has been found in endothelial cells, monocytes, macrophages and many cancer cells (Bharadwaj et al., 2013). In cancer cells, ANXA2 and its binding partners, such as S100A10, have been shown to promote metastasis by remodeling actin and regulating cytoskeleton structures (Lokman et al., 2011). As a mediator of the plasminogen activator system, ANXA2 also plays a role in regulating thrombolysis, fibrinolysis, and wound healing (Lokman et al., 2011).

The N-terminal domain can regulate the function of ANXA2 by altering calcium affinities at protein-interaction sites in the core domain, also as a direct result of tyrosine phosphorylation (Gerke et al., 2005). Membrane interactions of ANXA2 also play a significant role in mediating cellular functions. Annexin A2 binds to and aggregates vesicles containing the anionic phospholipids phosphatidic acid, phosphatidylserine, and phosphatidylinositol; but not vesicles containing phosphatidylcholine, phosphatidylethanolamine, or cholesterol (Bharadwaj et al., 2013). When ANXA2 associates with cholesterol and phosphatidylinositol 4,5-bisphosphate ($PI_{(4,5)}P_2$) rich-domains, it promotes the formation and influences the dynamics of those domains. Cholesterol appears to improve the membrane-binding affinity of ANXA2 by aiding the formation of domains containing high concentrations of anionic phospholipids (Bharadwaj et al., 2013).

There are still a lot of questions regarding the mechanism by which domains form and the functional role these lipid domains serve when bound to ANXA2 (Valapala & Vishwanatha, 2011). By uncovering this lipid-protein puzzle, much can be learned about the function of ANXA2.

2.6 Fluorescence Microscopy

Fluorescence microscopy is a commonly used method for protein-interaction studies (Yan & Marriott, 2003). Types of fluorescence microscopy include: Fluorescence resonance energy transfer (FRET), fluorescence lifetime imaging microscopy (FLIM), and fluorescence correlation spectroscopy (FCS). The advent of new fluorescent probe technology and labeling strategies has improved the use of fluorescence in various biological applications. Fluorescence spectroscopy is capable of making time-resolved measurements which can be used to characterize protein dynamics and to study conformational changes (Yengo & Berger, 2010).

2.6.1 FRET

FRET is used to measure the non-radiative energy transfer which occurs when a high-energy donor fluorophore excites a lower-energy acceptor fluorophore. In order for this interaction to occur (Piston & Kremers, 2007):

(1) The emission and absorption spectra of the two fluorophores must overlap (Fig. 2.4)

(2) The fluorophores must be separated by a distance of 10-100 angstroms

(3) The transition dipoles of the fluorophores must be oriented parallel to each other

The likelihood a FRET transfer will occur for a given acceptor and donor is described by the Forster distance, which is the distance the donor is from the acceptor when there is a 50% possibility of energy transfer which results in donor inactivation (Loura et al., 2010).

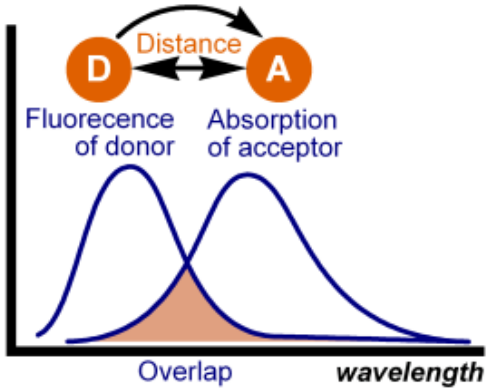

Figure 2.4: The overlap of the donor and acceptor fluorophores required for FRET transfer (http://www.calctool.org/CALC/chem/photochemistry/fret)

FRET is useful in determining protein-protein interactions which result from changes in affinity between two fluorescently labeled proteins or changes in binding conformation (Piston & Kremers, 2007). FRET can identify the extent of the interaction between two proteins, which surfaces they use to make contact, and the spatial location of the two proteins in relation to each other (Mendelsohn & Brent, 1999). Theoretically, FRET can be used to study interactions between proteins in any cellular compartment (Mendelsohn & Brent, 1999). When a FRET transfer occurs the intensity and lifetime of the donor fluorophore decrease while the intensity of the acceptor fluorophore increases. FLIM can be used to improve the quality of FRET-based imaging of protein-protein interactions within cells (Yan & Marriott, 2003).

2.6.2 FLIM

FLIM is used to measure nanosecond FRET events between two fluorescently labeled proteins within a cell (Yan & Marriott, 2003). FLIM works by recording images in terms of the fluorescence lifetime of the donor independent of the local concentrations of donor and acceptor fluorophores (Becker et al., 2004). Since the concentration of the fluorophore is inessential, FLIM can directly study phenomena involving energy transfer. Fluorescence lifetime is a direct indicator of the energy transfer rate from donor to acceptor (Becker et al., 2004).

2.6.3 FCS

FCS is a high resolution spatiotemporal analysis technique which measures fluctuations in thermal equilibrium which occur when single molecules alter their fluorescence intensity or leave the observation lens. Using a sensitive confocal microscope, it is possible to determine the local molecular concentration, mobility coefficients (such as translational and rotational mobility), the viscosity of the solution, and the size or shape of the molecules passing through the lens. Rate

constants of intermolecular and intramolecular reactions of fluorescently-labeled molecules can also be measured. If the brightness (η) is known, it is also possible to quantify the rate of fluorescence quenching. This method functions at nanomolar concentrations of a biological sample by using principles of relaxation analysis. The strength and duration of fluctuations are measured by autocorrelating the intensity signal with the time, which measures the deviation in signal over time (Schwille, 2005). Collectively, these fluorescent techniques are useful in studying protein-protein and protein-lipid interactions, but there are other methods, such as cross-linker experiments, co-immunoprecipitation and co-pelleting assays, which can also elucidate the behavior of ANXA2 *in vivo* and *in vitro*.

CHAPTER 3—CO-PELLETING ASSAYS AND CROSS-LINKER EXPERIMENTS ELUCIDATE THE ROLE OF ANXA2 DIMERIZATION

This chapter begins with a brief introduction (3.1) about the potential for ANXA2 to dimerize in the presence of calcium, the role of dimerization, and the role of the N-terminal domain in these interactions. Then, the Materials and Methods (3.2) describes how the Sulfo-EGS cross-linker experiments and liposome co-pelleting assays were performed on ANXA2 WT and the ANXA2 10X and 6X mutants. Finally, Section 3.3 discusses the results of these experiments.

3.1 Introduction

Annexin A2 (ANXA2) is a peripheral membrane protein which binds anionic phospholipids in a calcium-dependent manner. Alterations in phospholipid and calcium binding allows ANXA2 to function in vesicle trafficking, lipid raft formation, signaling, and cytoskeletal interactions (Bharadwaj et al., 2013). By studying the functional mechanism by which ANXA2 influences these many processes, we can learn how these peripheral membrane proteins play important roles in human health and disease.

In 2004, Rosengarth and Luecke crystallized full length ANXA2 in order to determine the propensity of ANXA2 to induce membrane aggregation by forming a multimeric state. Their research revealed that in the presence of calcium, ANXA2 dimerizes at repeat 3 in an "upside-down" fashion in which the concave side of one monomer faces the convex side of another monomer, as shown in Fig. 3.1. They identified the residues that make up the dimer interface using protein crystallography.

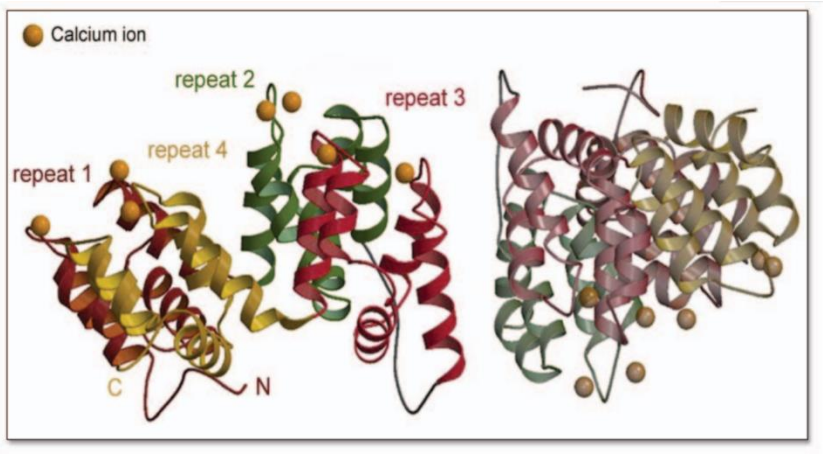

***Figure 3.1**: "Arrangement of the full-length ANXA2 dimer in the presence of calcium. The dimer contact is established through repeat 3" (Rosengarth & Luecke, 2004).*

In order to evaluate the functional purpose of dimerization in altering calcium binding affinities and protein-protein interactions, two mutant forms of ANXA2 were developed by the Gerke lab. ANXA2 6X, has 6 mutations at the salt bridges and calcium binding sites which make up the dimer interface: K81A, E189K, K206A, R196S, E219K, and K212S. The mutations are present on region 3, except K81A which is present on Region 1 where it has been shown to hydrogen bond to a neighboring ANXA2 dimer. These mutations convert polar amino acids into non-polar amino acids or positively charged amino acids into negatively charged amino acids which is intended to disrupt the salt bridges, preventing dimerization. The primers used for mutation can be found in Appendix A (8.1).

The second mutant form of ANXA2, ANXA2 10X has all of the mutations found in ANXA2 6X plus an additional 4 mutations: R36S, V53A, T54A, and K328A. These additional mutations also convert polar amino acids to nonpolar amino acids or alter the charge of the amino acid. The R36S mutation is next to the K81A mutation in Region 1, and both are believed to form a second region promoting dimerization in the wild type. The V53A, T54A, and K328A mutations were added to disrupt calcium-binding sites. A visual of the ANXA2 6X and 10X mutations (PDB ID 1XJL) is shown in Fig. 3.2 ANXA2 10X should prevent dimerization in the core domain, unless the N-terminal domain which could not be characterized through protein crystallography, plays a role in facilitating dimerization.

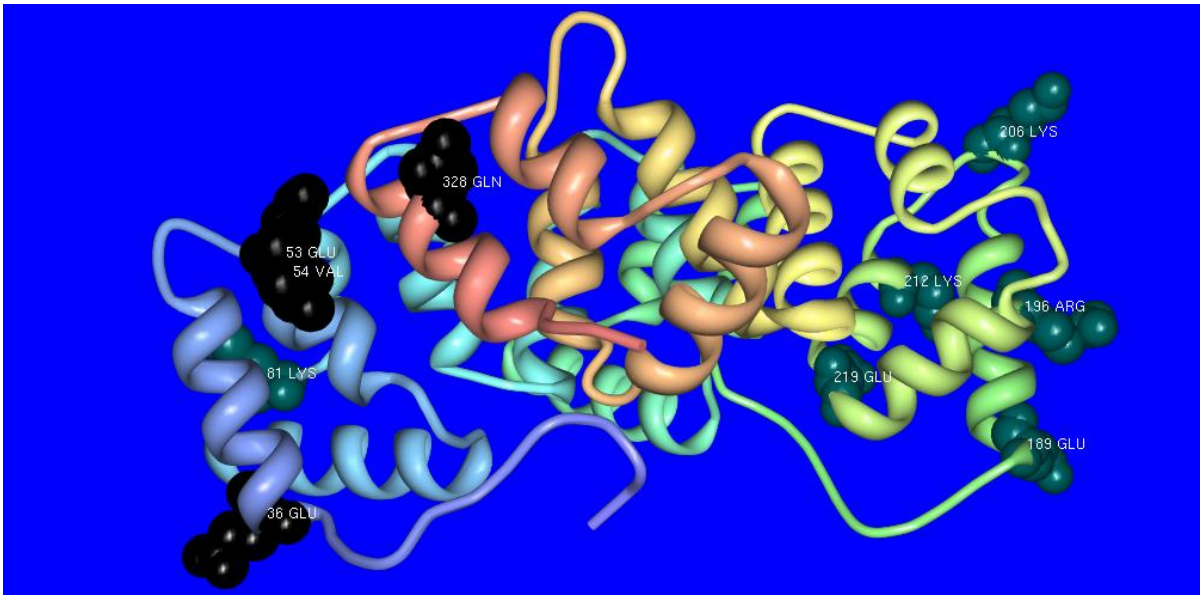

***Figure 3.2**: ANXA2 PDB ID 1XJL with 6x and 10x mutations highlighted in CPK atom and bond format. The 6x mutations are teal and the additional 10x mutations are black. The N-terminal residue is the periwinkle loop after the 36Glu residue (Protein Workshop).*

Currently, the role of the N-terminal domain in calcium-dependent membrane bridging is ambiguous (Ayala-San Martin Zibouche, 2008). This research was intended to elucidate the importance of dimerization in membrane bridging and the role of the N-terminal domain in this process by comparing the calcium-dependent binding of these mutants to the wild type by performing liposome co-pelleting assays and by performing Sulfo-EGS (ethylene glycolbis(succinimidylsuccinate)) cross-linking experiments to see if the N-terminal domain can form similar protein-protein interactions to the wild type.

3.2 Materials and Methods

3.2.1 ANXA2 10X, 6X, WT Expression

Glycerol stocks of ANXA2 WT, 10x, and 6x inserted into an *E.coli* BL21 (DE3)pLysS vectors, were used to inoculate an LB culture containing 150mM ampicillin. The cultures were grown to OD_{600} of 0.6 at 37°C, induced with 1mM IPTG, incubated in the shaker for 4 hours (250rpm, 37°C), and then chilled in the cold room for 30 minutes. The cell cultures were centrifuged at 5,000xg for 10 minutes at 4°C. The supernatant was discarded and the pellets were re-suspended in lysis buffer (50mM imidazole, 300mM NaCl, 10mM $MgCl_2$, 2mM DTT, 1 capsule Complete Protease Inhibitor EDTA-free, pH 7.4, 3 mL/g of wet pellet), and stored in -80°C.

3.2.2 ANXA2 10X, 6X, WT Purification

The protocol for the purification of ANXA2 WT can be found in Chapter 5 Section 3. The ANXA2 6X and 10X are purified in a similar manner. For the specific details of the equipment used and the antibodies used for the Western blot, refer to see the Methods section "Expression and Purification of Recombinant ANXA2" and "Antibodies, Expression Constructs, Proteins, and Synthetic Peptides" in Drucker et al. (2013) *Lipid segregation and membrane budding induced by the peripheral membrane binding protein annexin A2*.

3.2.2 Co-pelleting Liposome Assays

3.2.2.1 Liposome Preparation

Lipid samples were prepared according to the Avanti website[1] and lipid concentration was verified by performing phosphate assays. The desired lipid composition and concentration was measured and the lipids were dried using a stream of nitrogen while gently heating the lipids on a hot plate. The lipid films were stored in a vacuum overnight, then re-suspended in the experimental buffer (PBS or MES), heated to 60°C, vortexed, and extruded through a 200nm polycarbonate filter using an extrusion kit. The 200nm liposomes were prepared in a 20:60:20 POPS: POPC: Cholesterol ratio with 1mg of total lipid in 1mL. In these experiments, 300uL of liposomes were added (300ug).

3.2.2.2 Co-Pelleting Liposome Assay Protocol

20-60ug of ANXA2 WT, 6X, or 10X was added to 300ug of 20:60:20 POPS: POPC: Cholesterol and 250mM $CaCl_2$ which was brought to a volume of 250uL using MES or PBS buffer. The solution was incubated for 1hr at 4°C and placed in the Beckman Optima TL Ultracentrifuge at 100,000rpm (96,600xg) at 4°C for 15min. The supernatant was collected and labeled as "Calcium 1." The pellet was re-suspended in 250uL of MES or PBS buffer containing 250mM $CaCl_2$, incubated for 15min at 4°C, and then placed in the Beckman Optima TL Ultracentrifuge at 100,000rpm (96,600xg) at 4°C for 15min. The supernatant was collected and labeled as "Calcium 2." The pellet was re-suspended in 250uL of MES or PBS buffer containing 5mM EGTA, incubated for 15min at 4°C, and then placed in the Beckman Optima TL Ultracentrifuge at 100,000rpm (96,600xg) at 4°C for 15min. The supernatant was collected and labeled as "EGTA

[1] https://avantilipids.com/

1." The pellet was re-suspended in 250uL of MES or PBS buffer containing 5mM EGTA and labeled as EGTA 2. All fractions were ran on a denaturing 15% SGS-PAGE gel and scanned using the LI-COR.

3.2.3 Sulfo-EGS Cross-linker Experiments

The ANXA2 WT, 6X, and 10X proteins were dialyzed against HEPES buffer (20mM HEPES, 150mM NaCl, pH 7.4) and concentrated using an Amicon Ultra-4 Centrifugal Filter unit to a concentration of approximately 2mg/mL. The liposomes were prepared as described in *Section 3.2.2.1* using a ratio of DOPC: POPC: POPS: Cholesterol (20:40:20:20), and an overall lipid concentration of 1mg/0.3mL (3.34mg/mL). For each experiment, a control without cross-linker and liposomes was prepared, a control with EGTA without calcium, and a probe containing liposomes, cross-linker, and ANXA2 WT/6X/10X.

Initially, the controls and the probe are prepared without the Sulfo-EGS cross-linker and incubated at room temperature for 45minutes on the rocker. The control without cross-linker of liposomes has 60ug ANXA2 WT/6X/10X, 1mM $CaCl_2$, and is brought to a volume of 70uL with HEPES buffer. The EGTA control has 60ug ANXA2 WT/6X/10X, 100ug LUVs, 5mM EGTA, and is brought to a total volume of 70uL with HEPES buffer (including the volume of the cross-linker to be added later). The probe has 60ug ANXA2 WT/6X/10X, 100ug LUVs, 1mM $CaCl_2$, and is brought to a total volume of 70uL with HEPES buffer (including the volume of the cross-linker to be added later).

After 45 minutes, the Sulfo-EGS cross-linker was heated to 60°C and 0.3mM was added to the EGTA control and the probe. The controls and probe were then incubated at room temperature for an additional 45minutes on the rocker, then 15uL 5x SDS buffer without beta-mercaptoethanol was added to the controls and the probe. 3uL of 100mM EGTA was added to the probe and the samples were all left to sit at room temperature for 10min. 30uL of each sample was ran on a native 10% SDS-PAGE gel. The gel was rinsed 3x with water and stained with 30mL ThermoFisher Imperial Protein Stain for 2 hours. The gel was de-stained with Millipore water. The gels were scanned with a LI-COR.

In order to prevent the oxidized cysteine double bond which leads to the appearance of both the ANXA2 monomer and dimer in the control, the wild type ANXA2 was alkylated for 30minutes before it was ran on a 15% SDS-PAGE gel.

3.3 Results and Discussion

This section begins by discussing the results of the co-pelleting assays and ends by discussing the results of the Sulfo-EGS cross-linker experiments.

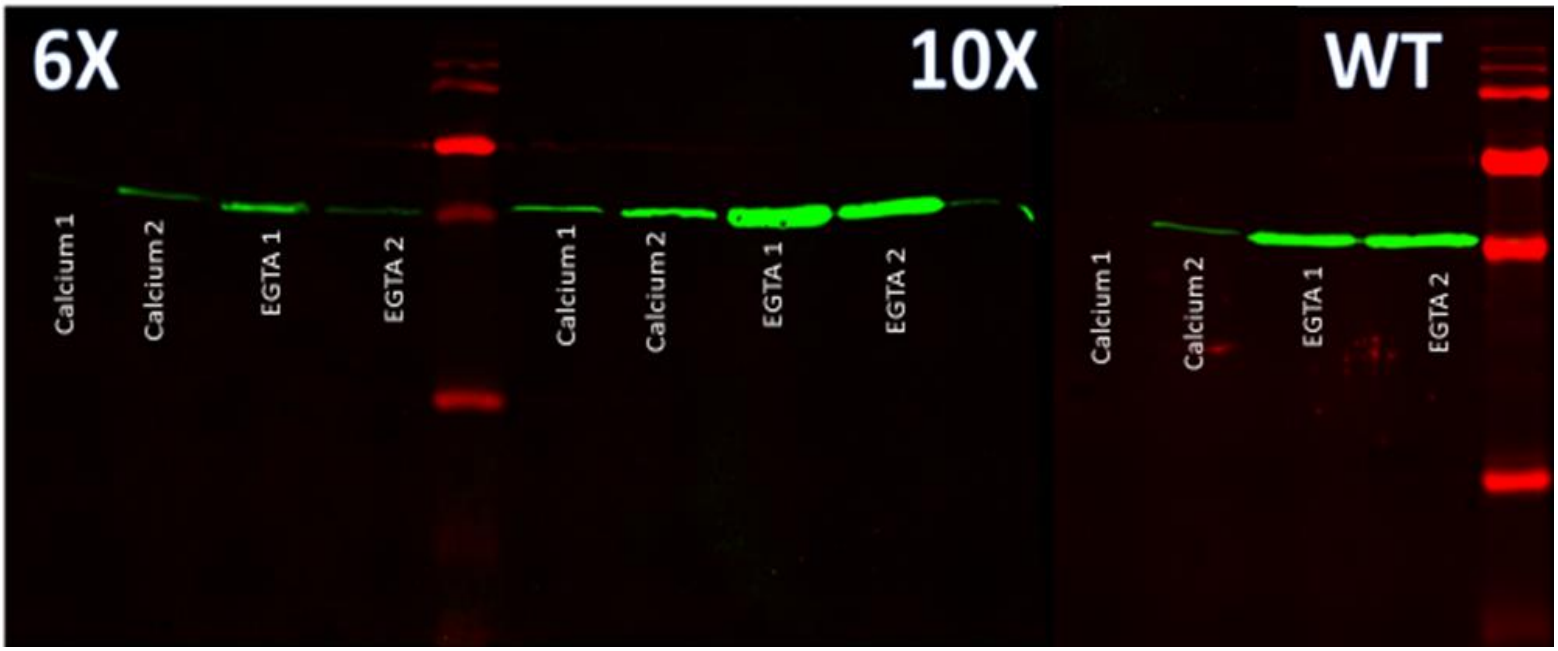

***Figure 3.3**: Co-pelleting liposome assays. Each experiment was performed in PBS buffer using 20ug ANXA2 6x, 60ug ANXA2 10X, 40ug ANXA2 WT, 250mM CaCl2 in the calcium fractions, and 5mM EGTA in the EGTA fractions in a total volume of 450Ul. For a detailed description of each fraction refer to the Methodology.*

Co-pelleting liposome assays were performed in order to assess the ability of wild type ANXA2 and the ANXA2 6X and ANXA2 10X mutants to reversibly bind anionic phospholipids in a calcium-dependent manner; a property of all forms of annexins, as shown in Fig. 3.3. By adding an excess of calcium chloride (250mM) in the presence of 100ug of 200nm liposomes containing 20:60:20 POPS: POPC: Cholesterol, the majority of the ANXA2 used in these experiments (20-60ug) was anticipated to bind liposomes in the presence of calcium and thus will be present in the pellet after the solution is centrifuged at 100,000rpm. 200nm vesicles were favorable to smaller vesicles because the larger size allows them to pellet at a lower speed. Upon the addition of EGTA, the ANXA2 protein should unbind the liposomes and be free in solution; allowing ANXA2 to show up in the supernatant after centrifugation.

In the first set of co-pelleting assays varying concentrations of ANXA2 were used to determine how much protein can bind 100ug of 20:60:20 POPS: POPC: Cholesterol liposomes. The co-pelleting experiment with 40ug of ANXA2, showed that the majority of the ANXA2 WT protein was bound to liposomes in the presence of calcium and upon the addition of EGTA, a chelator which preferentially targets divalent calcium ions, approximately half of the ANXA2 WT protein was released and half remained bound. The presence of large ANXA2 WT in the pellet after EGTA addition (5mM), suggests that more EGTA is needed to effectively chelate all of the Ca^{2+} ions, but that the ANXA2 WT can effectively bind liposomes in the presence of Ca^{2+} ions.

In comparison to the ANXA2 WT co-pelleting assay, the ANXA2 6X behaved similarly, although the ANXA2 6X experiment only had 20ug ANXA2 6X. There was a negligible amount of ANXA2 6X present in the first calcium fraction, and a small amount of ANXA2 6X was present in the second calcium fraction. The presence of ANXA2 6X in the second calcium fraction suggests that a small amount of the protein may have been damaged during resuspension and could no longer bind liposomes in a calcium-dependent manner. Upon EGTA addition, the majority of the ANXA2 6X was present in the supernatant, which indicates that ANXA2 6X binds reversibly to anionic phospholipids in the presence of calcium. The reduction in the amount of ANXA2 6X in the EGTA 2 fraction likely occurred because there was less ANXA2 6X present in this experiment than in the wild type. These findings suggest that the mutated residues did not significantly alter the ability of ANXA2 6X to bind lipids.

In order to further verify these findings, additional co-pelleting experiments were performed using 20ug of ANXA2 6X to replicate the cross-linker experiment in Fig.3.4 and another co-pelleting assay with 40ug of ANXA2 6X which exactly mimics the experimental conditions for the ANXA2 WT co-pelleting assay in Fig. 3.3. The 40ug ANXA2 6X co-pelleting assay appeared very similar to the 20ug ANXA2 6X co-pelleting assay.

Quantification of each band size using the LI-COR showed that in the 40ug experiment 3.5% ANXA2 6X (1.49ug/42.29ug) appeared in the first calcium fraction, 4.5% ANXA2 6X (1.90ug/42.49ug) appeared in the second calcium fraction, 74.4% ANXA2 6X (31.61ug/42.49ug) appeared in the first EGTA fraction, and 17.6% ANXA2 6X (17.49ug/42.49ug) appeared in the second EGTA fraction. In the 20ug ANXA2 6X experiment 2.7% ANXA2 6X (0.55ug/20.08ug) appeared in the first calcium fraction, 4.88% ANXA2 6X (0.98ug/20.08ug) appeared in the second calcium fraction, 77.1% ANXA2 6X (15.49ug/20.08ug) appeared in the first EGTA fraction, and 15.2% ANXA2 6X (3.06ug/20.08ug) appeared in the second EGTA fraction.

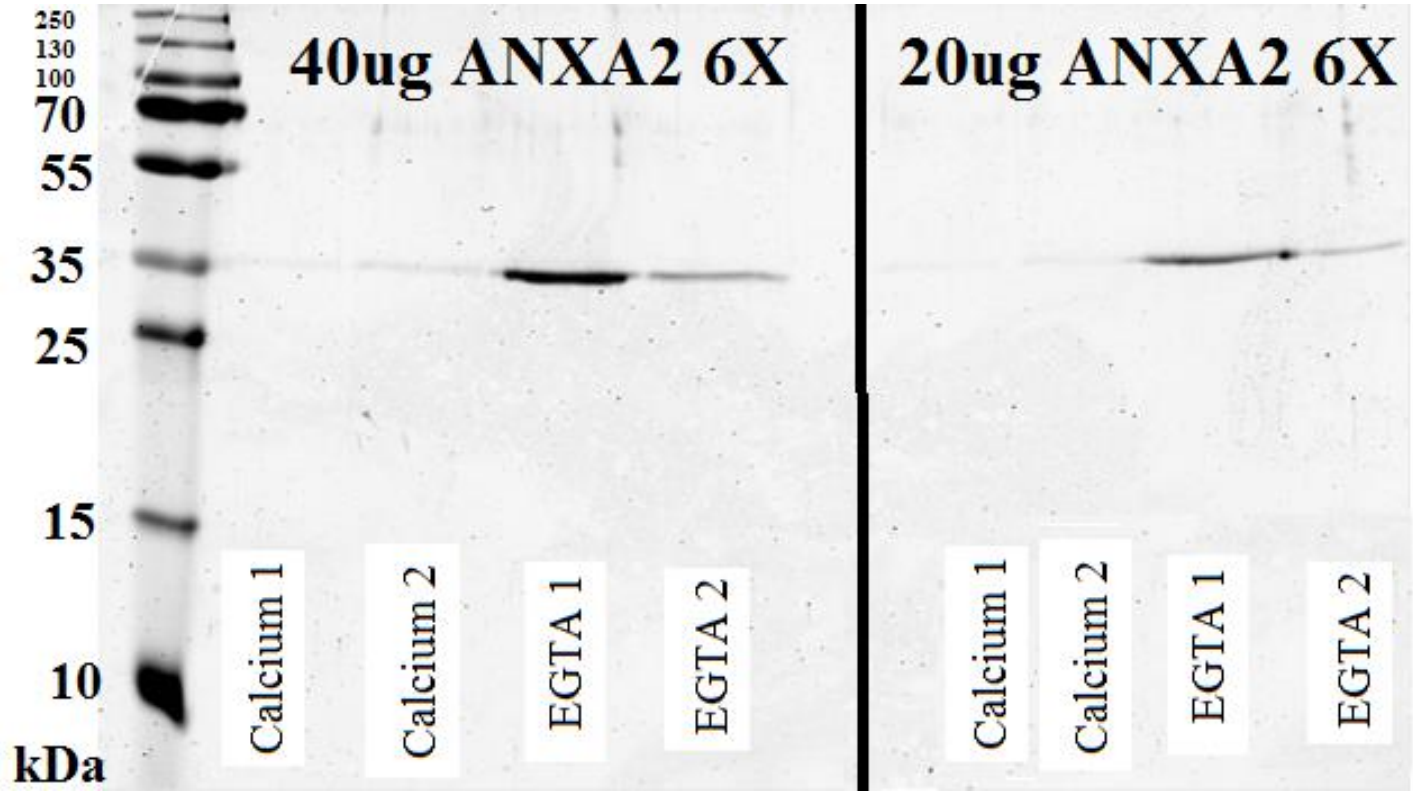

***Figure 3.4**: ANXA2 6X Co-pelleting liposome assay. Each experiment was performed in MES buffer using 250mM CaCl2 in the Calcium fractions and 5mM EGTA in the EGTA fractions. For a detailed description of each fraction refer to the Methodology. 40ug ANXA2 6X experiments Left to Right: 1.49ug ANXA2 6x in Calcium 1, 1.90ug in Calcium 2, 31.61ug in EGTA 1, and 7.49ug in EGTA 2. 20ug ANXA2 6X experiments Left to Right: 0.55ug ANXA2 6x in Calcium 1, 0.98ug in Calcium 2, 15.49ug in EGTA 1, and 3.06ug in EGTA 2.*

In comparison to the ANXA2 W co-pelleting assay, it appears that the ANXA2 6X is held more loosely by the membrane, allowing more of the ANXA2 6X mutant to become unbound from the membrane upon the addition of EGTA than the wild type.

Comparatively, the ANXA2 10X mutant bound the liposomes less effectively than the wild type and 6X mutant. The reduced binding was likely due to the presence of higher amounts of ANXA2

10X (60ug). The EGTA fractions contained the majority of the ANXA2 10X protein suggesting that ANXA2 10X also retained the ability to reversibly bind anionic phospholipids in the presence of calcium, even though additional calcium-binding sites were mutated in addition to the mutations present in the ANXA2 6X mutant. In future experiments, equivalent concentrations of the mutants and wild type should be studied and higher EGTA concentrations should be used to reduce the amount of ANXA2 WT/6X/10X in EGTA fraction 2. Overall though, these findings support that these mutations did not fully destroy the function of ANXA2, and thus they can be used for further experimentation.

In order to understand how these mutations affected the ability of ANXA2 to dimerize and form protein-protein interactions, Sulfo-EGS cross-linker experiments were performed as shown in Fig. 3.5. According to the ThermoFisher Scientific website[2], Sulfo-EGS is a water-soluble cross-linker which targets primary amine groups via a sulfo-NHS ester which is reactive at both ends and forms a 12-atom spacer arm. The lipids used in these experiments do not have primary amine groups, therefore only proteins which are within 12-atoms of each other will cross-link.

The ANXA2 WT showed numerous cross-linking protein bands in the probe lane of the native SDS-PAGE gel. The probe contained 60ug ANXA2 WT, 100ug liposomes, 1mM $CaCl_2$, and 0.3mM Sulfo-EGS cross-linker. There were no noticeable cross-linking bands in the in EGTA control or the control without cross-linker and liposomes. Cross-linking upon the addition of lipids and calcium suggests that when ANXA2 WT binds to anionic phospholipids, this produces a conformational change promoting further ANXA2 WT interactions.

Additionally, there are two protein bands present in the EGTA control and the control without cross-linker and liposomes because the N-terminal cysteine forms a double bond when oxidized which leads to additional cross-linking due to oxidative products. The majority of the ANXA2 WT appears around 70kDa, suggesting that when oxidative products do not inhibit dimerization, ANXA2 WT preferentially dimerizes.

[2] https://www.thermofisher.com/order/catalog/product/21566

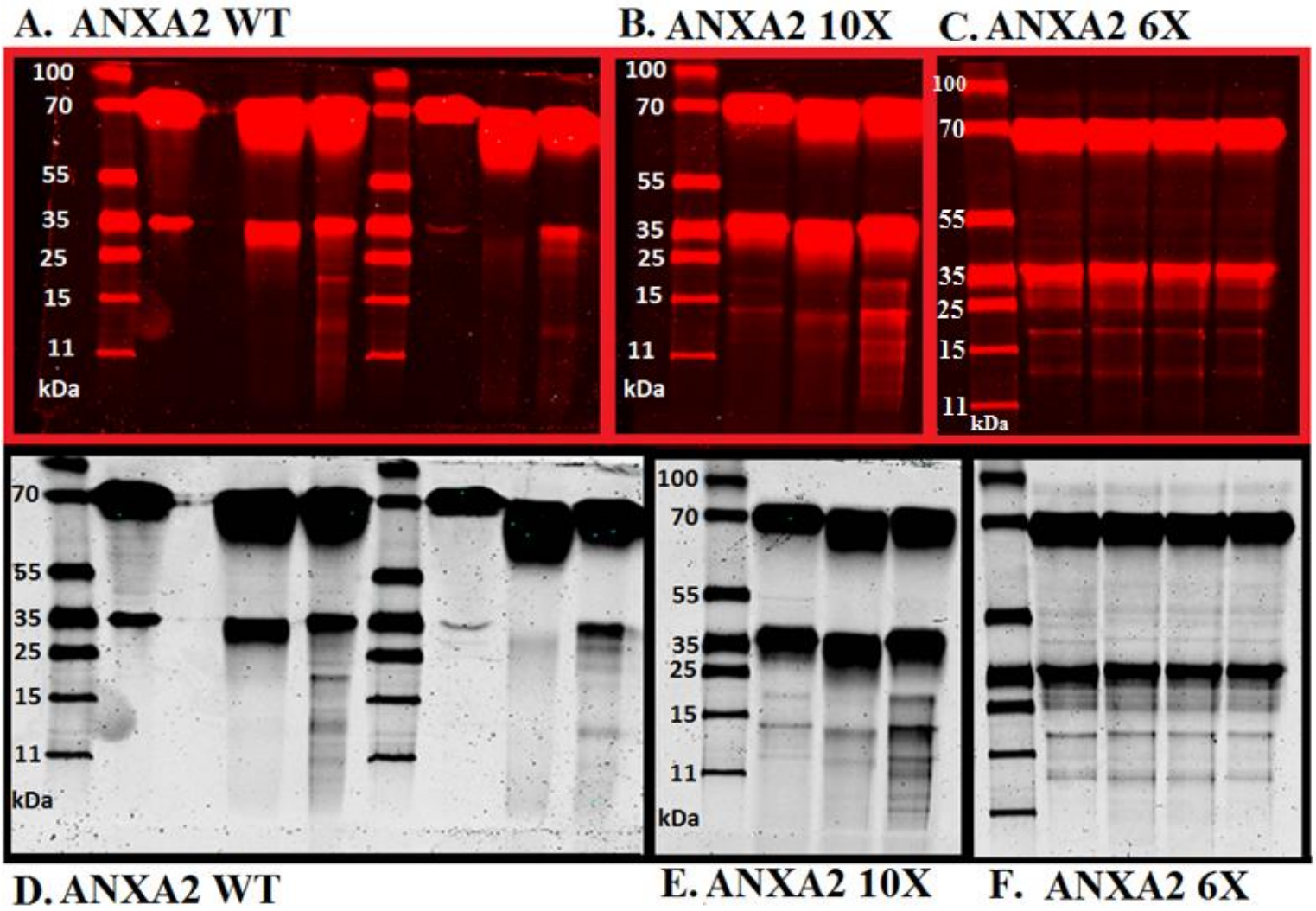

***Figure 3.5**: Sulfo-EGS Cross-linker Experiments. Top Native SDS-PAGE gels LI-COR scan, Bottom: Native SDS-PAGE gels in black and white. ANXA2 WT Lanes Left to Right: Protein Color Standard ladder, unalkylated control without cross-linker, empty lane, unalkylated EGTA control, unalkylated probe, Protein Color Standard ladder, alkylated control without cross-linker, alkylated EGTA control, alkylated probe. ANXA2 10X: Protein Color Standard ladder, control without cross-linker, EGTA control, probe. ANXA2 6X: Protein Color Standard ladder, Control without cross-linker, EGTA control, T1 probe, T2 probe.*

The ANXA2 10X behaves similarly to the ANXA2 WT, but the ANXA2 10X appeared to cross-link more strongly with fewer bands than the wild type. ANXA2 10X had approximately 6 highly visible protein bands from 11-35kDa in size, while the ANXA2 WT over 10 bands which were very faint after alkylation. In the control without cross-linker and liposomes, there are a few faint bands which suggest the presence of either small amounts of contamination or small amounts of protein degradation. There is also a faint band at 55kDa in the control without cross-linker and liposomes that is not present in the EGTA control, suggesting that calcium may produce conformational changes in the ANXA2 10X mutant, producing this additional band. The presence of equally strong protein bands at 35kDa and 70kDa indicates that ANXA2 can still dimerize even

though there are mutations in the dimerization site, suggesting that the N-terminal domain may play a stronger role than the residues in Region 1 and 3 of ANXA2 in promoting dimerization. Compared to ANXA2 WT, ANXA2 10X did not dimerize as efficiently which may have been due to the presence of more oxidative products causing a higher amount of cysteine double bonds, inhibiting dimerization. Future experiments should be performed in which the ANXA2 is alkylated to see how this effects the ratio of monomer to dimer.

Comparatively, the ANXA2 6X mutant was unaffected by the presence of the cross-linker, calcium, or lipids, suggesting that ANXA2 6X may have degraded prior to experimentation, likely after concentration and dialysis; suggesting that the mutation resulted in a less stable protein. The liposome assays indicated that ANXA2 binds anionic phospholipids in the presence of calcium, thus the ANXA2 6X was expected to undergo a conformational change, producing cross-linked ANXA2 proteins. There is a small possibility that ANXA2 does not change its protein-protein interactions upon membrane binding due to the nature of its mutations and is constantly shifting conformation due to lowered stability, but it would be expected that the ANXA2 10X mutation would have behaved similarly, if not less efficiently. Interestingly, ANXA2 6X still harbored a strong propensity to dimerize, indicating that the N-terminal domain must facilitate this interaction. In the future, the ANXA2 6X should be re-purified and these experiments should be repeated with and without alkylation. Overall, these findings support the notion that the N-terminal domain might play a role in ANXA2 dimerization. In order to further study the propensity of the N-terminal domain of ANXA2 to promote lipid aggregation and the formation of lipid rafts via self-association, the research aim and project approach were developed.

CHAPTER 4—ANXA2 MEDIATED LIPID CLUSTERING

Chapter 4: Research Aim and Project Approach, begins by discussing the importance of characterizing the interactions of ANXA2 with anionic phospholipids (4.1). Section 4.2 discusses the scope and aim of this research. Section 4.3 provides a review of related experiments conducted by others to provide the reader with an understanding of different methods which have previously been used to characterize the function of ANXA2. Lastly, Section 4.4 provides an overview of the project approach which includes the hypotheses to be tested and the specific aim of each experiment.

4.1 Importance of Characterizing the Interactions of ANXA2 with Anionic Phospholipids

ANXA2 is a physiologically relevant protein implicated in wide ranging cellular processes such as cell motility, tumorigenesis, osteoclast formation, fibrinolysis, membrane transport, and cellular signaling (Valapala & Vishwanatha, 2011). The role of this protein in human health and disease is far-reaching but its exact functional role in these processes is unknown. According to Blackwood et al. (1990), researching the ability of ANXA2 to bind to cellular membranes and calcium has elucidated the role this protein plays in mediating endocytosis, exocytosis, and other membrane trafficking events (Blackwood & Ernst, 1990).

As evidenced by a review by Gerke & Moss (2002), there is still much to be learned in order to determine the physiological importance of the calcium-dependent phospholipid and membrane binding of ANXA2 (Gerke & Moss, 2002). It is known that when ANXA2 associates with the plasma membrane or early endosomes, the core domain forms a compact disk whose convex side associates with membrane phospholipids and the concave portion is oriented away from the membrane (Fig. 2.2). ANXA2 binds anionic phospholipids at evolutionarily conserved annexin repeats within the core domain (Hedhli et al., 2012). ANXA2 binding to the plasma membrane is believed to cause cytosolic anionic phospholipids to cluster. The clustering activity of anionic phospholipids has a number of possible mechanisms. For example, when ANXA2 binds to the plasma membrane, this could promote self-association, promoting further clustering, aiding the development of a domain primarily comprised of anionic phospholipids. This clustering activity is believed to produce membrane domains or lipid rafts which function as signaling platforms (Gerke & Moss, 2002). Understanding the creation and function of these signaling platforms could provide useful clues about the importance of ANXA2 in signal transduction pathways.

The ability of annexins to self-associate and to bind anionic phospholipids differs between different forms of annexins and the nature of how these two processes function together is largely unknown. In 1991, research performed by Zaks and Creutz, suggested that calcium concentrations may dictate the relationship between self-association and phospholipid binding. At low concentration of calcium ions, membrane binding may require self-association. While at higher calcium ion concentrations, annexins likely monomerically bind two membranes. Self-association may be an evolutionary advantage allowing annexins to aggregate at membrane contact sites, strengthening this interaction (Zaks & Creutz, 1991). Other researchers, such as Hong et al. (1982), discount the notion of self-aggregation, preferring the idea that each annexin has multiple membrane binding locations to cross-link membranes (Hong, Düzgüneş, Ekerdt, & Papahadjopoulos, 1982). Differing annexins have variable N-terminal domains, and it has been found that some annexins have the propensity to self-associate while others do not.

Another interesting feature of ANXA2 is its capacity to aggregate membranes. When ANXA2 binds membranes comprised of anionic phospholipids, annexins A1, A2, A4, A6, and A7 participate in membrane vesicle aggregation (Gerke & Moss, 2002). Blackwood et al. (1990) has shown that the amino-terminus of ANXA2 plays an important role in aggregating cellular membranes. Structurally, the role of the N-terminus in membrane aggregation is difficult to explain because the phospholipid binding sites are on the opposite side of ANXA2 (Blackwood & Ernst, 1990). A proposed method for membrane vesicle aggregation, is the self-association of ANXA2 molecules already bound to different portions of cellular membrane.

The heterotetrameric form of ANXA2 promotes self-association and consequently aggregates membranes more efficiently than monomeric ANXA2. The heterotetramer also has an increased phospholipid binding affinity (Hedhli et al., 2012). ANXA2 forms a heterotetramer by preferentially binding to S100A10, also known as p11, a calcium-binding protein with an EF-hand motif (Hedhli et al., 2012). The heterotetramer form of ANXA2 aggregates membranes at micromolar calcium levels which are much lower than the calcium concentrations required for the monomer form (Gerke & Moss, 2002). A similar form of annexin, annexin A1, binds calcium, which induces a conformational change making the amino-terminal domain accessible for heterotetramer formation (Fig. 4.1), (Rescher, Zobiack, & Gerke, 2000). Zibouche et al. (2008),

has shown that ANXA2 associates with the membrane without any significant changes in the structure of the core domain (Zibouche, Vincent, Illien, Gallay, & Ayala-Sanmartin, 2008).

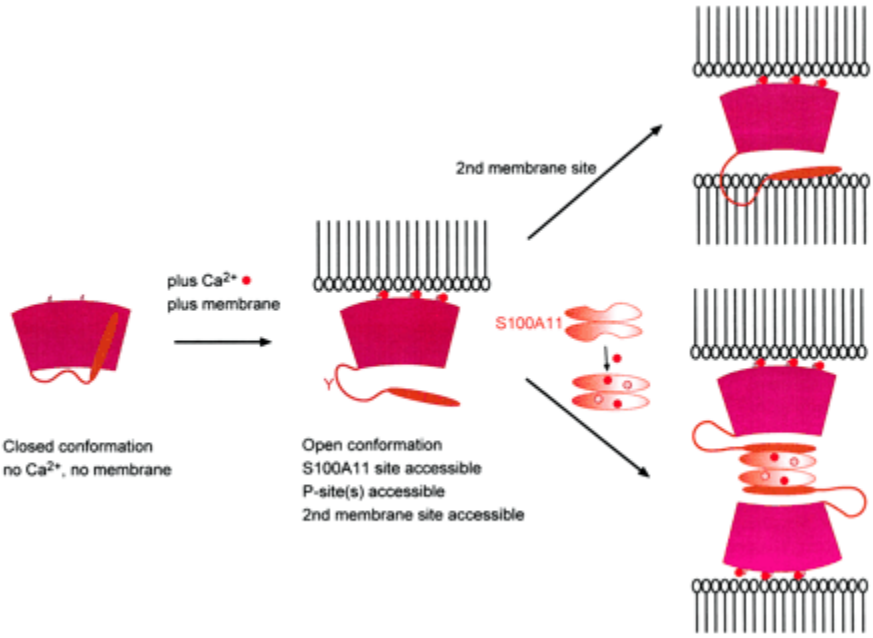

***Figure 4.1**: Annexin A1 Heterotetramer Formation. Annexin A1 binds calcium, inducing a conformational change which makes the amino-terminal domain accessible for heterotetramer formation (Rescher, Zobiack, & Gerke,2000)*

ANXA2 has been shown to form membrane-cytoskeleton interactions in addition to its membrane-membrane interactions. These calcium-dependent interactions assist numerous biological processes such as membrane trafficking and the maintenance of the shape of cells and organelles (Jost, Zeuschner, Seemann, Weber, & Gerke, 1997). The calcium-dependent binding of ANXA2 is reversible, and calcium chelating agents, such as EGTA, can be used to release annexins from binding anionic phospholipids. Conversely, the absence of calcium should nullify the interactions between ANXA2 and anionic phospholipids.

Understanding the importance of calcium in the function of ANXA2 can yield an array of important information. Calcium ions serve as secondary messengers in a number of cellular processes, enabling extracellular calcium signals to produce an intracellular response and vice versa. Regulation of intracellular Ca^{2+} concentrations helps to maintain this calcium signaling network. ANXA2 binds calcium ions within cells and is believed to participate directly in calcium signaling by creating conformational changes, and other altered cellular states as a result of calcium binding. The exact role of ANXA2 within the calcium signaling network still needs to be

determined (Gerke & Moss, 2002). There is evidence that ANXA2 can function in the absence of calcium under certain cellular conditions. For instance, Jost et al. (1997), found that at a neutral pH, ANXA2 binds endosomal membranes calcium independent.

Cellular signaling is highly interconnected and it is often difficult to determine how multiple molecules interacting together elicit a particular cellular response *in vivo*. By working to understand how ANXA2 interacts with calcium and anionic phospholipids to facilitate cellular processes such as exocytosis and thrombolysis, *in vitro*, it is then possible to understand how the body works and why diseases such as antiphospholipid syndrome or acute promyelocytic leukemia are linked to mutations in the ANXA2 gene.

By researching the protein-protein and protein-lipid interactions of ANXA2, its functional role in cellular processes can be elucidated. Protein and lipid interactions comprise most cellular events, and by understanding the spatiotemporal nature of the interaction, the reaction conditions required for interaction, and the result of the interaction it is then possible to determine the function of this interaction in the body. Different calcium concentrations, pH levels, and anionic phospholipid composition have been shown to alter ANXA2 interactions with anionic phospholipids both *in vitro* and *in vivo* (Zaks & Creutz, 1991).

Knockout models in cells and animals and dominant negative mutant ANXA2 proteins have been developed in order to study the function of annexins (Gerke & Moss, 2002). Microscopy techniques such as cryoelectron microscopy and atomic force microscopy have been used to identify the formation of membrane domains and to study the interactions of different types of annexins with anionic phospholipids. Transmission and total internal reflection fluorescence microscopy (TIRF) have provided evidence that some annexins change conformation upon binding anionic phospholipids (Gerke & Moss, 2002). In considering the many different ways of studying annexins and the research equipment available, the Project Aim was developed.

4.2 Project Aim

This project was intended to characterize ANXA2 interactions with the anionic phospholipids PS and $PI_{(4,5)}P_2$, by studying whether altering calcium and anionic phospholipid concentrations promote or prevent ANXA2 self-association *in vitro*. The *in vitro* system used in these studies was

developed to shed light on the mechanism by which ANXA2 interacts with cellular membranes and anionic phospholipids *in vivo* to cause membrane rearrangement, producing lipid rafts which may serve as signaling platforms.

This research was performed by analyzing the ability of the N-terminal domains of adjacent ANXA2 molecules to interact with other ANXA2 molecules in the presence and absence of PS and $PI_{(4,5)}P_2$.Purified ANXA2 protein was divided in half and fluorescently labeled. One half was labeled with a donor fluorophore (AlexaFluor 488 C5 Maleimide) and the other half was labeled with an acceptor fluorophore (AlexaFluor 568 C5 Maleimide). The fluorescent dye labeled the singular exposed cysteine residue on the N-terminal domain of ANXA2 (Fig. 4.2). After the protein was labeled, FRET experiments were performed in which lipid was titrated into a solution containing calcium chloride (0.5Mm) and varying concentrations of the acceptor and donor. After assessing the nature of this interaction, the importance of calcium in these experiments was elucidated by performing $CaCl_2$ titrations into a solution containing 0.5mM EGTA, 0.5uM donor, and 2.0uM acceptor ANXA2. The ability of ANXA2 to aggregate membranes was evaluated using dynamic light scattering (DLS). This research was intended to provide a platform for future ANXA2 characterization studies as well as to complement existing data regarding the interactions of ANXA2. Additionally, this research should expand current understanding regarding membrane domain formation by peripherally associated proteins. The FRET experiments may reveal useful information about changes in the quaternary structure of ANXA2 near its N-terminal cysteine residue upon lipid binding.

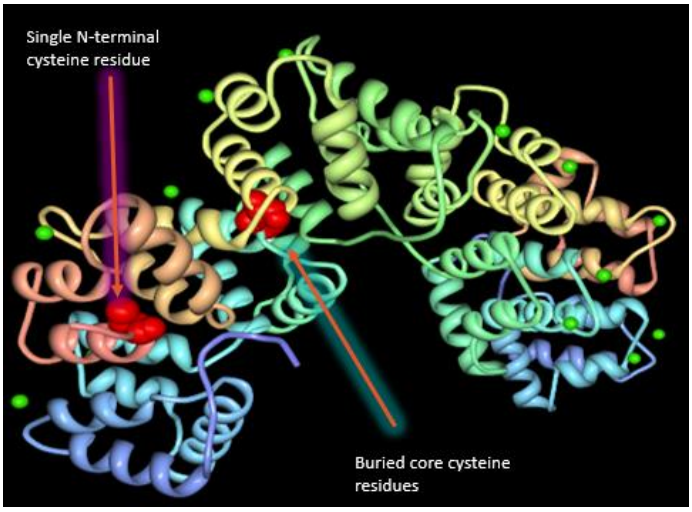

***Figure 4.2**: Cysteine residues on ANXA2 ribbon diagram (Protein Workshop).*

4.3 Literature Review of Related Experiments

There have been a number of experiments performed by others which have elucidated the nature of the interactions between ANXA2 and anionic phospholipids. This subsection will discuss those experiments which are closely related to the Project Aim (4.2) and aided in the development of the Methodology (Chapter 5) as well as the Hypotheses and Project Goals (4.4).

In 2013, Drucker et al. performed experiments with giant unilamellar vesicles (GUVs) in order to study the ability of ANXA2 to induce membrane domain formation. Upon binding GUVs containing $PI_{(4,5)}P_2$and cholesterol, ANXA2 (monomer and a mutant containing only the core domain) clustered the anionic lipids inducing lipid phase separation. Additionally, ANXA2 was shown to link adjacent GUVs and to induce membrane indentations in the presence of $PI_{(4,5)}P_2$, (Fig. 4.3). The membrane indentations produced by ANXA2 resulted in the inward vesiculation of the clustered lipids (also known as "membrane domains"). This phenomenon highlighted the potential role of ANXA2 in membrane trafficking. In these studies, the protein and calcium ion concentration were altered as well as the ratio of anionic lipids in the GUVs. These alterations indicated that increasing the concentration of anionic POPS (5-20% total lipid composition, 5ug) and $CaCl_2$ (50-500uM) allows ANXA2 to bind more lipids as shown by an increase in the number of GUV-bound AlexaFluor® 568 fluorescence (Drücker et al., 2013).

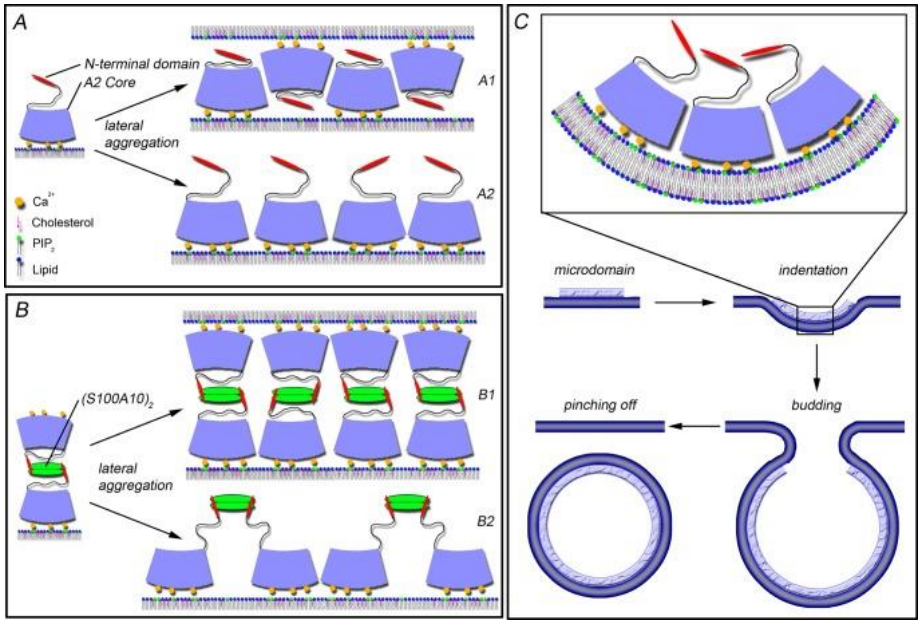

***Figure 4.3**: Lipid segregation and membrane budding induced by the peripheral membrane binding (Drücker et al., 2014).*

The following year, Drucker et al. (2014) published a paper characterizing ANXA2 binding to solid-supported lipid bilayers (SLBs) containing varying concentrations of anionic phospholipids, such as $PI_{(4,5)}P_2$and POPS, using Quartz Crystal Microbalance (QCM). As a result of the piezoelectric effect, QCM measures mass variation per unit area or viscosity by calculating the resonance frequency of a sample using a quartz crystal oscillator. QCM is used to determine protein affinity on surfaces such as SLBs. These experiments were conducted in the presence and absence of cholesterol. This research indicated that ANXA2 cooperatively binds $PI_{(4,5)}P_2$to form 0.5–2 ± 0.2μm TopFluor $PI_{(4,5)}P_2$ domains that co-localize with labeled ANXA2. In the presence of cholesterol, the dissociation constant of monomeric ANXA2-lipid binding varied from 22.1-32.2nM, depending on the lipid composition. These numbers indicate that binding is of high specificity and affinity (Drücker et al., 2014).

The cause of the cooperativity which occurs when ANXA2 binds the plasma membrane in the presence of cholesterol, $PI_{(4,5)}P_2$, and POPS is unclear. The cooperativity of ANXA2 binding is believed to occur a result of one of the following phenomena (Drücker et al., 2014):

> ANXA2 Induces Lipid Reorganization: Bilayer reorganizations occur as a result of ANXA2 binding
>
> Lipids Stimulate Protein-Protein Interactions: Conformational change in AnxA2 results from lipid binding, enabling protein-protein contacts which facilitates further binding
>
> Lipid Reorganization Induces ANXA2 Binding: pre-existing domains of $PI_{(4,5)}P_2$ and cholesterol effect ANXA2 binding properties

It is also possible that cooperativity results from a combination of these mechanisms. Lipid reorganization and protein-protein interactions could both be stimulated by lipid binding (Drücker et al., 2014).

A study performed by Illien et al. (2012), characterized the role of calcium and pH in causing ANXA2 to aggregate membranes containing $PI_{(4,5)}P_2$ and POPS in the presence and absence of cholesterol. By looking at turbidimetry using a Cary spectrophotometer, Illien et al. (2012) studied the ability of ANXA2 to aggregate large unilamellar vesicles (LUVs) via membrane bridging at differing concentrations of calcium or hydronium ions. Under acidic conditions, ANXA2 has been shown to bind anionic phospholipids independent of calcium. A lipid/protein ratio of 25 was used. This research indicated that PS-containing membranes interact with ANXA2 to form membrane

bridges at a lower calcium concentrations than membranes comprised of $PI_{(4,5)}P_2$. The calcium concentrations required for half maximal membrane bridging (EC50) by monomeric ANXA2 (5ug) was between 1.55uM and 91.2uM for POPS-containing membranes and between 3.31uM and 190.5uM for $PI_{(4,5)}P_2$-containing membranes. The calcium requirements for ANXA2 interactions with PS-containing membranes is further lowered in the presence of cholesterol. The role of cholesterol in altering the calcium ion sensitivity of $PI_{(4,5)}P_2$–containing membranes is unclear. Unexpectedly, calcium ion sensitivity did not correlate with the concentration of anionic phospholipids involved in membrane binding. $PI_{(4,5)}P_2$is more negatively charged than POPS and should require more calcium ions to lower the electrostatic repulsion, enabling ANXA2 to form membrane bridges. Additionally, ANXA2 alters membrane fluidity upon lipid binding. $PI_{(4,5)}P_2$-containing membranes lower membrane fluidity more than those containing POPS. This effect is most pronounced under acidic conditions than under high Ca^{2+} concentrations. Cholesterol further reduces membrane fluidity. These findings highlighted key differences between the ability of ANXA2 to aggregate membranes calcium dependently and calcium independently (Illien, Piao, Coué, Di Marco, & Ayala-Sanmartin, 2012).

The role of the N-terminal domain in membrane bridging by ANXA2 was studied by Zibouche et al. (2008) using steady-state and time-resolved FRET of ANXA2 proteins fluorescently labeled at Cys-8 using acrylodan or *N*-(1-pyrene)maleimide and doxyl-labeled phospholipids (POPS/POPC) at different pH values. This study revealed a direct interaction between the N-terminal domain and the membrane. The distance of the labeled cysteine from the center of the bilayer (10.7 Å) was estimated from the quenching efficiency of 5-doxyl PC and 12-doxyl PC. Under mildly acidic conditions, N-terminal dimerization is not necessary for membrane bridging. An ANXA2 mutant lacking the N-terminal domain was capable of bridging membranes with a 2 to 3-fold lowered efficiency compared to the wild type suggesting that the N-terminal domain enhances the formation of membrane bridges under acidic conditions, but is not required for membrane binding (Zibouche et al., 2008).

In addition to membrane binding, Zibouche et al. (2008) discovered interactions between the N-terminal domains of adjacent ANXA2 proteins that were not in contact with the membrane as well as alterations in ANXA2 organization at the membrane as a result of changes in pH and Ca^{2+} concentration, suggesting that ANXA2 changes conformation under differing reaction conditions

which could help to explain its diverse role within the human body. By performing fluorimetry experiments Zibouche et al. found that vesicle aggregation was stronger under acidic conditions than under high Ca^{2+} conditions (pH 7). This finding led them to perform cryo-electron microscopy where they saw that under mildly acidic conditions ANXA2 appears to organize in a single protein layer while in the presence of Ca^{2+} (pH 7), two layers of ANXA2 protein form. The presence of two layers indicates face-to-face dimerization of ANXA2 molecules. The presence of differing protein arrangements was further supported by calculating that the amount ANXA2 required for half-maximal membrane aggregation under high Ca^{2+} conditions (3.1mM, pH 7) was approximately double (5.1 ± 0.2 $\mu g ml^{-1}$) the amount of ANXA2 required under acidic conditions (2.5 ± 0.2 $\mu g\ ml^{-1}$, pH 4). The degree of cooperativity was also found to be one molecules greater in the presence of Ca^{2+} (Hill number 0.90) than under acidic conditions (Hill number 0.34). Collectively, this data suggests that changes in the physiological conditions of a cell dictate the arrangement of ANXA2 molecules. By studying the nature of the conformational changes and organization of ANXA2 much can be learned about its functional role in various bodily functions (Zibouche et al., 2008).

The ability of ANXA2 to self-associate is controversial. There is still much that needs to be learned about how and why this occurs. In 1991, Zaks and Creutz studied annexin association using 90° light scattering and resonance energy transfer with an eosin–labeled acceptor annexin protein and a fluorescein–labeled donor annexin protein. Annexin IV, annexin VI, and annexin VII were studied. In solution, all of the annexins exhibited self-association in a calcium-dependent fashion that varied in reproducibility and consistency. When these proteins were bound to chromaffin granules (neuroendocrine cells found in the adrenal glands), self-association was more consistent and reproducible. Calcium levels of 10.0uM-31.6uM (pCa5.0-4.5) were studied. POPS and POPE-containing vesicles self-associated poorly compared to POPS and POPC-containing vesicles. At calcium concentrations less than 100uM (pCa 4), annexins VII and IV self-associated when bound to chromaffin granules while at higher calcium concentrations (more than pCa 4, 100uM), there was no self-association. Therefore at higher calcium concentrations it appears that ANX IV, VI, and VII binds membranes as a monomer, which is the exact opposite of Zibouche et al.(2008)'s findings, which suggests that ANXA2 binds membranes as a monomer at high calcium concentrations (Zaks & Creutz, 1991), which may be due to differences in the size of the N-terminal domain of each type of annexin protein.

In 2005, Patel et al. further found that annexin A5 and B12 associate strongly in the presence of anionic phospholipids (0.1mM) and calcium (0.5mM) but annexin A1 and A2 do not. These studies used 4nM ANXA2 labeled with acceptor dye (AlexaFluor 532 C5 Maleimide), 10nM ANXA2 labeled with donor dye (AlexaFluor 647 C5 Maleimide), anionic phospholipid vesicles (2:1 PS: PC), and HEPES buffer (20mM HEPES, pH 7.4). In some experiments, they observed small change in the acceptor of ANXA2 upon membrane binding likely due to chance interactions of a donor and acceptor bound to the same vesicle. The probability of these chance interactions occurring could be amplified by raising the concentration of ANXA2 in the interaction. Further research needs to be performed to further validate these findings as well as to uncover how the differing lengths and amino acid sequences of the N-terminal domain can interact with anionic phospholipids in vastly different manners (Patel et al., 2005).

4.4 Hypotheses and Goals

1. **To determine if ANXA2 self-associates in the presence and absence of lipid vesicles containing $PI_{(4,5)}P_2$, PS, and PC.**

This goal was designed to see if the addition of $PI_{(4,5)}P_2$will promote the self-association of ANXA2 upon lipid binding, as shown in Figure 4.4. I hypothesize that $PI_{(4,5)}P_2$will promote self-association upon membrane binding. As shown by Drucker et al. (2013), $PI_{(4,5)}P_2$ induces membrane indentations leading to the inward vesiculation of membrane domains, which could be assisted by the self-association of the N-terminal domains of adjacent ANXA2 molecules. It has previously been shown that ANXA2 should not self-associate when free in solution or in the absence of Ca^{2+} at neutral pH. Patel et al. (2005) found that the N-terminal domains of ANXA2 and ANXA1 self-associate poorly in response to vesicles containing POPS and POPC, but small amounts of interaction were detectable by FRET. These studies will be carried out by performing FRET experiments in a similar fashion to the experiments performed by Patel et al. (2005). As a result of these experiments it will be possible to further characterize how ANXA2 interacts with anionic phospholipids on membranes by determining the role of $PI_{(4,5)}P_2$in membrane trafficking by evaluating the self-association of ANXA2 in the presence of $PI_{(4,5)}P_2$.

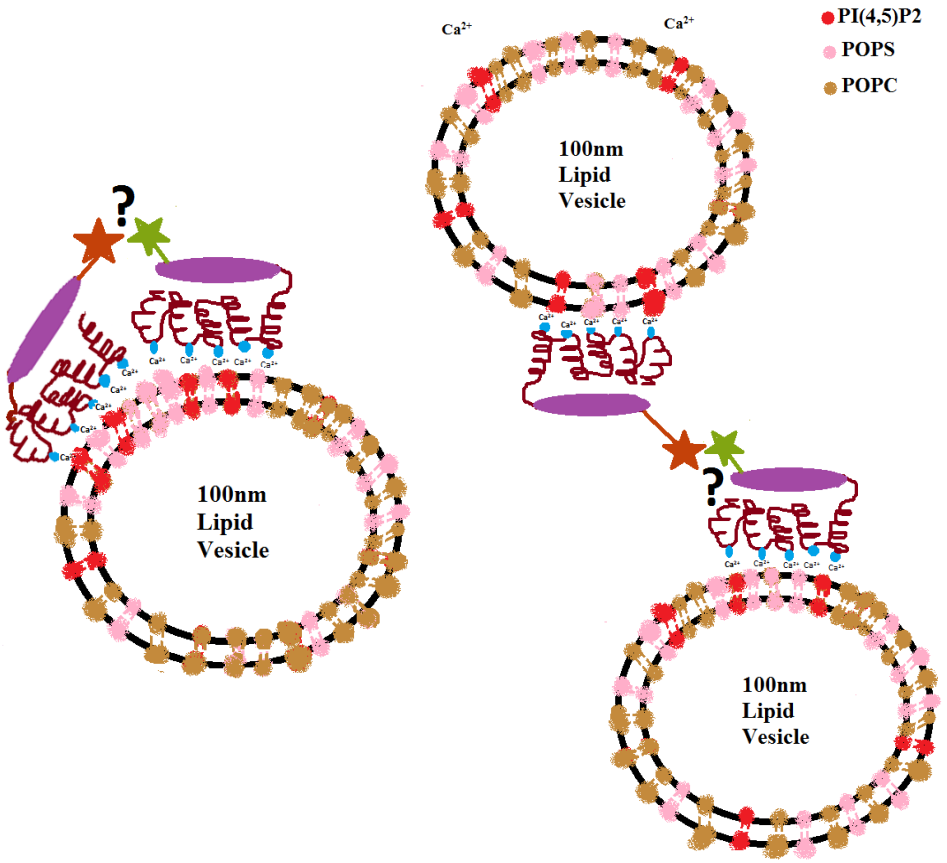

***Figure 4.4**: Predicted manners in which the N-terminally labeled cysteine residues of ANXA2 A488 and ANXA2 A568 can self-associate in the presence of anionic lipids*

2. To determine if altering the calcium concentration affects self-association.

In order to determine if ANXA2 self-association is promoted at high or low concentrations of Ca^{2+} ($CaCl_2$) Ca^{2+} titrations were performed at pH 7.4 into a solution containing 0.5uM acceptor, 2uM donor, and 0.5mM EGTA. I hypothesize that at high Ca^{2+} concentrations the rate of self-association will decrease. These experiments should indicate the role of self-association of ANXA2 upon membrane binding and the role of ANXA2 in the formation of membrane domains. This information could be used to predict the effects of increases or decreases in Ca^{2+} concentration *in vivo*, which could be helpful in assessing the role and mechanism of calcium signaling regulation in the interactions of ANXA2.

3. **To determine whether altering the concentrations and composition of anionic phospholipids affects the interaction of the N-terminal domains of ANXA2.**

This goal has two purposes. The first is to assess the effects of light scattering by lipid vesicles to determine whether or not the Ca^{2+} was causing the lipids to aggregate in such a way that it inhibited ANXA2 interactions with the membrane. This will be done by using differing ratios of PC and $PS/PI_{(4,5)}P_2$ which will have the same reaction conditions and volume. PC is a neutral phospholipid which does not bind ANXA2. Therefore, I hypothesize that there should be no FRET transfer with 100% PC vesicles and any decreases in donor excitation will be due to light scattering by lipids. This will serve as a control for assessing the validity of ANXA2 interactions.

The second purpose was due to findings by Patel et al. (2005) which suggested that high concentrations of ANXA2 can cause chance association of the N-terminal domain of two ANXA2 molecules. Therefore, it was necessary to use both low, medium, and high concentrations of lipids to interpret whether self-association was a chance occurrence or a reproducible phenomenon.

CHAPTER 5—METHODOLOGY

Chapter 5: Methodology begins by discussing ANXA2 WT plasmid preparation (Section 5.1). Section 5.2 describes the protein expression protocol. Section 5.3 outlines the steps necessary for ANXA2 WT purification. Section 5.4 describes how the protein was quantified, how the purity was assessed, and how the protein was stored. Section 5.5 explains how ANXA2 WT was concentrated and fluorescently labeled. Section 5.6 outlines how the FRET experiments were performed.

5.1 Plasmid Preparation

The ANXA2 WT DNA used in these experiments was inserted into a pSE420 vector, the vector map can be found in Appendix B (8.2). The DNA sequence of ANXA2 WT used in these experiments is PDB ID 1XJL. The DNA and protein sequence for ANXA2 WT can be found in Appendix C (8.3). In order to amplify the DNA for expression, 117 ng of ANXA2 WT DNA was transformed into TOP10F' super competent cells. The cells were regenerated by adding 350uL of SOB recovery media and the transformant was incubated at 37°C for 1hr on a rotator. 20uL of transformant was plated onto an LB-AMP plate (150mg/mL ampicillin). The plate was left overnight in a 37°C incubator. A single colony was inoculated into 4mL of LB broth containing 150mg/mL ampicillin and placed in the shaker (270rpm, 37°C) overnight. The culture was centrifuged at 11,000xg for 3 minutes using an accuSpin^{TM} 1R swing bucket rotor. The pellet was suspended in 600uL of autoclaved water. A Zippy maxi-prep plasmid purification kit was used to isolate and purify the plasmid DNA. The DNA concentration was measured using a Nanodrop and sent out for sequencing. The forward primers designed for sequencing was 5'GCTGGGAACCGACGAGGACT3' and the reverse primer was 5'TAGACTCTG TTAATTTCCTGCAGCTC 3.' The sequence alignment can be found in Appendix C (8.3).

5.2 Protein Expression

In order to express the protein, 237ng purified ANXA2WT plasmid DNA was transformed into BL21 super competent cells. The cells were regenerated by adding 350uL of SOB recovery media and the transformant was incubated at 37°C for 1hr on a rotator. The transformant was pipetted into a 100mL LB starter culture containing 150mg/mL ampicillin and was grown overnight in a shaker (250rpm, 37°C). The entire starter culture was added to a flask containing 900mL LB, 150mg/mL ampicillin and 200uL of antifoaming agent. The flask was placed into the shaker

(250rpm, 37°C) and incubated until it reached an OD of 0.7. At an OD of 0.7 the culture was induced with 1mM IPTG, incubated in the shaker for 3 hours (250rpm, 37°C), and chilled in the cold room for 30 minutes. The cell culture was centrifuged at 5,000xg for 10 minutes at 4°C. The supernatant was discarded and the pellets were resuspended in lysis buffer (50mM imidazole, 300mM NaCl, 10mM $MgCl_2$, 2mM DTT, 1 capsule Complete Protease Inhibitor EDTA-free, pH 7.4, 3 mL/g of wet pellet), and stored in -80°C.

5.3 Protein Purification

5.3.1 French Press

The ANXAT WT cell pellets (-80°C) were thawed in a hot water bath (37°C) and lysis buffer was added to a total volume of 40mL and placed on ice. The mixture was passed through the French press three times at 1,000 psi and then centrifuged at 30,000rpm in a Beckman Coulter Ultracentrifuge (1hr, 4°C). The supernatant was dialyzed overnight in the cold room in 3L of DE buffer (10mM imidazole, 10mM NaCl, 1mM EGTA, 2mM DTT, pH 7.4) at 4°C using 10,000MWCO SnakeSkin® Dialysis Tubing (3.7mL/cm). The DE buffer was replaced with an additional 3L of DE buffer and dialyzed for 2-3 hours.

5.3.2 DE Column

The GE Healthcare DEAE Sephacel column material (5mL in 4, 50mL conical tubes, 20mL total) was hydrated by adding 40mL of DE buffer and rocking at 4°C for 15 minutes. The tubes were centrifuged in an accuSpin™1R swing bucket rotor at 1,500xg for 2 minutes and the buffer was removed and 40mL of DE buffer was added. These steps were repeated three times and then the ANXA2WT protein was transferred from the dialysis tubing and aliquoted into the hydrated DE column material. The ANXA2 WT protein was incubated with the DE column material on the rocker in the cold room for 2 hours. The protein and column material was added to a column and left to settle for 30 minutes. The flow through was collected and then 40mL of DE buffer was passed through and collected ("wash" fraction). The flow through and wash fractions were centrifuged in the Beckman Coulter Ultracentrifuge at 30,000 rpm for1 hour at 4°C. The supernatant of the wash and flow through were placed into separate 10,000MWCO SnakeSkin® Dialysis Tubing (3.7mL/cm) and were dialyzed in the cold room overnight in 3L of CM buffer (20mM sodium acetate, 10mM NaCl, 1mM EGTA, 2mM DTT, pH 5.6). The buffer was replaced with an additional 3L of CM buffer once and allowed to dialyze for 2-3 hours.

5.3.3 CM Column

The Sigma Carboxymethyl Sepharose® (CM) column material (2.5mL in 6, 50mL conical tubes, 15mL total) was hydrated by adding 42.5mL of CM buffer and rocking at 4°C for 15 minutes. The tubes were centrifuged in an accuSpin^{TM}1R swing bucket rotor at 1500xg for 2 minutes and the buffer was removed and 42.5mL of CM buffer was added. These steps were repeated three times and then the ANXA2 WT wash and flow through fractions were transferred from the dialysis tubing and aliquoted into the hydrated CM column material (5mL column material for the wash and 10mL column material for the flow through). The ANXA2 WT protein was incubated with the CM column material on the rocker in the cold room for 2 hours. Two columns were set up, CM buffer was passed and the columns were stoppered. The flow through and column material was added to one column and the wash and column material to another. The columns were allowed to settle for 30 minutes. The flow through in each column was drained and 15mL of CM buffer was passed through each column twice. Then, 15mL of CM buffer containing an additional 100mM NaCl was passed three times through the column. The ANXA2 WT protein was eluted by passing 10mL of CM buffer containing an additional 600mM NaCl three times. Each 10mL fraction was collected separately.

5.4 Purity Assessment, Quantification of Protein Concentration, and Storage

A 15% denaturing SDS-PAGE gel was run with 20uL of sample and 5uL of 5x SDS running buffer. The gels were stained with Fairbanks staining (25% isopropanol, 10% acetic acid, 0.05% Coomassie R) and destained with a 10% acetic acid solution. The gel bands were sent out and assessed by mass spectrometry, as shown in Appendix D (8.4). Additionally, a Western Blot was performed. A 15% SDS-PAGE gel was ran with 20uL of sample and 5uL of 5x SDS running buffer and transferred onto a Thermo-Scientific Nitrocellulose Membrane (0.45micron, prod#88018) at 150mA for 1.5 hours. After washing the membrane in Millipore water, the membrane was incubated with the primary antibody, Cell Signaling Technology Annexin A2 (D11G2) Rabbit mAb (#8235), overnight on a rocker at 4°C. The primary antibody (10uL) was prepared in a 1X TBS (pH 7.4) solution containing 5% milk fat (10mL). The membrane was washed, by adding 1x TBS-Tween (pH 7.4) buffer to the membrane and rocking for 15 minutes at room temperature (3x). The secondary antibody was incubated with the membrane on the rocker at room temperature for 1 hour. The secondary antibody, Cell Signaling Technology Anti-rabbit goat IgG, was prepared in a 1x TBS-Tween solution containing 1% milk fat (10mL). The membrane was washed, by

adding 1x TBS-Tween buffer to the membrane and rocking for 15 minutes at room temperature (3x). The membrane was then washed in water. Clarity™ Western ECL Substrate (1mL, prod#170-5061) was added to the membrane and the membrane was scanned using a Bio-Rad Chemi-Doc XRS+.

A Malvern Instruments DLS (Dynamic Light Scattering) was used with Zetasizer® software to monitor protein aggregation. The samples were scanned using a low volume (50uL) quartz cuvette with a 3.00mm path length. A measurement angle of 173° was used.

For storage purposes, the protein was dialyzed into MES buffer (20mM MES, 150mM NaCl, 2mM DTT, 1mM NaN_3, pH 6.0) using 3-12mL 10,000MWCO Slide-A-Lyzer® dialysis cassettes (Prod#66810). The dialyzed protein was stored on ice in the cold room (4°C). For experiments, the ANXA2 WT protein was dialyzed into HEPES buffer (20mM HEPES, 150mM NaCl, pH 7.4).

The protein was concentrated to approximately 1mg/mL using 5mL Amicon® Ultra Centrifugal Filters, Ultracel®-10K. The filters were hydrated by adding 5mL of HEPES buffer and spinning the filters for 9 minutes at 2,000rcf in an accuSpin™ 1R swing bucket rotor. Then, 5mL of ANXA2 WT (5mL) was added to the filters and the protein was concentrated to 1mL in the accuSpin™ 1R swing bucket rotor at 2,500rcf for approximately 6 minutes. The protein concentration of the wash and flow through elution fractions was assessed using a NanoDrop at an absorbance of A280. The extinction coefficient (30,250 M^{-1} cm^{-1}) and the molecular weight (38,485Da) were used to calculate the protein concentration. Three samples of each protein were taken and the average value was used.

5.5 Fluorescent Labeling

Concentrated ANXA2 WT protein in HEPES buffer was separated into two 500mL fractions. Half of the protein was labeled overnight (4°C) with a 10x molar excess of AlexaFluor488 C5 Maleimide Dye and the other half was labeled overnight in a 10x molar excess of AlexaFluor568 C5 Maleimide Dye. The dye was quenched with a 10x molar excess of Sigma Aldrich® beta-mercaptoethanol for 20 minutes. Unlabeled dye was removed by dialyzing the protein in 100mL of HEPES buffer using 0.1-0.5 10,000MWCO Slide-A-Lyzer® dialysis cassettes (Prod#66383). The buffer was changed every 30 minutes for 4 hours. The degree of labeling and the protein concentration was assessed using the NanoDrop. The extinction coefficient (30,250 M^{-1} cm^{-1}) and the molecular weight (38,485Da) were used to calculate the protein concentration. Three samples

of each protein were taken and the average protein concentration was used. The samples were stored on ice at 4°C.

5.6 FRET

5.6.1 Spectrometer Settings

A F-4500 FL Fluorescence Spectrometer was used for these experiments. The excitation wavelength was set to 493nm. The emission wavelength was scanned from 500nm-750nm. The scan speed was 60nm/min and the PMT voltage was 950V. The response time used was 8sec, the cycle time was 5 minutes, and the delay time was 0 sec. The excitation and emission slits were 2.5nm and the reaction temperature was 20°C.

5.6.2 Sample Preparation

The samples were prepared in a low volume (50uL) quartz cuvette with a 3.00mm path length. The total sample volume was 60uL. Before each experiment the fluorescently labeled ANXA2 WT was scanned in the DLS to monitor protein aggregation. All experiments were performed in HEPES buffer.

5.6.2.1 Lipid Titrations

For all experiments, a starting concentration of 0.5mM $CaCl_2$ was used. The acceptor to donor concentration (0.5uM) was 4 to 1, 3 to 1, or 2 to 1. The lipid vesicles (0.3mM) were titrated in increments of either 2uL or 3uL.

5.6.2.2 Calcium Chloride Titrations

Starting concentrations of 0.5uM EGTA, 0.5uM donor, 2uM acceptor, and 75uM lipid were used. 10uM $CaCl_2$ solution was titrated in increments of either 2uL or 3uL.

5.6.3 Lipid Preparation

Lipid samples were prepared according to the Avanti website[3] and lipid concentration was verified by performing phosphate assays. The desired lipid composition and concentration was measured and the lipids were dried using a stream of nitrogen while gently heating the lipids on a hot plate. The lipid films were stored in a vacuum overnight, then resuspended in the experimental buffer (HEPES), vortexed, and extruded through a 100nm polycarbonate filter using an extrusion kit.

[3] https://avantilipids.com/

Lipid vesicle size distribution was verified using A Malvern Instruments DLS (Dynamic Light Scattering) with Zetasizer® software. The samples were scanned using a low volume (50uL) quartz cuvette with a 3.00mm path length at a temperature of 20ºC. The measurement angle was 173°, the count rate was 339.9kcps, and the measurement position was 4.20mm.

CHAPTER 6—RESULTS AND DISCUSSION

This chapter will begin by discussing the results of the ANXA2 purification (6.1). Then the following sections will discuss the results of the FRET titration experiments in order of the varying lipid compositions: 95% POPC 5% $PI_{(4,5)}P_2$ (6.2), 65% POPC 5% $PI_{(4,5)}P_2$30% POPS (6.3), 55% POPC 15% $PI_{(4,5)}P_2$30% POPS (6.4), and 85% POPC 15% $PI_{(4,5)}P_2$.

6.1 ANXA2 Purification and Quality Assessment

In order to study the interaction of the N-terminal domains of adjacent ANXA2 proteins, the ANXA2 wild type protein was expressed in BL21 bacterial cells which produced cell pellets of approximately 2.5g per 1L of culture. Approximately 7.5g of ANXA2 cell pellet were lysed and purified in order to eliminate cellular debris which could inhibit the specific activity of ANXA2. Purifying ANXA2 also improves the collisional efficiency of fluorescent labeling of the singular exposed cysteine residues on the N-terminal domain of ANXA2, leading to a better degree of labeling. Additionally, if ANXA2 were labeled immediately after lysis, the fluorescent signal in the FRET assays would be strongly diminished. ANXA2 purification resulted in a large band at approximately 32KDa, with greater than 95 % purity as shown by the denatured SDS-PAGE gel in Fig.6.1A. This band was lower than expected, accordingly a Western blot was performed, as shown in Fig. 6.1B, to ensure that the bands were ANXA2. The Western blot verified that the bands on the SDS-PAGE gel were ANXA2, which was further verified using mass spectroscopy as shown in Appendix D (8.1). Mass spectrometry was performed to verify that the small band beneath the ANXA2 band in the SDS-PAGE gel was not a protein which could have cysteine residues which could be labeled by the AlexaFluor dye. The band was found to be a small amount of *E.coli* contamination which would not affect the fluorescence experiments.

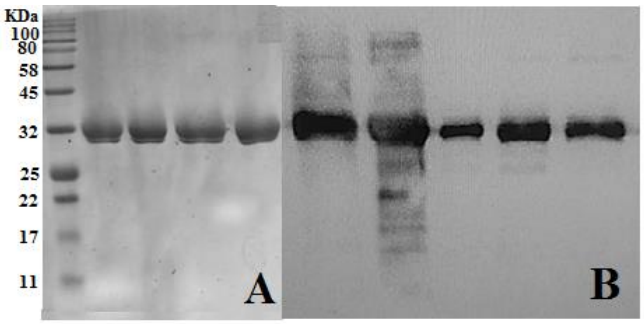

***Figure 6.1**: (A) Denatured SDS-PAGE Gel of ANXA2 Purification. Left to Right: 6 HEPES Buffer, CM Fraction 6 MES Buffer, CM Fraction 7 HEPES Buffer, CM Fraction 7 MES Buffer. (B) Western Blot after ANXA Purification. Left to Right: (1) French Press Flow through, (2) French Press pellet, (3) DE Flow Through,(4) CM Flow Through Fraction 6, (5) CM Wash Fraction 6.*

After ensuring that the ANXA2 was pure, the protein was concentrated to approximately 1.3mg/mL to improve the collisional efficiency of the ANXA2 protein with either the AlexaFluor C5 488 Maleimide dye or the AlexaFluor C5 568 Maleimide dye. The optimal protein concentration for protein labeling with this dye is 2mg/mL, but the ANXA2 protein has a propensity to aggregate at higher concentrations, therefore a lower protein concentration was favored to maintain the stability of the protein. The concentrated ANXA2 protein was then dialyzed against 20mM HEPES, 150mM NaCl, pH 7.4 buffer to remove the MES storage buffer which contains DTT and sodium azide which interfere with FRET experiments. After concentrating and dialyzing, the protein was labeled and the unreacted dye was deactivated and removed through dialysis. The degree of labeling was found to be 1.2 for the AlexaFluor C5 488 Maleimide-labeled ANXA2 and 0.44 for the AlexaFluor C5 568 Maleimide-labeled ANXA2. This degree of labeling was sufficient for experimentation.

Prior to experimentation, the ANXA2 A488 and the ANXA2 A568 proteins were assessed for aggregation using the Dynamic Light Scattering (DLS) Zetasizer software. According to the Malvern website, this software measures the size of a sample by measuring particle diffusion according to Brownian motion and converts this to a size distribution using the Stokes-Einstein relationship. The size of the ANXA2 A488 was approximately 5.7 nm and the size of the ANXA2 A568 was approximately 4.6nm, which indicated that the proteins were not aggregated as shown in Fig. 6.2 and Fig.6.3, respectively.

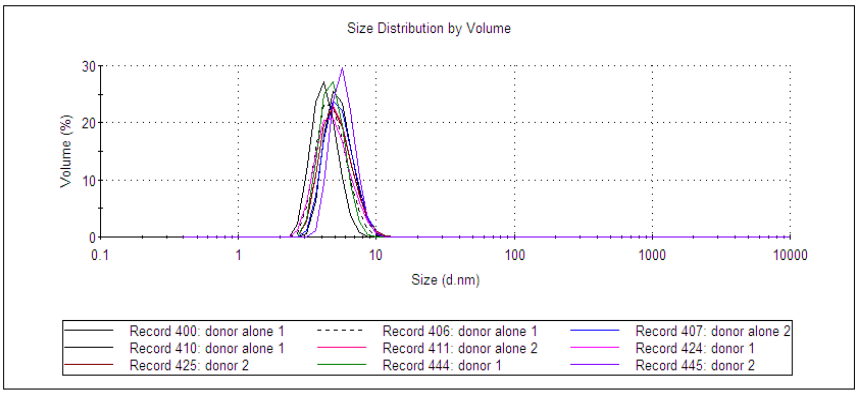

***Figure 6.2**: DLS Size Distribution by Volume of ANXA2 Fluorescently Labeled with the Donor AlexaFluor488 Prior to Experimentation. All of the donor ANXA2 used in these experiments had a singular peak with a size of approximately 5.7nm.*

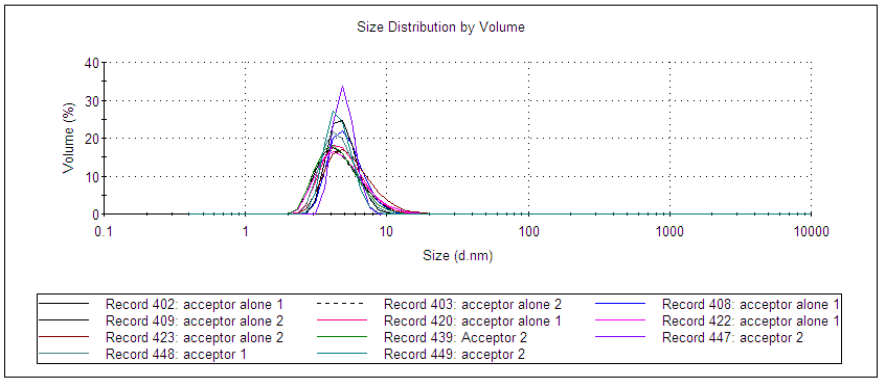

***Figure 6.3**: DLS Size Distribution by Volume of ANXA2 Fluorescently Labeled with the Acceptor AlexaFluor568 Prior to Experimentation. All of the acceptor ANXA2 used in these experiments had a singular peak with a size of approximately 4.6nm.*

The lipid vesicles used in these experiments were all size-verified using the DLS Zetasizer software in order to ensure that the extrusion kit produced vesicles of approximately 100nm. The lipid vesicles used in all experiments has a Z-average (d.nm) of 100±17 and were of good quality as shown in Fig. 6.4.

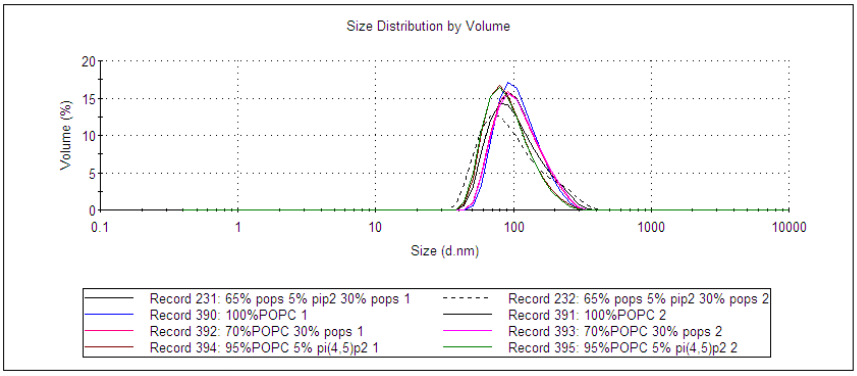

***Figure 6.4**: DLS Size Distribution by Volume of Lipid Vesicles after Extrusion. All of the lipid vesicles used in these experiments had a Z-Average (d.nm) of approximately 100 ± 17 and were of good quality according to the DLS Zetasizer software.*

6.2 FRET Experiments with 95% POPC, 5% $PI_{(4,5)}P_2$ Lipid Composition

In order to determine the role of $PI_{(4,5)}P_2$ in stimulating the association of the N-terminal domains of ANXA2, 95% POPC, 5% $PI_{(4,5)}P_2$was used in order to mimic the physiological ratio of $PI_{(4,5)}P_2$present at the inner leaflet of the plasma membrane. Varying ratios of ANXA2 acceptor (ANXA2 A5568) to donor (ANXA2 A488) were used to identify the optimal ratio for FRET interaction. Preliminary experiments were performed with 2 to 1 acceptor to donor concentrations using 100% POPC lipids and 70% POPC, 30% POPS lipids, but the acceptor band emitted poorly at 493nm excitation, therefore higher ratios were tried in these experiments (Appendix E, Section 8.5).

A donor alone experiment was performed as a control to ensure that the changes in donor fluorescence was due to FRET transfer and not a byproduct of light scattering by lipids, direct excitation or other aspects of the experimental setup. The donor alone titration had an average donor emission fluorescence intensity which was 90.5% of the fluorescence intensity of the donor emission at 493nm excitation prior to lipid addition; an overall 9.5% decrease in fluorescence intensity. Table 1 in Appendix F shows that in the Trial 1 donor alone experiment the average change in the fluorescence intensity of the donor emission was 89.5% (10.5% decrease), Trial 2 had an average change of 87.2% (12.8% decrease), and Trial 3 had an average change of 93.6% (6.4% decrease).

A graph of the dilution corrected emission spectra after each lipid addition for each trial as well as a graph in the changes in fluorescence intensity upon lipid addition can be found in Fig. 6.5. Increasing the lipid to protein ratio which can be found in Table 17 in Appendix G, did not lead to a steady decrease in the donor fluorescence which could have numerous causes. The fluctuation in fluorescence intensity may have resulted from the degree of mixing of the solution, which would alter whether or not aggregated proteins were at the bottom of the cuvette when the fluorescence emission was scanned.

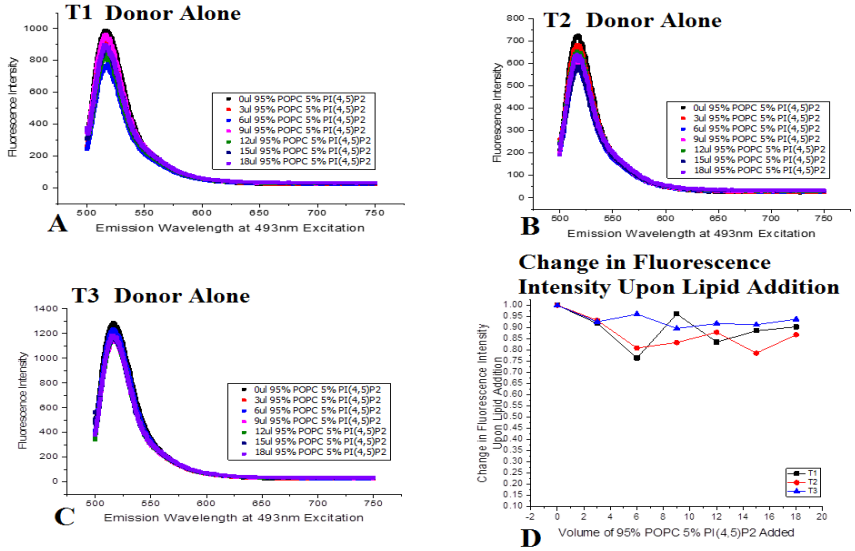

Figure 6.5: *95% POPC 5% $PI_{(4,5)}P_2$ Donor Alone Lipid Titration. Starting concentration: 0.5uM donor AlexaFluor 488 ANXA2 and 0.5mM CaCl2. The emission spectra were dilution corrected to better display changes in fluorescence intensity upon lipid addition. See Table 17 Appendix G for a summary of the different ratios of lipid to protein and the calcium concentration differences upon lipid addition. (A) T1- Change in Fluorescence intensity of the Emission Spectra Upon Lipid Addition (B) T2- Change in Fluorescence intensity of the Emission Spectra Upon Lipid Addition (C) T3- Change in Fluorescence intensity of the Emission Spectra Upon Lipid Addition (D)Change in Ratio of Fluorescence Intensity Upon Lipid Addition, all values for each trial were divided by the fluorescence intensity when there were no lipids present.*

The 3 to 1 ratio of acceptor to donor (2.0uM, 0.5uM), showed similar results to the donor alone graph with more variation in the change in the donor and acceptor emission at an excitation of 493nm. The average donor emission fluorescence intensity of the 3 to 1 acceptor donor was 92.5% of the fluorescence intensity of the donor emission at 493nm excitation prior to lipid addition; an overall 7.5% decrease in fluorescence intensity; which is a slightly smaller decrease in the donor emission fluorescence intensity compared to the donor alone average decrease of 9.5% indicating that no FRET transfer occurred. Table 2 in Appendix F shows that in the Trial 1 the average change in the fluorescence intensity of the donor emission was 97.6% (2.4% decrease) and Trial 2 had an average change of 92.8% (7.2% decrease). The 3 to 1 experiment likely had a smaller decrease in the fluorescence intensity of the donor emission because there was a smaller lipid to protein ratio (Table 18 Appendix G) because there was more ANXA2 present in the system.

The change in acceptor emission upon lipid addition were also recorded in Table 2 Appendix F to show if the changes in fluorescence intensity were a result of the conditions of the experiment or whether actual FRET transfer was occurring. As evidenced by the graph of the change in fluorescence intensity upon lipid addition in Fig. 6.6, it appears that the acceptor and donor emissions for each trial follow similar patterns of increases and decreases upon lipid addition. If FRET transfer were occurring the acceptor emission should increase while the donor emission decreases. These changes are likely a result of variations in mixing which alters which labeled ANXA2 proteins are aggregated at the bottom of the solution and which ANXA2 protein's signals are being clouded by the lipids.

Interestingly, it appears that the ANXA2 A568 acceptor protein slightly increased in fluorescence intensity, with the average ratio of the change of the acceptor emission being 104% (4% increase) in both trials, as shown in Table 2 Appendix F, indicating that lipid scattering effects lowers the donor emission while increasing the acceptor emission. An acceptor alone trial will need to be performed in the future in order to further verify this difference.

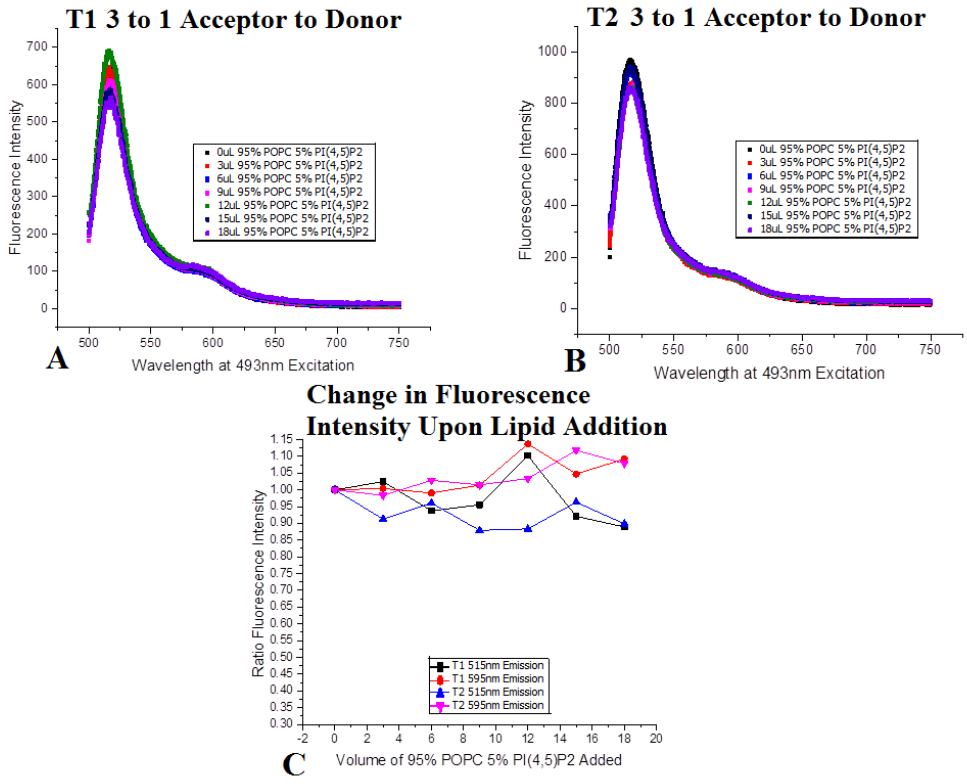

Figure 6.6: *95% POPC 5% $PI_{(4,5)}P_2$ 3 to 1 Acceptor to Donor Lipid Titration. Starting concentration: 0.5uM donor AlexaFluor 488 ANXA2, 1.5uM acceptor AlexaFluor 568 ANXA2, and 0.5mM CaCl2. The emission spectra were dilution corrected to better display changes in fluorescence intensity upon lipid addition. See Table 18 Appendix G for a summary of the different ratios of lipid to protein and the calcium concentration differences upon lipid addition. (A) T1- Change in Fluorescence intensity of the Emission Spectra Upon Lipid Addition (B) T2- Change in Fluorescence intensity of the Emission Spectra Upon Lipid Addition (C) Change in Ratio of Fluorescence Intensity Upon Lipid Addition, all values for each trial were divided by the fluorescence intensity when there were no lipids present.*

The ratio of acceptor to donor ANXA2 was further raised to 4 to 1 (2.0uM, 0.5uM), as shown in Table 19 Appendix G, in order to further diminish the lipid to protein ratio to see if this would raise the chance that the ANXA2 A488 and ANXA2 A568 would interact with each other when there are no accessible anionic lipid binding sites for it to bind to. In this system, the fluorescence intensity of the donor emission was lower than the 3 to 1 acceptor to donor experiments and the donor alone experiments, as shown in Fig. 6.7. The average change in donor emission fluorescence intensity was 71.2% of the starting fluorescence intensity, with the donor emission fluorescence intensity decreasing 39% immediately upon adding 14.29uM 95% POPC 5% $PI_{(4,5)}P_2$ to the solution (Table 3, Appendix F). This difference suggested that a FRET transfer may have occurred, but the acceptor ANXA2 A568 emission fluorescence intensity only increases approximately 8%, as shown in Table 3 Appendix F, which is not consistent with a 39% decrease in the donor

intensity. Inconsistencies in FRET transfer may be due to the nature of the spectral overlap, thus a different donor/acceptor pair with a larger Forster distance should be used in the future.

There is little change in the fluorescence intensity after the first lipid addition, which suggests that by chance, there may have been a lot of $PI_{(4,5)}P_2$ in the first lipid addition and not in the subsequent additions. If there was enough $PI_{(4,5)}P_2$it is possible that all of the donor ANXA2 A88 was bound to the membrane in such a manner that they could no longer interact with the acceptor ANXA2 A568. In the future, more trials of the 4 to 1 acceptor to donor 95% POPC 5% $PI_{(4,5)}P_2$ should be performed to see if these findings are consistent.

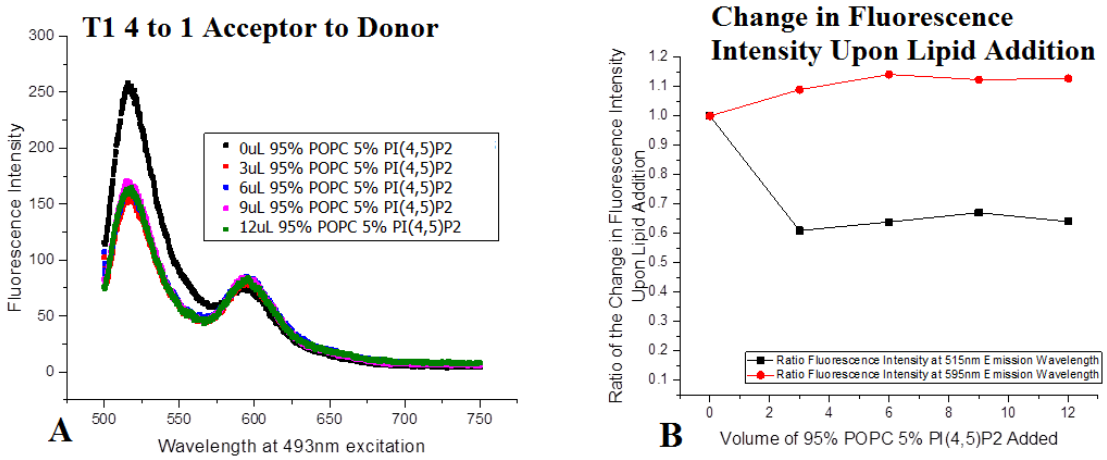

Figure 6.7: *95% POPC 5% $PI_{(4,5)}P_2$ 4 to 1 Acceptor to Donor Lipid Titration. Starting concentration: 0.5uM donor AlexaFluor 488 ANXA2, 2.0uM acceptor AlexaFluor 568 ANXA2, and 0.5mM CaCl2. The emission spectra were dilution corrected to better display changes in fluorescence intensity upon lipid addition. See Table 19 Appendix G for a summary of the different ratios of lipid to protein and the calcium concentration differences upon lipid addition. (A) T1- Change in Fluorescence intensity of the Emission Spectra Upon Lipid Addition (B) Change in Ratio of Fluorescence Intensity Upon Lipid Addition, all values for each trial were divided by the fluorescence intensity when there were no lipids present.*

At the end of each of the 95% POPC 5% $PI_{(4,5)}P_2$FRET titrations experiments, the DLS Zetasizer was used to monitor aggregation in the solution. There was minimal lipid aggregation which could alter the FRET signal by affecting lipid scattering as indicated by using the DLS Zetasizer data in Fig. 6.8. There were two peaks, one at approximately 130nm which comprises 88.3% of the samples and the other at approximately 4800nm which is 11.7% of the solution. The 130nm peak was likely the lipid peak and the 4800nm peak was likely the aggregated lipid and ANXA2 protein. This indicated that although high concentrations of calcium chloride (0.384mM-0.5mM, factoring in the dilution caused by lipid addition) were used in these experiments, which can cause $PI_{(4,5)}P_2$containing vesicles to aggregate by altering electrostatic interactions (Ellenbroek et al.,

2011) and can facilitate ANXA2-mediated aggregation of membrane containing anionic phospholipids (Gerke & Moss, 2002), the concentrations of $PI_{(4,5)}P_2$ was low enough that it did not overly cloud the system.

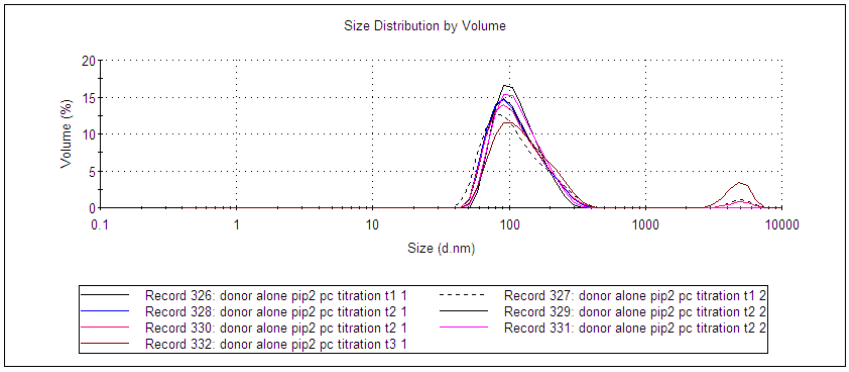

***Figure 6.8**: DLS Size Distribution by Volume of the ANXA2 Labeled with AlexaFluor 488 and ANXA2 Labeled with AlexaFluor 568 after titration with 95% POPC 5% $PI_{(4,5)}P_2$.*

6.3 FRET Experiments with 65% POPC, 5% $PI_{(4,5)}P_2$, 30% POPS Lipid Composition

After performing the 95% POPC 5% $PI_{(4,5)}P_2$FRET assays, POPS was added to the vesicles to see if this would effect ANXA2 self-association at the N-terminal domain. Previously, Patel et al. (2005), indicated that the N-terminal domain of ANXA1 and ANXA2 cannot self-associate in the presence of POPS unless their core domains are swapped with annexin proteins with a known propensity to self-associate, such as ANXA5 and ANXB12. Even so, Patel et al. (2005) occasionally detected small amounts of FRET transfer with wild type ANXA2. For the 4 to 1 acceptor to donor ANXA2 ratio and 95% POPC, 5% $PI_{(4,5)}P_2$vesicles, only small amounts of possible FRET transfer was observed. Both systems suggested a similarly low propensity for self-association, but adding POPS to the $PI_{(4,5)}P_2$system may cooperatively assist self-association by improving membrane binding by ANXA2. In 2013, Drucker et al. found that ANXA2 binds cooperatively to membranes containing $PI_{(4,5)}P_2$, POPS, and cholesterol using a quartz crystal microbalance (QCM).

In order to determine this, a 4 to 1 acceptor to donor FRET lipid titration experiment was performed using 65% POPC, 5% $PI_{(4,5)}P_2$, and 30% POPS. The physiological mol concentration of POPS in the inner leaflet of the plasma membrane is approximately 30%. Donor alone control titrations was performed to determine the baseline change in fluorescence transfer due to lipid scattering and other factors which could alter the fluorescence intensity of the donor emission. The donor alone experiments highlighted an average decrease in fluorescence intensity of the donor emission

compared to the donor emission before lipid addition of 6.4% (fluorescence intensity which is 93.6% of the fluorescence intensity without lipid). The changes in fluorescence intensity upon lipid addition is graphed in Fig. 6.9 and the actual numerical values can be found in Table 4 and 5, Appendix F. In the 4 to 1 acceptor to donor trials, the alterations in donor and acceptor emissions varied per trial and there was no significant alteration in fluorescence intensity which would suggests that FRET transfer occurred.

By evaluating the change in the acceptor emission in the donor alone graph, upon lipid addition when no acceptor was present, it was possible to see the natural fluctuations in the acceptor peak, as shown in Table 5, Appendix F. This evaluation made it appear that the reduction in the donor emission fluorescence intensity upon lipid addition was not due to FRET transfer. The clearest indication that FRET transfer did not occur was indicated by Fig. 6.9E which divides the 4 to 1 acceptor to donor fluorescence intensities of the donor emission by the donor alone emission which produced relatively flat lines around 1.0, indicating that the values of each are roughly the same. A more detailed evaluation showing how lipid addition altered the lipid to protein ratio, the calcium concentration, and the concentrations of acceptor ANXA2 A568 and ANXA2 A488 can be found in Tables 20-21, Appendix G.

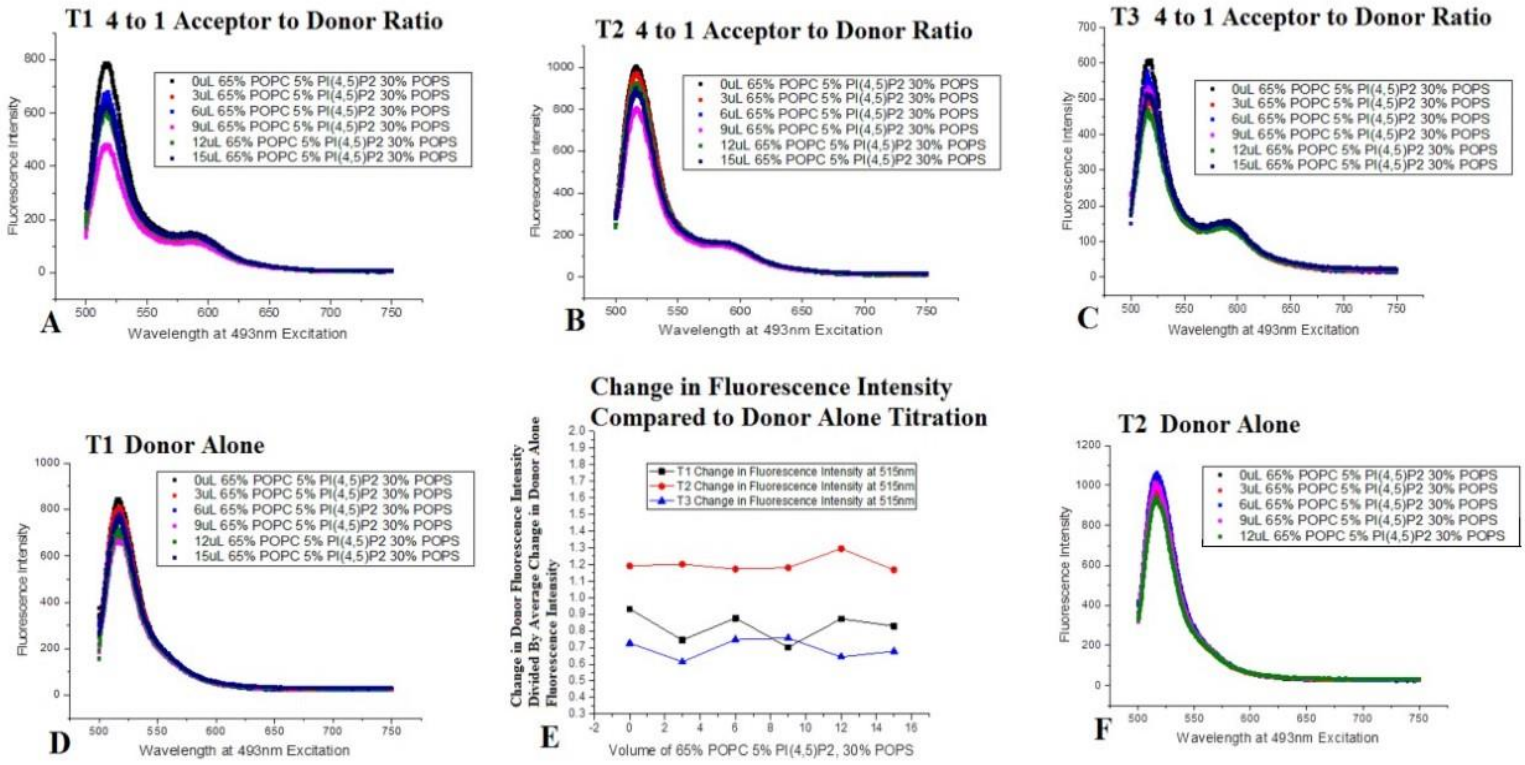

Figure 6.9: *65% POPC 5% $PI_{(4,5)}P_2$ 30% POPS 4 to 1 Acceptor to Donor Lipid Titration. Starting concentration: 0.5uM donor AlexaFluor 488 ANXA2, 2.0uM acceptor AlexaFluor 568 ANXA2, 0.5mM starting calcium chloride concentration. The emission spectra were dilution corrected to better display changes in fluorescence intensity upon lipid addition. See Tables 20-21 Appendix G for a summary of the different ratios of lipid to protein and the calcium concentration differences upon lipid addition. (A-C, D, F) Change in fluorescence intensity emission spectra upon lipid addition divided by fluorescence intensity prior to lipid addition (E) Change in fluorescence intensity of the donor emission of the 4 to 1 acceptor to donor experiment divided by the donor emission of the T1 donor alone experiment.*

The lack of observed FRET transfer may be due to an increased amount of protein and lipid aggregation making it difficult to detect changes in fluorescence. At the end of each of the 65% POPC, 5% $PI_{(4,5)}P_2$, 30% POPS FRET titrations experiments, the DLS Zetasizer was used to monitor aggregation in the solution. The entire solution was aggregated. Most trials had two broad peaks at 1489nm (97.3%) and 5384nm (2.7%), as shown in Fig. 6.10. If FRET transfer had occurred it would have been negligible because although the donor emission should was lower while the acceptor emission remained constant, the changes did not vary enough from the donor alone emission graphs.

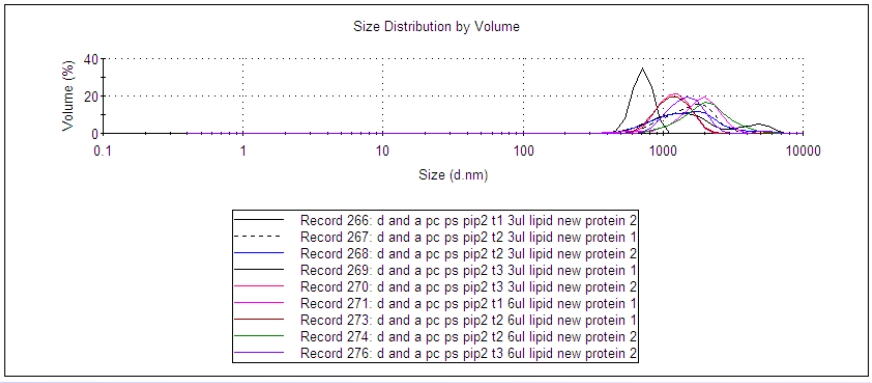

Figure 6.10: *Size Distribution by Volume of the ANXA2 WT AlexaFluor 488 and AlexaFluor 568 after titration with 65% POPC 5% $PI_{(4,5)}P_2$ 30% POPS.*

6.4 FRET Experiments with 55% POPC, 15% $PI_{(4,5)}P_2$, 30% POPS Lipid Composition

In order to try to promote a FRET interaction, the percentage of $PI_{(4,5)}P_2$used to make the lipid films was raised to 15%, while maintaining the 4 to 1 acceptor to donor concentration ratio used in the previous experiments. Additionally, the calcium chloride was titrated instead of the lipids to determine whether lower calcium concentrations would promote a FRET interaction by lowering the amount of light scattering by lipids by reducing the amount of calcium available to promote aggregation. This was done by adding 0.5mM EGTA, which has a high affinity for chelating Ca^{2+}, thus it removes any Ca^{2+} ions present in the solution, ensuring that the only Ca^{2+} ions present in the solution was the 10mM $CaCl_2$ titrated into the solution.

Using Stanford's Maxchelator, the amount of free calcium present in solution was calculated using a temperature of 20°C, pH 7.4, and an ionic concentration of 0.15M. After adding the first 4uL of 10mM $CaCl_2$ to the titration there was 625uM of total $CaCl_2$ in solution, approximately 468.77uM was bound and 156.22uM was free in solution. When 6uL of 10mM $CaCl_2$ was added to the titration there was 909uM of total $CaCl_2$ in solution, approximately 453.95uM was bound and 455.04uM was free in solution. Adding 8uL 10mM CaCl2 resulted in 1176uM (1.176mM) of total $CaCl_2$ in solution, approximately 441.00uM was bound and 735.02uM was free in solution. 10uL 10mM $CaCl_2$ resulted in 1,429uM (1.429mM) of total $CaCl_2$ in solution, approximately 429.00uM was bound and 1,000uM (1mM) was free in solution. 12uL 10mM $CaCl_2$ resulted in 1,667uM (1.667mM) of total $CaCl_2$ in solution, approximately 417.00uM was bound and 1,250.00uM (1.250mM) was free in solution. Finally, 14uL 10mM $CaCl_2$ resulted in 1,892uM (1.892mM) of total $CaCl_2$ in solution, approximately 405.00uM was bound and 1487.00uM (1.487mM) was free in solution. Thus overall in these experiments the concentration of free Ca^{2+} ions ranged from 0uM-1.487mM, and after the first 6uL of 10mM $CaCl_2$ was added, the concentration of free Ca^{2+} ions was higher than in the previous experiments of approximately 0.5mM $CaCl_2$ throughout the titration. Tables 22 and 23 in Appendix G, will show the exact $CaCl_2$, EGTA, donor, acceptor, and lipid concentrations used in these experiments.

These experiments further verified that no FRET transfer was occurring, as indicated by the dilution corrected graphs of the change in fluorescence intensity of the emission spectra upon $CaCl_2$ addition in Fig. 6.11, below. These titrations appeared to minimize lipid scattering, producing a flat line when dividing the fluorescence intensity of the donor emission upon $CaCl_2$ addition by the fluorescence intensity of the donor emission prior to $CaCl_2$ addition (Fig.6.11D). The values plotted in Fig. 6.11D can be found in Tables 7 and 8, Appendix F. T1 saw the highest decrease in donor emission which was on average 88.5% of the donor emission prior to $CaCl_2$ addition, an 11.5% overall decrease in fluorescence intensity of the donor emission, while the acceptor emission experienced a decrease of approximately 5%, suggesting that this change was not due to FRET transfer.

By averaging all the trials, the change in fluorescence intensity of the donor emission showed a 1% increase in the fluorescence intensity of the donor emission compared to the fluorescence intensity before $CaCl_2$ addition, and the acceptor emission experienced a 2% increase. The donor

alone titration, saw an average increase of approximately 9% in the donor emission fluorescence intensity and the acceptor emission has an 11% increase, which suggests that initially adding 75uM 55% POPC 15% $PI_{(4,5)}P_2$, 30% POPS as the calcium aggregates the lipids this somehow makes the ANXA2 fluorophores more visible when the solution is scanned, likely because the aggregated lipid is sinking to the bottom of the cuvette. By definition, the ANXA2 protein should facilitate this aggregation process and it should also sink to the bottom of the cuvette. Thus, it seems, that the aggregated vesicles have the ANXA2 bound to them, with the N-terminal domains facing outwards, and the cuvette was mixed enough prior to the scan, allowing the aggregated protein to be scanned while the ANXA2 is still floating in the aqueous phase didn't sink. Additionally, decreasing the lipid to protein ratio from 30 to 15.6 throughout the titration, would make the fluorescently labeled ANXA2 more visible.

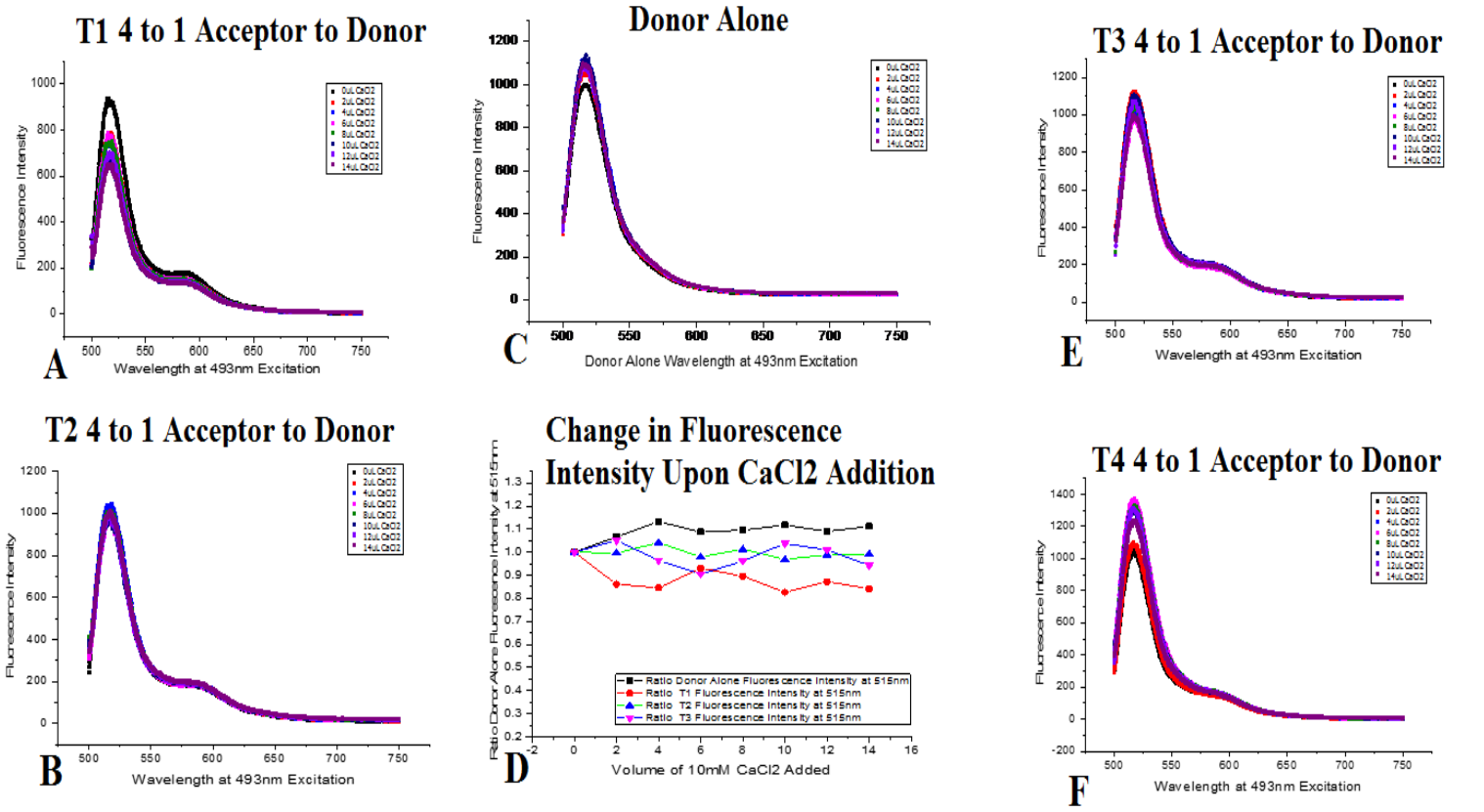

Figure 6.11: *55% POPC 15% PI(4,5)P2 30% POPS 4 to 1 Acceptor to Donor Calcium Chloride Titration. Starting concentration: 0.5uM donor AlexaFluor 488 ANXA2, 2.0uM acceptor AlexaFluor 568 ANXA2, 0.5mM EGTA. The emission spectra were dilution corrected to better display changes in fluorescence intensity upon lipid addition. See Tables 22 and 23 Appendix G for a summary of the different ratios of lipid to protein and the EGTA concentration alterations upon calcium chloride addition. (A-C, E-F) Change in the fluorescence intensity of the emission spectra upon CaCl2 addition (D) Change in the fluorescence intensity of the donor emission of the 4 to 1 acceptor to donoe experiments upon CaCl2 addition divided by the donor emission prior to CaCl2 emission*

In order to better monitor the presence of lipid and ANXA2 aggregation, at the end of each titration the sample was scanned with the DLS using the Zetasizer software as shown in Fig. 6.12, below. There were two peaks the lipid peak was 109.7nm and it made up 55.20% of the solution and the aggregation peak was 2138nm and comprised 44.8% of the solution, thus about half of the solution was aggregated. The aggregation level is higher than the 95% POPC, 5% $PI_{(4,5)}P_2$ trial but much less than the 65% POPC, 5% $PI_{(4,5)}P_2$, 30% POPS trial. The lowered presence of aggregation upon increasing the concentration of $PI_{(4,5)}P_2$, suggested that the signal was less affected by light scattering produced by lipids.

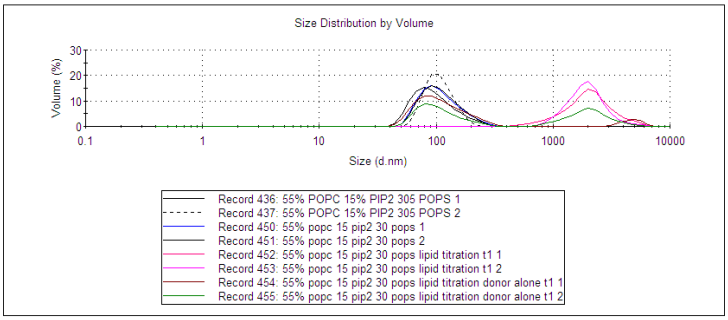

***Figure 6.12**: Size Distribution by Volume of the ANXA2 WT AlexaFluor 488 and AlexaFluor 568 after titration with 55% POPC 15% $PI_{(4,5)}P_2$ 30% POPS.*

6.5 FRET Experiments with 85% POPC, 15% $PI_{(4,5)}P_2$ Lipid Composition

In order to further see how $PI_{(4,5)}P_2$affected FRET transfer, the next series of experiments remove POPC from the system while maintaining an elevated level of $PI_{(4,5)}P_2$ (85% POPC 15% $PI_{(4,5)}P_2$) and the 4 to 1 ANXA2 acceptor to donor concentration. Lipid and $CaCl_2$ titrations were performed in order to compare the results from each. The $CaCl_2$ titration used the same range of free Ca^{2+} ions (0uM-1.487mM) as the 55% POPC 15% $PI_{(4,5)}P_2$, 30% POPS $CaCl_2$ titration. The exact concentrations of lipid, acceptor ANXA2, donor ANXA2, EGTA, and calcium, as well as the lipid to protein ratio can be found in Table 24-25 Appendix G for the $CaCl_2$ titration and Table 26-27 Appendix G for the lipid titration.

The $CaCl_2$ titration bore similar results to the 65% POPC 5% $PI_{(4,5)}P_2$, 30% POPS $CaCl_2$ titration. The first trial showed the strongest decrease in the donor emission upon $CaCl_2$ addition. The biggest decrease (approximately 24% lowered fluorescence intensity of the donor emission), displayed in Table 9) occurred in Trial 1 and the donor alone emissions when 8uL 10mM $CaCl_2$ was added which resulted in a total $CaCl_2$ concentration of 1,176uM (1.176mM) with approximately 441.00uM was bound and 735.02uM was free in solution. In order to best show that there was no FRET transfer occurring, the donor emission of the 4 to 1 acceptor to donor titration trials upon $CaCl_2$ addition was divided by the donor alone donor emission upon $CaCl_2$ addition, as shown in Fig. 6.13, the tabulated values for this graph can be found in Table 10. Trial 2 and 3 yielded flat lines around 1, indicating no FRET transfer occurred while Trial 1 had a small increase in slope between 4uL $CaCl_2$ addition and 8uL, because these numbers are smaller than 1, there is a small decrease in the donor emission intensity at this location. This decrease falls around the time when the $CaCl_2$ has fully bound the EGTA and is free in solution indicating that in some trials FRET transfer may have occurred. If FRET transfer occurred, the acceptor emission should have

increased noticeably, which it did not according to the graphs of the changes in the fluorescence intensity of the donor emission upon $CaCl_2$ addition, Fig13A-C, therefore the light scattering by the lipids may influence the acceptor emission, or the FRET transfer is very transient and the scan speed was too slow (60nm/min) to register the FRET transfer.

The 85% POPC 15% $PI_{(4,5)}P_2$ lipid titration further supported the belief that FRET transfer is not occurring. In this experiment the increase in lipid volume appears to have lowered the fluorescence intensity signal of the donor emission as shown in Fig.6.13E. In viewing the DLS data with the

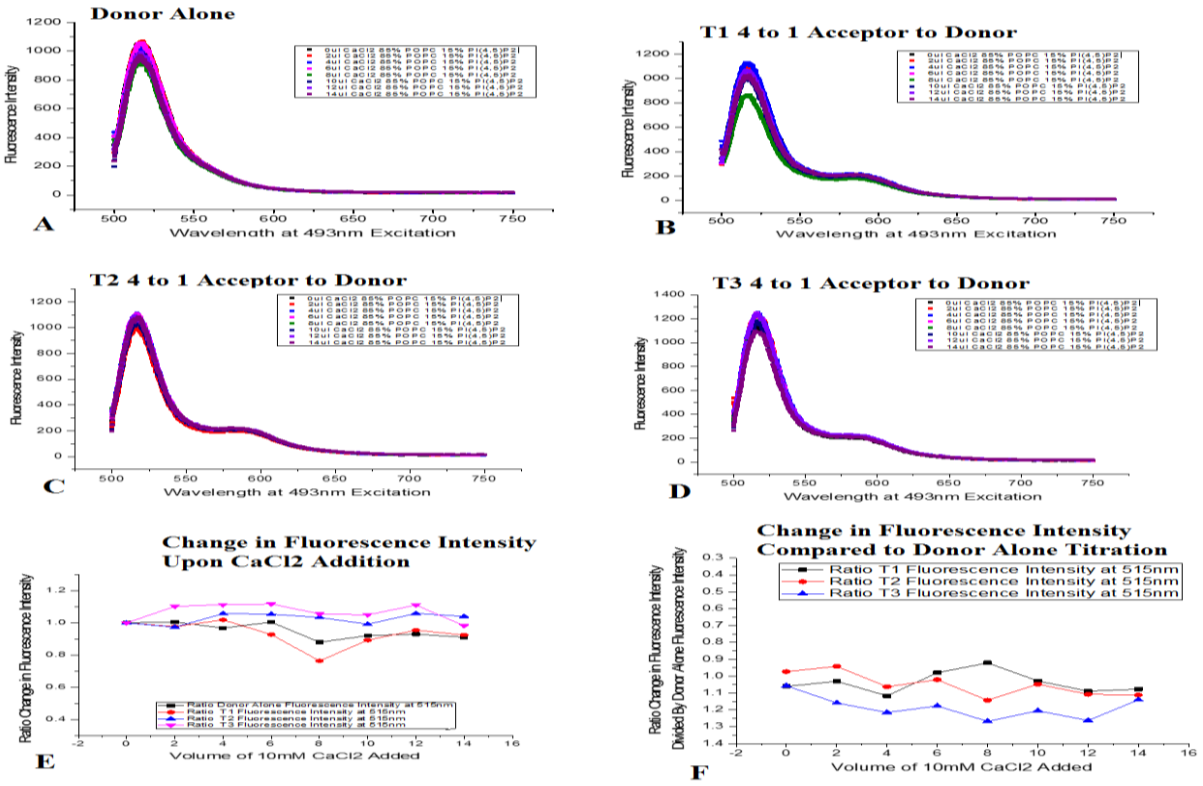

Figure 6.13: *85% POPC 15% PI(4,5)P2 4 to 1 Acceptor to Donor Calcium Chloride Titration. Starting concentration: 0.5uM donor AlexaFluor 488 ANXA2, 2.0uM acceptor AlexaFluor 568 ANXA2, 0.5mM EGTA. The emission spectra were dilution corrected to better display changes in fluorescence intensity upon lipid addition. See Tables 24-25 Appendix G for a summary of the different ratios of lipid to protein and the EGTA concentration alterations upon calcium chloride addition. (A-D) Change in the fluorescence intensity of the emission spectra upon CaCl2 addition (E) Change in the fluorescence intensity of the donor emission of the 4 to 1 acceptor to donor experiments upon CaCl2 addition divided by the donor emission prior to CaCl2 emission (F) Change in the fluorescence intensity of the donor emission of the 4 to 1 acceptor to donor experiments upon CaCl2 addition divided by the donor emission of the donor alone experiments.*

Zetasizer software (Fig. 6.14) to monitor aggregation after each titration, there were numerous peaks and high amounts of aggregation. In one trial, the lipid peak ran high at 151nm and it comprised 9.7% of the solution, 77% of the solution was aggregated in 1,740nm clusters, and the remaining 3.2% of the solution aggregated in giant 5,225nm clumps. It is highly likely that the

aggregation will cause bigger particle size over time. This discovery supports the belief that light scattering by lipids caused the steady decrease in donor fluorescence. It was originally expected that increasing the $PI_{(4,5)}P_2$ would produce two clear peaks (lipid and aggregation) as observed in the 95% POPC 5% $PI_{(4,5)}P_2$ graph, instead it appears that the presence of a high enough concentration of either $PI_{(4,5)}P_2$of POPS will produce high amounts of aggregation regardless of lipid type.

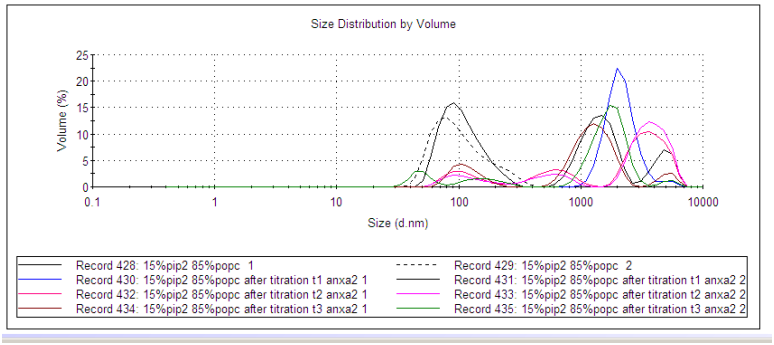

***Figure 6.14**: Size Distribution by Volume of the ANXA2 WT AlexaFluor 488 and AlexaFluor 568 after titration with 85% POPC 15% $PI_{(4,5)}P_2$*

The lowered donor emission fluorescence signal appears to directly correlate with the increase in lipid vesicle concentration. Fig. 6.15A, C and D and the acceptor emission peak does not decrease as significantly compared to the donor emission suggesting that FRET transfer may be occurring. If FRET transfer is taking place the signal is low. The donor alone emission fluorescence intensity decreased an average of 82% of the donor emission signal prior to lipid addition (18% less fluorescence), with the lowest decrease in signal (65% 35% less fluorescence) occurring when 18uL of 85% POPC, 5% $PI_{(4,5)}P_2$ (69.23uM, Table 26 Appendix G), as shown in Table 11. Similarly, Trial 1 experienced an average decrease in the donor emission fluorescence intensity divided by the donor emission fluorescence intensity prior to lipid addition of approximately 79% (21% less fluorescence) with the lowest decrease in signal (63%, 37% less fluorescence) occurring when 15uL of 85% POPC, 5% $PI_{(4,5)}P_2$ (60.0uM, Table 27 Appendix G). Therefore, it seems that about 3% of the decrease in fluorescence intensity could have resulted from a FRET transfer, which is a very low possibility.

Trial 2 experienced an average decrease in the donor emission fluorescence intensity divided by the donor emission fluorescence intensity prior to lipid addition of approximately 80.5% (19.5% less fluorescence) with the lowest decrease in signal (65%, 35% less fluorescence) occurring when

18uL of 85% POPC, 15% $PI_{(4,5)}P_2$ (69.23uM, Table 27 Appendix G), as shown in Table 11. This graph is very similar to the donor alone graph and T1. The graph of the 4 to 1 acceptor to donor trials donor emission divided by the donor alone fluorescence intensity in Fig. 6.15F, indicated the unlikely possibility of FRET transfer because these graphs should have had a decreasing slope if FRET transfer is occurring, because values higher than 1 indicate that the 4 to 1 trial had a higher fluorescence emission than the donor alone graph.

Thus Trial 3, which shows a flat line with an increase in slope towards the end of the titration likely did not experience FRET transfer. These findings seem to contradict the 4 to 1 acceptor to donor lipid titration with 95% POPC and 5% $PI_{(4,5)}P_2$which suggests that FRET transfer does occur. Even so, both experiments show decreases in the donor emission fluorescence intensity of approximately 30%. The 95% POPC 5% $PI_{(4,5)}P_2$trial showed an immediate decrease of 39% in donor fluorescence (Table 3) and then the fluorescence intensity leveled out suggesting that the donor had been quenched immediately. This difference is likely because the 95% POPC 5% $PI_{(4,5)}P_2$trial had a acceptor concentration of 1uM and a donor concentration of 0.25uM while the 85% POPC, 15% $PI_{(4,5)}P_2$ trial had an acceptor concentration of 2.0uM and a donor concentration of 0.5uM. Therefore, the lipid to protein ratio was higher in the 95% POPC 5% $PI_{(4,5)}P_2$trial and donor quenching may have occurred faster and was thus easier to detect. In the future, lower concentrations of acceptor and donor should be used to monitor this difference.

In 2005, Patel et al. found that at high ANXA2 concentrations the likelihood of chance co-localization increases, which can give the false appearance of FRET transfer. There is also a possibility that FRET transfer is not occurring and the donor fluorophore may be burying itself in the membrane. In 2008, Zibouche et al. observed FRET transfer between the fluorescently labeled the N-terminal domain of ANXA2 and fluorescently labeled phospholipids (POPS/POPC), which suggests that there is a direct interaction between ANXA2 and anionic phospholipids. Zibouche et al. (2008) also observed interactions between neighboring annexins, which suggests that there may be mixed roles for the N-terminal domain depending on how many ANXA2 molecules are able to bind to the anionic phospholipids. The acceptor (ANXA2 568) may not experience a similar decrease in fluorescence intensity because the acceptor is bigger (880.92g/mol) than the donor

(720.66g/mol) and it may alter the properties of ANXA2, preventing it from burying itself in the membrane.

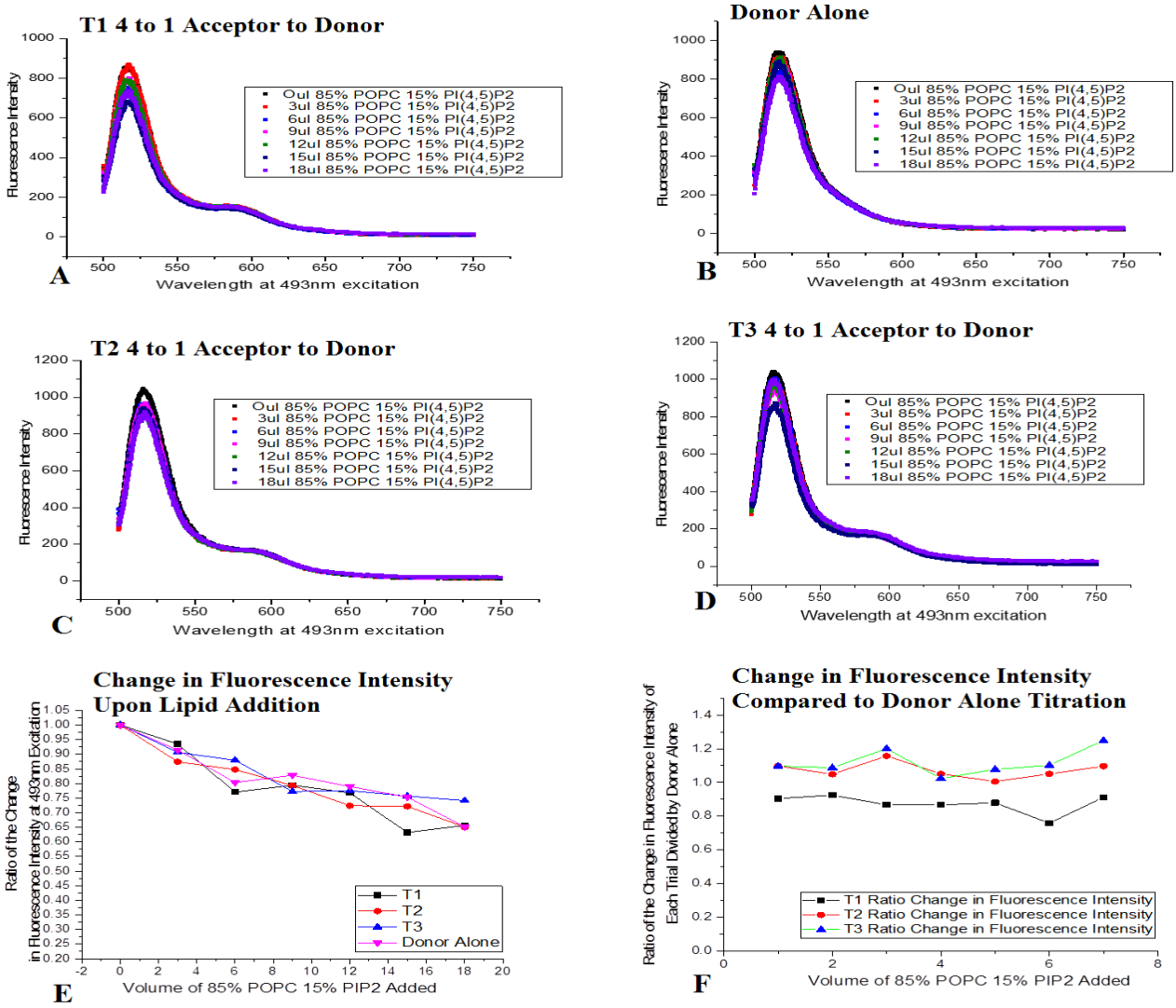

Figure 6.15: *<u>85% POPC 15% $PI_{(4,5)}P_2$ 4 to 1 Acceptor to Donor Lipid Titration</u>. Starting concentration: 0.5uM donor AlexaFluor 488 ANXA2. 2.0uM acceptor AlexaFluor 568 ANXA2, 0.5mM calcium chloride. The emission spectra were dilution corrected to better display changes in fluorescence intensity upon lipid addition. See Tables 26-27 Appendix G for a summary of the different ratios of lipid to protein and the calcium concentration differences upon lipid addition. (A-D) Change in the fluorescence intensity of the emission spectra upon lipid addition. (E) Change in the fluorescence intensity of the donor emission of the 4 to 1 acceptor to donor experiments upon lipid addition divided by the donor emission prior to lipid emission (F) Change in the fluorescence intensity of the donor emission of the 4 to 1 acceptor to donor experiments upon lipid addition divided by the donor emission of the donor alone experiments.*

CHAPTER 7—CONCLUSIONS AND FUTURE WORK

In summary, there was no significant FRET transfer observed between the N-terminal domains of adjacent ANXA2 acceptor and donor proteins with any lipid composition used. Protein and lipid aggregation and light scattering by lipids was observed and may have clouded the FRET signal. Alternatively, the cysteine residue may be inaccessible due to interactions with anionic phospholipids in the membrane as was observed by Zibouche et al. (2008). At this point, it cannot be conclusively stated whether or not ANXA2 promotes domain formation by self-associating with the N-terminal domain of adjacent ANXA2 proteins upon binding anionic phospholipids.

In the future, a different acceptor/donor pair with a larger Forster distance (R^0) and better spectral overlap might yield different results. In these experiments, the acceptor labeled poorly and due to slight size differences in the acceptor and donor, it is possible that the AlexaFluor 568 C5 maleimide dye altered the conformation and possibly the functionality of ANXA2. The FRET experiments could also be improved by using faster scan speeds and quicker mixing to improve the probability of observing a FRET signal before the ANXA2 proteins and the lipids aggregate and sink to the bottom of the cuvette. Additionally, co-pelleting assays should be performed to ensure that the fluorescently labeled ANXA2 is functional. Acceptor alone controls should be done in order to better observe how light scattering by lipids effects the acceptor emission. When the experimental setup is fully optimized, it would be interesting to alter the pH instead of the calcium concentration because Illien et al. (2012) observed that in the absence of calcium, ANXA2 can aggregate membranes containing POPS and $PI_{(4,5)}P_2$ at acidic pH. Ultimately, the best method to monitor this interaction, would be to perform FCS-FLIM experiments in cells.

REFERENCES

Ayala-Sanmartin, J., Zibouche, M., Illien, F., Vincent, M., & Gallay, J. (2008). Insight into the location and dynamics of the annexin A2 N-terminal domain during Ca 2+-induced membrane bridging. *Biochimica et Biophysica Acta (BBA)-Biomembranes, 1778*(2), 472-482.

Becker, W., Bergmann, A., Biscotti, G., Koenig, K., Riemann, I., Kelbauskas, L., & Biskup, C. (2004). *High-speed FLIM data acquisition by time-correlated single-photon counting.* Paper presented at the Biomedical Optics 2004.

Bharadwaj, A., Bydoun, M., Holloway, R., & Waisman, D. (2013). Annexin A2 Heterotetramer: Structure and Function. *International Journal of Molecular Sciences, 14*(3), 6259-6305. doi: 10.3390/ijms14036259

Blackwood, R., & Ernst, J. (1990). Characterization of Ca2+-dependent phospholipid binding, vesicle aggregation and membrane fusion by annexins. *Biochemical Journal, 266*(1), 195-200.

Bogdanov, M., Mileykovskaya, E., & Dowhan, W. (2008). Lipids in the assembly of membrane proteins and organization of protein supercomplexes: implications for lipid-linked disorders *Lipids in Health and Disease* (pp. 197-239): Springer.

Drücker, P., Pejic, M., Galla, H.-J., & Gerke, V. (2013). Lipid segregation and membrane budding induced by the peripheral membrane binding protein annexin A2. *Journal of Biological Chemistry, 288*(34), 24764-24776.

Drücker, P., Pejic, M., Grill, D., Galla, H.-J., & Gerke, V. (2014). Cooperative binding of annexin A2 to cholesterol-and phosphatidylinositol-4, 5-bisphosphate-containing bilayers. *Biophysical journal, 107*(9), 2070-2081.

Gerke, V., Creutz, C. E., & Moss, S. E. (2005). Annexins: linking Ca2+ signalling to membrane dynamics. *Nature reviews Molecular cell biology, 6*(6), 449-461.

Gerke, V., & Moss, S. E. (2002). Annexins: from structure to function. *Physiological reviews, 82*(2), 331-371.

Glomset, J. A. (1999). Lipids protein-lipid interactions on the surfaces of cell membranes. *Current opinion in structural biology, 9*(4), 425-427.

Hajjar, K. A. (2015). The Biology of Annexin A2: From Vascular Fibrinolysis to Innate Immunity. *Transactions of the American Clinical and Climatological Association, 126*, 144-155.

Hedhli, N., Falcone, D. J., Huang, B., Cesarman-Maus, G., Kraemer, R., Zhai, H., . . . Hajjar, K. A. (2012). The annexin A2/S100A10 system in health and disease: emerging paradigms. *BioMed Research International, 2012*.

Hong, K., Düzgüneş, N., Ekerdt, R., & Papahadjopoulos, D. (1982). Synexin facilitates fusion of specific phospholipid membranes at divalent cation concentrations found intracellularly. *Proceedings of the National Academy of Sciences, 79*(15), 4642-4644.

Illien, F., Piao, H.-R., Coué, M., Di Marco, C., & Ayala-Sanmartin, J. (2012). Lipid organization regulates annexin A2 Ca 2+-sensitivity for membrane bridging and its modulator effects on membrane fluidity. *Biochimica et Biophysica Acta (BBA)-Biomembranes, 1818*(11), 2892-2900.

Jacobson, K., Mouritsen, O. G., & Anderson, R. G. W. (2007). Lipid rafts: at a crossroad between cell biology and physics. *Nat Cell Biol, 9*(1), 7-14.

Jost, M., Zeuschner, D., Seemann, J., Weber, K., & Gerke, V. (1997). Identification and characterization of a novel type of annexin-membrane interaction: Ca2+ is not required for the association of annexin II with early endosomes. *Journal of cell science, 110*(2), 221-228.

Liu, L. (1999). Calcium-dependent self-association of annexin II: a possible implication in exocytosis. *Cellular signalling, 11*(5), 317-324.

Lizarbe, M. A., Barrasa, J. I., Olmo, N., Gavilanes, F., & Turnay, J. (2013). Annexin-phospholipid interactions. Functional implications. *International journal of molecular sciences, 14*(2), 2652-2683.

Lokman, N. A., Ween, M. P., Oehler, M. K., & Ricciardelli, C. (2011). The role of annexin A2 in tumorigenesis and cancer progression. *Cancer Microenvironment, 4*(2), 199-208.

Loura, L. M., Prieto, M., & Fernandes, F. (2010). Quantification of protein–lipid selectivity using FRET. *European Biophysics Journal, 39*(4), 565-578.

Luckey, M. (2014). *Membrane structural biology: with biochemical and biophysical foundations*: Cambridge University Press.

Maxfield, F. R. (2002). Plasma membrane microdomains. *Current opinion in cell biology, 14*(4), 483-487.

McIntosh, T. J. (2015). Stepping between Membrane Microdomains. *Biophysical journal, 108*(4), 783-784.

Mendelsohn, A. R., & Brent, R. (1999). Protein interaction methods--toward an endgame. *Science, 284*(5422), 1948.

Patel, D. R., Isas, J. M., Ladokhin, A. S., Jao, C. C., Kim, Y. E., Kirsch, T., . . . Haigler, H. T. (2005). The conserved core domains of annexins A1, A2, A5, and B12 can be divided into two groups with different Ca2+-dependent membrane-binding properties. *Biochemistry, 44*(8), 2833-2844.

Piston, D. W., & Kremers, G.-J. (2007). Fluorescent protein FRET: the good, the bad and the ugly. *Trends in biochemical sciences, 32*(9), 407-414.

Rescher, U., & Gerke, V. (2004). Annexins–unique membrane binding proteins with diverse functions. *Journal of cell science, 117*(13), 2631-2639.

Rescher, U., Zobiack, N., & Gerke, V. (2000). Intact Ca (2+)-binding sites are required for targeting of annexin 1 to endosomal membranes in living HeLa cells. *Journal of cell science, 113*(22), 3931-3938.

Rossy, J., Ma, Y., & Gaus, K. (2014). The organisation of the cell membrane: do proteins rule lipids? *Current opinion in chemical biology, 20*, 54-59.

Saxena, V., Lai, C.-K., Chao, T.-C., Jeng, K.-S., & Lai, M. M. (2012). Annexin A2 is involved in the formation of hepatitis C virus replication complex on the lipid raft. *Journal of virology, 86*(8), 4139-4150.

Schwille, P. (2005). Fluorescence correlation spectroscopy *Encyclopedic Reference of Genomics and Proteomics in Molecular Medicine* (pp. 576-578): Springer.

Valapala, M., & Vishwanatha, J. K. (2011). Lipid raft endocytosis and exosomal transport facilitate extracellular trafficking of annexin A2. *Journal of Biological Chemistry, 286*(35), 30911-30925.

Yan, Y., & Marriott, G. (2003). Analysis of protein interactions using fluorescence technologies. *Current opinion in chemical biology, 7*(5), 635-640.

Yengo, C. M., & Berger, C. L. (2010). Fluorescence anisotropy and resonance energy transfer: powerful tools for measuring real time protein dynamics in a physiological environment. *Current opinion in pharmacology, 10*(6), 731-737.

Zaks, W. J., & Creutz, C. E. (1991). Calcium (2+)-dependent annexin self-association on membrane surfaces. *Biochemistry, 30*(40), 9607-9615.

Zibouche, M., Vincent, M., Illien, F., Gallay, J., & Ayala-Sanmartin, J. (2008). The N-terminal domain of annexin 2 serves as a secondary binding site during membrane bridging. *Journal of Biological Chemistry, 283*(32), 22121-22127.

CHAPTER 8—APPENDIX

8.1 Appendix A: ANXA2 6X and 10x Primers for Mutation

6x Mutations

K81A (AAG→GCG)

K81A_For: 5' CCAGAGAAGGACCAAAGCGGAACTTGCATCAGCAC 3'

K81A_Rev: 5' GTGCTGATGCAAGTTCCGCTTTGGTCCTTCTCTGG 3'

E189K (GAA→AAA)

E189K_For: 5' GGCTCTGTCATTGATTATAAACTGATTGACCAAGATGCTC 3'

E189K_Rev: 5' GAGCATCTTGGTCAATCAGTTTATAATCAATGACAGAGCC 3'

K206A (AAA→GCA)

K206A_For: 5' CGCTGGAGTGAAGAGGGCAGGAACTGATGTTCCC 3'
K206A_Rev: 5' GGGAACATCAGTTCCTGCCCTCTTCACTCCAGCG 3'

R196S (CGG→AGT)

R196S_For: 5' CTGATTGACCAAGATGCTAGTGATCTCTATGACGCTGGAG 3'

R196S_Rev: 5' CTCCAGCGTCATAGAGATCACTAGCATCTTGGTCAATCAG 3'

E219K (GAG→AAG)

E219K_For: 5' ATCAGCATCATGACCAAGCGGAGCGTGCCC 3'

E219K_Rev: 5' GGGCACGCTCCGCTTGGTCATGATGCTGAT 3'

K212S (AAG→TCG)

K212S_For_N: 5' CAGGAACTGATGTTCCCTCGTGGATCAGCATCATG 3'

K212S_Rev_N: 5' CATGATGCTGATCCACGAGGGAACATCAGTTCCTG 3'

Additional 10x Mutations

R36→S (CGG→AGC)
R36S_For: 5` TATACTAACTTTGATGCTGAGAGCGATGCTTTGAACATTGAAACA 3`
R36s_Rev: 5` ATATGATTGAAACTACGACTCTCGCTACGAAACTTGTAACTTTGT 3`

V53→A and T54→A (GTC→GCC and ACC→GCC)
For_5` CAAAGGTGTGGATGAGGCCGCCATTGTCAACATTTTG 3`
Rev_5` CAAAATGTTGACAATGGCGGCCTCATCCACACCTTTG 3`

K328→A (AAA→GCA)
K328A_For 5` TAAGGGCGACTACCAGGCAGCGCTGCTGTACCTG 3`
K328A_Rev 5` AGGTACAGCAGCGCTGCCTGGTAGTCGCCCTTAG 3`

8.2 Appendix B: pSE420 Vector Map and ANXA2 Insertion Information

Comments for pSE420:
4617 nucleotides

Trc promotor: bases 191-221
Lac operator: bases 228-248
rrnB antitermination sequences: bases 264-333
T7 gene 10 translational enhancer: bases 346-354
Ribosome binding site: bases 370-374
Mini-cistron: bases 383-409
Superlinker MCS: bases 411-763
Ampicilin resistance ORF: bases 1283-2143
LacI^{q} ORF: bases 3615-4574

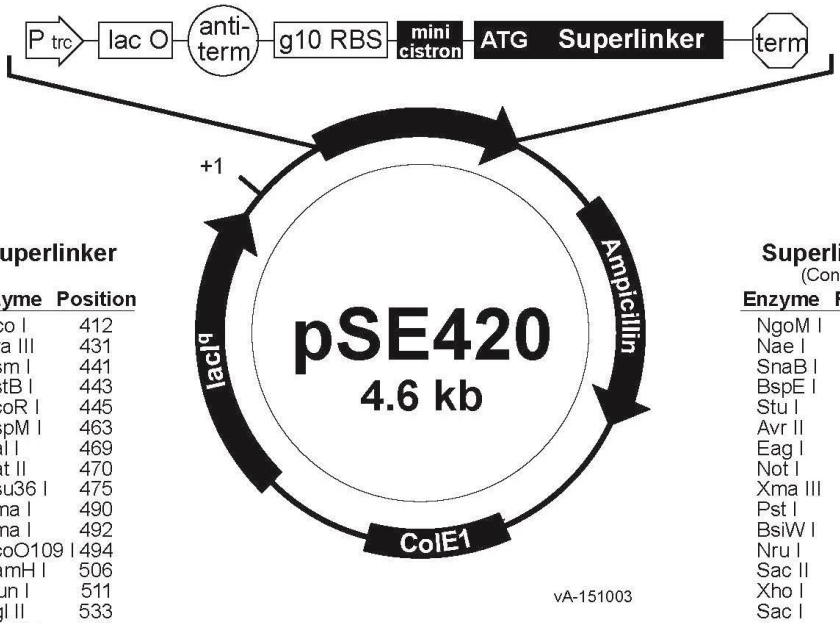

Superlinker

Enzyme	Position
Nco I	412
Dra III	431
Bsm I	441
BstB I	443
EcoR I	445
BspM I	463
Sal I	469
Aat II	470
Bsu36 I	475
Xma I	490
Sma I	492
EcoO109 I	494
BamH I	506
Mun I	511
Bgl II	533
BsaB I	549
Eco47 III	557
Nhe I	575
Xba I	587
Acc65 I	593
Age I	596
Kpn I	597

Superlinker (Cont.)

Enzyme	Position
NgoM I	613
Nae I	615
SnaB I	621
BspE I	628
Stu I	644
Avr II	645
Eag I	661
Not I	661
Xma III	661
Pst I	672
BsiW I	691
Nru I	699
Sac II	706
Xho I	721
Sac I	722
Spe I	731
Msc I	738
Pml I	742
Sfi I	744
Afl II	756
Hind III	759

pse420 Detailed Sequence

```
ID   PSE420     preliminary; circular DNA; SYN; 4613 BP.
XX
AC   IG1117;
DE   E. coli plasmid vector pSE420 - complete.
XX
KW   cloning vector.
XX
OS   Cloning vector
OC   Artificial sequences; Cloning vehicles.
XX
RN   [1]
RC   pRSETA from pET-3 & pBluescript series
RC   pRSETB from pET-3 & pBluescript series
RC   pRSETC from pET-3 & pBluescript series
```

```
RC   pSE280 from pKK233-2
RC   pSE380 from pTrc99A
RC   pSE420 from pSE380
RC   pTRCHISA from pSE420
RC   pTRCHISB from pSE420
RC   pTRCHISC from pSE420
RA   Abdel-Malek H.;
RT   ;
RL   The Digest 4:1-3(1991).
XX
RN   [2]
RC   pKK421-1 from pKK233-2
RC   pSLD7, pSLE1, pSLF1, pSLJ10 from pBluescript KS+
RC   pSL180 from pUC18 & linker
RC   pSL189 from pUC19 & linker
RC   pSL190 from pSL189
RC   pSL1180 from pUC118 & linker
RC   pSL1190 from pUC119 & linker
RC   pSL300 from pSLJ10 & linker
RC   pSL250 from pSL300
RC   pSL260 from pSL250
RC   pSL270 from pSL250
RC   pSL251 from pSL250
RC   pSL261 from pSL260
RC   pSL271 from pSL270
RC   pSL301 from pSL300
RC   pSE1200 from pUC120 & linker
RC   pSE1201 from pUC120 & linker
RC   pSE1202 from pUC120 & linker
RC   pSE219 from pKK233-2
RC   pSE220 from pSE219
RC   pSE280 from pKK421-1
RC   pSE380 from pTrc99A
RA   Brosius J.;
RT   "Superpolylinkers in cloning and expression vectors";
RL   DNA 8:759-777(1989).
XX
CC   NM (pSE420)
CC   CM (yes)
CC   NA (ds-DNA)
CC   TP (circular)
CC   ST ()
CC   TY (plasmid)
CC   SP (Invitrogen)
CC   HO (E.coli NM522)(E.coli INValphaF')
CC   CP ()
CC   FN (expression)
CC   SE ()
CC   PA (pSE380)
CC   BR ()
CC   OF ()
CC   OR ()
XX
FH   Key             Location/Qualifiers
FH
FT   misc_feature    0..0
FT                   /note="1. pSE380 4476bp
```

```
FT                   -> pSE420 4613bp"
FT   promoter        0..0
FT                   /note="PRO E. coli trc (trp & lac)"
FT   promoter        0..0
FT                   /note="PRO E. coli lacO gene"
FT   promoter        0..0
FT                   /note="PRO E. coli antitermination"
FT   RBS             0..0
FT                   /note="RBS E. coli g10 gene"
FT   misc_feature    0..0
FT                   /note="E. coli mini-cistron"
FT   misc_feature    0..0
FT                   /note="ATG"
FT   promoter        0..0
FT                   /note="PRO bacteriophage T7"
FT   misc_binding    0..0
FT                   /note="MCS SL2 superlinker"
FT   promoter        0..0
FT                   /note="PRO bacteriophage T3"
FT   terminator      0..0
FT                   /note="TER"
FT   CDS             0..0
FT                   /note="ANT E. coli beta-lactamase gene (bla)
FT                   ampicillin resistance gene (apr/amp)"
FT   rep_origin      0..0
FT                   /note="ORI E. coli pMB1 (ColE1 and pBR322)"
FT   promoter        0..0
FT                   /note="PRO E. coli lacIq gene"
XX
SQ   Sequence 4613 BP; 1132 A; 1154 C; 1225 G; 1102 T; 0 other;
     gtttgacagc ttatcatcga ctgcacggtg caccaatgct tctggcgtca ggcagccatc
     ggaagctgtg gtatggctgt gcaggtcgta aatcactgca taattcgtgt cgctcaaggc
     gcactcccgt tctggataat gtttttgcg ccgacatcat aacggttctg gcaaatattc
     tgaaatgagc tgttgacaat taatcatccg gctcgtataa tgtgtggaat tgtgagcgga
     taacaatttc acacaggaaa cagcgccgct gagaaaaagc gaagcggcac tgctctttaa
     caatttatca gacaatctgt gtgggcactc gaccggaatt atcgattaac tttattatta
     aaaattaaag aggtatatat taatgtatcg attaaataag gaggaataaa ccatggctgg
     tgaccacgtc gtggaatgcc ttcgaattca gcacctgcac atgggacgtc gacctgaggt
     aattataacc cgggccctat atatggatcc aattgcaatg atcatcatga cagatctgcg
     cgcgatcgat atcagcgctt taaatttgcg catgctagct atagttctag aggtaccggt
     tgttaacgtt agccggctac gtatactccg gaatattaat aggcctagga tgcatatggc
     ggccgcctgc agctggcgcc atcgatacgc gtacgtcgcg accgcggaca tgtacagagc
     tcgagaagta ctagtggcca cgtgggccgt gcaccttaag cttggctgtt ttggcggatg
     agagaagatt ttcagcctga tacagattaa atcagaacgc agaagcggtc tgataaaaca
     gaatttgcct ggcggcagta gcgcggtggt cccacctgac cccatgccga actcagaagt
     gaaacgccgt agcgccgatg gtagtgtggg gtctccccat gcgagagtag ggaactgcca
     ggcatcaaat aaaacgaaag gctcagtcga aagactgggc ctttcgtttt atctgttgtt
     tgtcggtgaa cgctctcctg agtaggacaa atccgccggg agcggatttg aacgttgcga
     agcaacggcc cggagggtgg cgggcaggac gcccgccata aactgccagg catcaaatta
     agcagaaggc catcctgacg gatggccttt ttgcgtttct acaaactctt tttgtttatt
     tttctaaata cattcaaata tgtatccgct catgagacaa taaccctgat aaatgcttca
     ataatattga aaaaggaaga gtatgagtat tcaacatttc cgtgtcgccc ttattccctt
     ttttgcggca ttttgccttc ctgtttttgc tcacccagaa acgctggtga aagtaaaaga
     tgctgaagat cagttgggtg cacgagtggg ttacatcgaa ctggatctca acagcggtaa
     gatccttgag agttttcgcc ccgaagaacg ttttccaatg atgagcactt ttaaagttct
     gctatgtggc gcggtattat cccgtgttga cgccgggcaa gagcaactcg gtcgccgcat
     acactattct cagaatgact tggttgagta ctcaccagtc acagaaaagc atcttacgga
```

tggcatgaca gtaagagaat tatgcagtgc tgccataacc atgagtgata acactgcggc
caacttactt ctgacaacga tcggaggacc gaaggagcta accgcttttt tgcacaacat
gggggatcat gtaactcgcc ttgatcgttg ggaaccggag ctgaatgaag ccataccaaa
cgacgagcgt gacaccacga tgcctgtagc aatggcaaca acgttgcgca aactattaac
tggcgaacta cttactctag cttcccggca acaattaata gactggatgg aggcggataa
agttgcagga ccacttctgc gctcggccct tccggctggc tggtttattg ctgataaatc
tggagccggt gagcgtgggt ctcgcggtat cattgcagca ctggggccag atggtaagcc
ctcccgtatc gtagttatct acacgacggg gagtcaggca actatggatg aacgaaatag
acagatcgct gagataggtg cctcactgat taagcattgg taactgtcag accaagttta
ctcatatata ctttagattg atttaaaact tcatttttaa tttaaaagga tctaggtgaa
gatccttttt gataatctca tgaccaaaat cccttaacgt gagttttcgt tccactgagc
gtcagacccc gtagaaaaga tcaaaggatc ttcttgagat cctttttttc tgcgcgtaat
ctgctgcttg caaacaaaaa aaccaccgct accagcggtg gtttgtttgc cggatcaaga
gctaccaact ctttttccga aggtaactgg cttcagcaga gcgcagatac caaatactgt
ccttctagtg tagccgtagt taggccacca cttcaagaac tctgtagcac cgcctacata
cctcgctctg ctaatcctgt taccagtggc tgctgccagt ggcgataagt cgtgtcttac
cgggttggac tcaagacgat agttaccgga taaggcgcag cggtcgggct gaacgggggg
ttcgtgcaca cagcccagct tggagcgaac gacctacacc gaactgagat acctacagcg
tgagctatga gaaagcgcca cgcttcccga agggagaaag gcggacaggt atccggtaag
cggcagggtc ggaacaggag agcgcacgag ggagcttcca gggggaaacg cctggtatct
ttatagtcct gtcgggtttc gccacctctg acttgagcgt cgatttttgt gatgctcgtc
aggggggcgg agcctatgga aaaacgccag caacgcggcc tttttacggt tcctggcctt
ttgctggcct tttgctcaca tgttctttcc tgcgttatcc cctgattctg tggataaccg
tattaccgcc tttgagtgag ctgataccgc tcgccgcagc cgaacgaccg agcgcagcga
gtcagtgagc gaggaagcgg aagagcgcct gatgcggtat tttctcctta cgcatctgtg
cggtatttca caccgcatat ggtgcactct cagtacaatc tgctctgatg ccgcatagtt
aagccagtat acactccgct atcgctacgt gactgggtca tggctgcgcc ccgacacccg
ccaacacccg ctgacgcgcc ctgacgggct tgtctgctcc cggcatccgc ttacagacaa
gctgtgaccg tctccgggag ctgcatgtgt cagaggtttt caccgtcatc accgaaacgc
gcgaggcagc agatcaattc gcgcgcgaag gcgaagcggc atgcatttac gttgacacca
tcgaatggcg caaaaccttt cgcggtatgg catgatagcg cccggaagag agtcaattca
gggtggtgaa tgtgaaacca gtaacgttat acgatgtcgc agagtatgcc ggtgtctctt
atcagaccgt ttcccgcgtg gtgaaccagg ccagccacgt ttctgcgaaa acgcgggaaa
aagtggaagc ggcgatggcg gagctgaatt acattcccaa ccgcgtggca caacaactgg
cgggcaaaca gtcgttgctg attggcgttg ccacctccag tctggccctg cacgcgccgt
cgcaaattgt cgcggcgatt aaatctcgcg ccgatcaact gggtgccagc gtggtggtgt
cgatggtaga acgaagcggc gtcgaagcct gtaaagcggc ggtgcacaat cttctcgcgc
aacgcgtcag tgggctgatc attaactatc cgctggatga ccaggatgcc attgctgtgg
aagctgcctg cactaatgtt ccggcgttat ttcttgatgt ctctgaccag acacccatca
acagtattat tttctcccat gaagacggta cgcgactggg cgtggagcat ctggtcgcat
tgggtcacca gcaaatcgcg ctgttagcgg gcccattaag ttctgtctcg gcgcgtctgc
gtctggctgg ctggcataaa tatctcactc gcaatcaaat tcagccgata gcggaacggg
aaggcgactg gagtgccatg tccggttttc aacaaaccat gcaaatgctg aatgagggca
tcgttcccac tgcgatgctg gttgccaacg atcagatggc gctgggcgca atgcgcgcca
ttaccgagtc cgggctgcgc gttggtgcgg atatctcggt agtgggatac gacgataccg
aagacagctc atgttatatc ccgccgtcaa ccaccatcaa acaggatttt cgcctgctgg
ggcaaaccag cgtggaccgc ttgctgcaac tctctcaggg ccaggcggtg aagggcaatc
agctgttgcc cgtctcactg gtgaaaagaa aaaccaccct ggcgcccaat acgcaaaccg
cctctccccg cgcgttggcc gattcattaa tgcagctggc acgacaggtt tcccgactgg
aaagcgggca gtgagcgcaa cgcaattaat gtgagttagc gcgaattgat ctg

8.3 APPENDIX C: FASTA DNA Sequence and Sequence Alignment Data

FASTA:

Homo sapiens annexin A2 (ANXA2), transcript variant 3, mRNA

NCBI Reference Sequence: NM_004039.2

GenBank Graphics

>gi|50845389:56-1075 Homo sapiens annexin A2 (ANXA2), transcript variant 3, mRNA
ATGTCTACTGTTCACGAAATCCTGTGCAAGCTCAGCTTGGAGGGTGATCACTCTACACCCCCAAGTGCAT
ATGGGTCTGTCAAAGCCTATACTAACTTTGATGCTGAGCGGGATGCTTTGAACATTGAAACAGCCATCAA
GACCAAAGGTGTGGATGAGGTCACCATTGTCAACATTTTGACCAACCGCAGCAATGCACAGAGACAGGAT
ATTGCCTTCGCCTACCAGAGAAGGACCAAAAAGGAACTTGCATCAGCACTGAAGTCAGCCTTATCTGGCC
ACCTGGAGACGGTGATTTTGGGCCTATTGAAGACACCTGCTCAGTATGACGCTTCTGAGCTAAAAGCTTC
CATGAAGGGGCTGGGAACCGACGAGGACTCTCTCATTGAGATCATCTGCTCCAGAACCAACCAGGAGCTG
CAGGAAATTAACAGAGTCTACAAGGAAATGTACAAGACTGATCTGGAGAAGGACATTATTTCGGACACAT
CTGGTGACTTCCGCAAGCTGATGGTTGCCCTGGCAAAGGGTAGAAGAGCAGAGGATGGCTCTGTCATTGA
TTATGAACTGATTGACCAAGATGCTCGGGATCTCTATGACGCTGGAGTGAAGAGGAAAGGAACTGATGTT
CCCAAGTGGATCAGCATCATGACCGAGCGGAGCGTGCCCCACCTCCAGAAAGTATTTGATAGGTACAAGA
GTTACAGCCCTTATGACATGTTGGAAAGCATCAGGAAAGAGGTTAAAGGAGACCTGGAAAATGCTTTCCT
GAACCTGGTTCAGTGCATTCAGAACAAGCCCCTGTATTTTGCTGATCGGCTGTATGACTCCATGAAGGGC
AAGGGGACGCGAGATAAGGTCCTGATCAGAATCATGGTCTCCCGCAGTGAAGTGGACATGTTGAAAATTA
GGTCTGAATTCAAGAGAAAGTACGGCAAGTCCCTGTACTATTATATCCAGCAAGACACTAAGGGCGACTA
CCAGAAAGCGCTGCTGTACCTGTGTGGTGGAGATGACTGA

1020 bp with Methionine

Anx A2 seq.

PSE 420 Vector Seq.

5'->3' : 5'-
ATGTCTACTGTTCACGAAATCCTGTGCAAGCTCAGCTTGGAGGGTGATCACTCTACACCCCCAAGTGCATATGGGT
CTGTCAAAGCCTATACTAACTTTGATGCTGAGCGGGATGCTTTGAACATTGAAACAGCCATCAAGACCAAAGGTGT
GGATGAGGTCACCATTGTCAACATTTTGACCAACCGCAGCAATGCACAGAGACAGGATATTGCCTTCGCCTACCAG
AGAAGGACCAAAAAGGAACTTGCATCAGCACTGAAGTCAGCCTTATCTGGCCACCTGGAGACGGTGATTTTGGGC
CTATTGAAGACACCTGCTCAGTATGACGCTTCTGAGCTAAAAGCTTCCATGAAGGGGCTGGGAACCGACGAGGAC
TCTCTCATTGAGATCATCTGCTCCAGAACCAACCAGGAGCTGCAGGAAATTAACAGAGTCTACAAGGAAATGTACA
AGACTGATCTGGAGAAGGACATTATTTCGGACACATCTGGTGACTTCCGCAAGCTGATGGTTGCCCTGGCAAAGG
GTAGAAGAGCAGAGGATGGCTCTGTCATTGATTATGAACTGATTGACCAAGATGCTCGGGATCTCTATGACGCTG
GAGTGAAGAGGAAAGGAACTGATGTTCCCAAGTGGATCAGCATCATGACCGAGCGGAGCGTGCCCCACCTCCAG
AAAGTATTTGATAGGTACAAGAGTTACAGCCCTTATGACATGTTGGAAAGCATCAGGAAAGAGGTTAAAGGAGAC
CTGGAAAATGCTTTCCTGAACCTGGTTCAGTGCATTCAGAACAAGCCCCTGTATTTTGCTGATCGGCTGTATGACTC
CATGAAGGGCAAGGGGACGCGAGATAAGGTCCTGATCAGAATCATGGTCTCCCGCAGTGAAGTGGACATGTTGA

AAATTAGGTCTGAATTCAAGAGAAAGTACGGCAAGTCCCTGTACTATTATATCCAGCAAGACACTAAGGGCGACT
ACCAGAAAGCGCTGCTGTACCTGTGTGGTGGAGATGACTGAAGCTTGGCTGTTTTGGCGGATGAGAGAAGATTTT
CAGCCTGATACAGATTAAATCAGAACGCAGAAGCGGTCTGATAAAACAGAATTTGCCTGGCGGCAGTAGCGCGGT
GGTCCCACCTGACCCCATGCCGAACTCAGAAGTGAAACGCCGTAGCGCCGATGGTAGTGTGGGGTCTCCCCATGC
GAGAGTAGGGAACTGCCAGGCATCAAATAAAACGAAAGGCTCAGTCGAAAGACTGGGCCTTTCGTTTTATCTGTT
GTTTGTCGGTGAACGCTCTCCTGAGTAGGACAAATCCGCCGGGAGCGGATTTGAACGTTGCGAAGCAACGGCCCG
GAGGGTGGCGGGCAGGACGCCCGCCATAAACTGCCAGGCATCAAATTAAGCAGAAGGCCATCCTGACGGATGGC
CTTTTTGCGTTTCTACAAACTCTTTTTGTTTATTTTTCTAAATACATTCAAATATGTATCCGCTCATGAGACAATAACC
CTGATAAATGCTTCAATAATATTGAAAAAGGAAGAGTATGAGTATTCAACATTTCCGTGTCGCCCTTATTCCCTTTT
TTGCGGCATTTTGCCTTCCTGTTTTTGCTCACCCAGAAACGCTGGTGAAAGTAAAAGATGCTGAAGATCAGTTGGG
TGCACGAGTGGGTTACATCGAACTGGATCTCAACAGCGGTAAGATCCTTGAGAGTTTTCGCCCCGAAGAACGTTTT
CCAATGATGAGCACTTTTAAAGTTCTGCTATGTGGCGCGGTATTATCCCGTGTTGACGCCGGGCAAGAGCAACTCG
GTCGCCGCATACACTATTCTCAGAATGACTTGGTTGAGTACTCACCAGTCACAGAAAAGCATCTTACGGATGGCAT
GACAGTAAGAGAATTATGCAGTGCTGCCATAACCATGAGTGATAACACTGCGGCCAACTTACTTCTGACAACGATC
GGAGGACCGAAGGAGCTAACCGCTTTTTTGCACAACATGGGGGATCATGTAACTCGCCTTGATCGTTGGGAACCG
GAGCTGAATGAAGCCATACCAAACGACGAGCGTGACACCACGATGCCTGTAGCAATGGCAACAACGTTGCGCAA
ACTATTAACTGGCGAACTACTTACTCTAGCTTCCCGGCAACAATTAATAGACTGGATGGAGGCGGATAAAGTTGCA
GGACCACTTCTGCGCTCGGCCCTTCCGGCTGGCTGGTTTATTGCTGATAAATCTGGAGCCGGTGAGCGTGGGTCTC
GCGGTATCATTGCAGCACTGGGGCCAGATGGTAAGCCCTCCCGTATCGTAGTTATCTACACGACGGGGAGTCAGG
CAACTATGGATGAACGAAATAGACAGATCGCTGAGATAGGTGCCTCACTGATTAAGCATTGGTAACTGTCAGACC
AAGTTTACTCATATATACTTTAGATTGATTTAAAACTTCATTTTTAATTTAAAAGGATCTAGGTGAAGATCCTTTTTG
ATAATCTCATGACCAAAATCCCTTAACGTGAGTTTTCGTTCCACTGAGCGTCAGACCCCGTAGAAAAGATCAAAGG
ATCTTCTTGAGATCCTTTTTTTCTGCGCGTAATCTGCTGCTTGCAAACAAAAAAACCACCGCTACCAGCGGTGGTTT
GTTTGCCGGATCAAGAGCTACCAACTCTTTTTCCGAAGGTAACTGGCTTCAGCAGAGCGCAGATACCAAATACTGT
CCTTCTAGTGTAGCCGTAGTTAGGCCACCACTTCAAGAACTCTGTAGCACCGCCTACATACCTCGCTCTGCTAATCC
TGTTACCAGTGGCTGCTGCCAGTGGCGATAAGTCGTGTCTTACCGGGTTGGACTCAAGACGATAGTTACCGGATA
AGGCGCAGCGGTCGGGCTGAACGGGGGGTTCGTGCACACAGCCCAGCTTGGAGCGAACGACCTACACCGAACTG
AGATACCTACAGCGTGAGCTATGAGAAAGCGCCACGCTTCCCGAAGGGAGAAAGGCGGACAGGTATCCGGTAAG
CGGCAGGGTCGGAACAGGAGAGCGCACGAGGGAGCTTCCAGGGGGAAACGCCTGGTATCTTTATAGTCCTGTCG
GGTTTCGCCACCTCTGACTTGAGCGTCGATTTTTGTGATGCTCGTCAGGGGGGCGGAGCCTATGGAAAAACGCCA
GCAACGCGGCCTTTTTACGGTTCCTGGCCTTTTGCTGGCCTTTTGCTCACATGTTCTTTCCTGCGTTATCCCCTGATT
CTGTGGATAACCGTATTACCGCCTTTGAGTGAGCTGATACCGCTCGCCGCAGCCGAACGACCGAGCGCAGCGAGT
CAGTGAGCGAGGAAGCGGAAGAGCGCCTGATGCGGTATTTTCTCCTTACGCATCTGTGCGGTATTTCACACCGCAT
ATGGTGCACTCTCAGTACAATCTGCTCTGATGCCGCATAGTTAAGCCAGTATACACTCCGCTATCGCTACGTGACTG
GGTCATGGCTGCGCCCCGACACCCGCCAACACCCGCTGACGCGCCCTGACGGGCTTGTCTGCTCCCGGCATCCGCT
TACAGACAAGCTGTGACCGTCTCCGGGAGCTGCATGTGTCAGAGGTTTTCACCGTCATCACCGAAACGCGCGAGG
CAGCAGATCAATTCGCGCGCGAAGGCGAAGCGGCATGCATTTACGTTGACACCATCGAATGGCGCAAAACCTTTC
GCGGTATGGCATGATAGCGCCCGGAAGAGAGTCAATTCAGGGTGGTGAATGTGAAACCAGTAACGTTATACGAT
GTCGCAGAGTATGCCGGTGTCTCTTATCAGACCGTTTCCCGCGTGGTGAACCAGGCCAGCCACGTTTCTGCGAAAA
CGCGGGAAAAAGTGGAAGCGGCGATGGCGGAGCTGAATTACATTCCCAACCGCGTGGCACAACAACTGGCGGGC
AAACAGTCGTTGCTGATTGGCGTTGCCACCTCCAGTCTGGCCCTGCACGCGCCGTCGCAAATTGTCGCGGCGATTA
AATCTCGCGCCGATCAACTGGGTGCCAGCGTGGTGGTGTCGATGGTAGAACGAAGCGGCGTCGAAGCCTGTAAA
GCGGCGGTGCACAATCTTCTCGCGCAACGCGTCAGTGGGCTGATCATTAACTATCCGCTGGATGACCAGGATGCC
ATTGCTGTGGAAGCTGCCTGCACTAATGTTCCGGCGTTATTTCTTGATGTCTCTGACCAGACACCCATCAACAGTAT

TATTTTCTCCCATGAAGACGGTACGCGACTGGGCGTGGAGCATCTGGTCGCATTGGGTCACCAGCAAATCGCGCT
GTTAGCGGGCCCATTAAGTTCTGTCTCGGCGCGTCTGCGTCTGGCTGGCTGGCATAAATATCTCACTCGCAATCAA
ATTCAGCCGATAGCGGAACGGGAAGGCGACTGGAGTGCCATGTCCGGTTTTCAACAAACCATGCAAATGCTGAAT
GAGGGCATCGTTCCCACTGCGATGCTGGTTGCCAACGATCAGATGGCGCTGGGCGCAATGCGCGCCATTACCGAG
TCCGGGCTGCGCGTTGGTGCGGATATCTCGGTAGTGGGATACGACGATACCGAAGACAGCTCATGTTATATCCCG
CCGTCAACCACCATCAAACAGGATTTTCGCCTGCTGGGGCAAACCAGCGTGGACCGCTTGCTGCAACTCTCTCAGG
GCCAGGCGGTGAAGGGCAATCAGCTGTTGCCCGTCTCACTGGTGAAAAGAAAAACCACCCTGGCGCCCAATACGC
AAACCGCCTCTCCCCGCGCGTTGGCCGATTCATTAATGCAGCTGGCACGACAGGTTTCCCGACTGGAAAGCGGGC
AGTGAGCGCAACGCAATTAATGTGAGTTAGCGCGAATTGATCTGGTTTGACAGCTTATCATCGACTGCACGGTGC
ACCAATGCTTCTGGCGTCAGGCAGCCATCGGAAGCTGTGGTATGGCTGTGCAGGTCGTAAATCACTGCATAATTC
GTGTCGCTCAAGGCGCACTCCCGTTCTGGATAATGTTTTTTGCGCCGACATCATAACGGTTCTGGCAAATATTCTGA
AATGAGCTGTTGACAATTAATCATCCGGCTCGTATAATGTGTGGAATTGTGAGCGGATAACAATTTCACACAGGAA
ACAGCGCCGCTGAGAAAAAGCGAAGCGGCACTGCTCTTTAACAATTTATCAGACAATCTGTGTGGGCACTCGACC
GGAATTATCGATTAACTTTATTATTAAAAATTAAAGAGGTATATATTAATGTATCGATTAAATAAGGAGGAATAAA
C -3'

Sequence Alignment Data

1. Anx WT 401-800

5’TGCAGGAAATTAACAGAGTCTACAAGGAAATGTACAAGACTGATCTGGAGAAGG
ACATTATTTCGGACACATCTGGTGACTTCCGCAAGCTGATGGTTGCCCTGGCAAAGG
GTAGAAGAGCAGAGGATGGCTCTGTCATTGATTATGAACTGATTGACCAAGATGCTC
GGGATCTCTATGACGCTGGAGTGAAGAGGAAAGGAACTGATGTTCCCAAGTGGATC
AGCATCATGACCGAGCGGAGCGTGCCCCACCTCCAGAAAGTATTTGATAGGTACAA
GAGTTACAGCCCTTATGACATGTTGGAAAGCATCAGGAAAGAGGTTAAAGGAGACC
TGGAAAATGCTTTCCTGAACCTGGTTCAGTGCATTCAGAACAAGCCCCTGTATTTTG
CTGATCGGCTGTATGACTCCATGAAGGGCAAGGGGACGCGAGATAAGGTCCTGATC
AGAATCATGGTCTCCCGCAGTGAAGTGGACATGTTGAAAATTAGGTCTGAGTTCAAG
AGAAAGTACGGCAAGTCCCTGTACTATTATATCCAGCAAGACACTAAGGGCGACTA
CCAGAAAGCGCTGCTGTACCTGTGTGGTGGAGATGACTGAAGCCCGACACGGCCTG
AGCGTCCAGAAATGGTGCTCACCAAGCTTGGCTGTTTTGGCGGATGAGAGAAGATTT
TCAGCCTGATACAGATTAAATCAGAACGCAGAAGCGGTCTGATAAAACAGAATTTG
CCTGGCGGCAGTAGCGCGGTGGTCCCACCTGACCCATGCCGAACTCAGAAGTGAAA
CGCCGTAGCGCCGATGGTAGTGTGGGGTCTCCCCATGCGAGAGTAGGGAACTGCCA
GGCATCAAATAAAACGAAAGGCTCAGTCGAAAGACTGGGCTTTCGTTTTATCTGTTG
TTTGTCGGTGAACGCTCTCCTGAGTAGGACAAATCCGCCGGGAGCGGATTTGAACGT
TGCGAGCACGGCCCGGGAGGGTGGCGGGCAGGACGCCCGCATAAACTGCCAGGCAT
CAAATTAAGCAGAAGCATCCTGACGATGACTTTTGCGTTTCTACAACTCTTTTGTTAT
TTTTCTAATACATCAAATATGTATCGCTCATGAACATAACCCTGATAATGCTCAATA
ATATGAAAAGANNNTGATATCAATTTCNNTCGCCTTATCTTTGCGCATTGCTCTGTTT
GCTACCGAACGTNAGTAAGATGCTGAATCTTGGGTGCAGAGGTGNTACTCGACTGT
GATCTCCACAGCGGGTATGA 3’

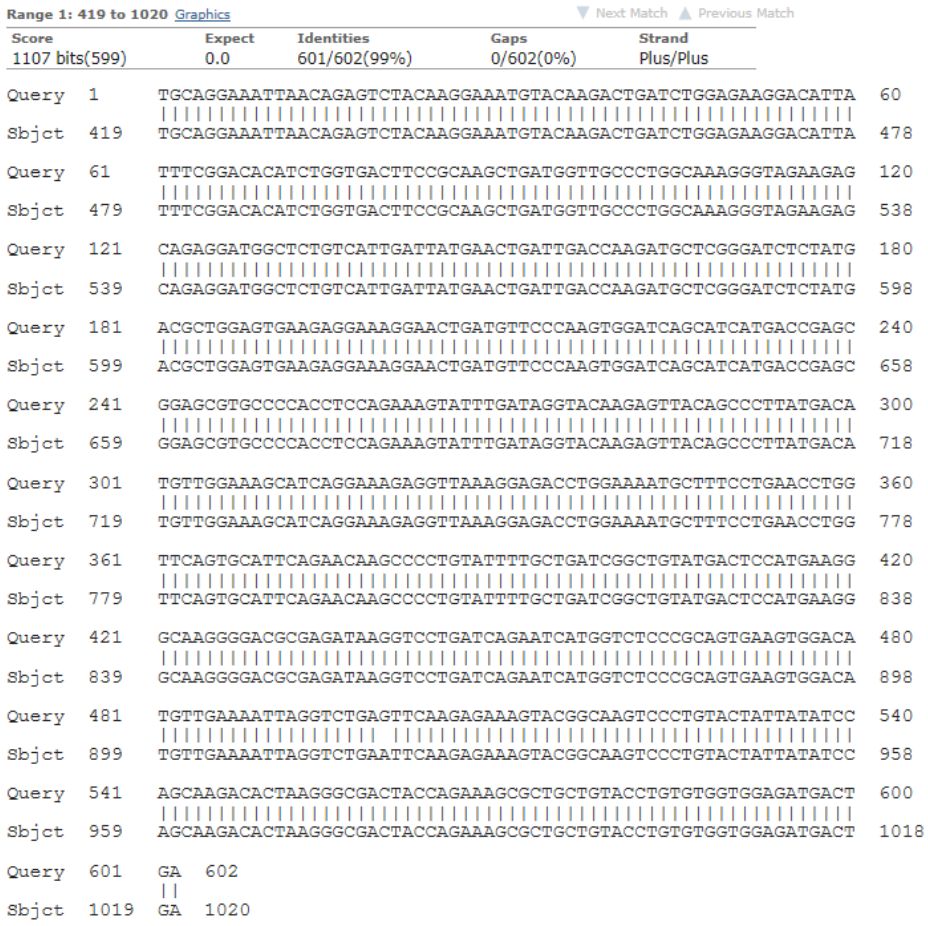

Range 1: 419 to 1020 Graphics Next Match Previous Match

Score	Expect	Identities	Gaps	Strand
1107 bits(599)	0.0	601/602(99%)	0/602(0%)	Plus/Plus

```
Query  1     TGCAGGAAATTAACAGAGTCTACAAGGAAATGTACAAGACTGATCTGGAGAAGGACATTA  60
             ||||||||||||||||||||||||||||||||||||||||||||||||||||||||||||
Sbjct  419   TGCAGGAAATTAACAGAGTCTACAAGGAAATGTACAAGACTGATCTGGAGAAGGACATTA  478

Query  61    TTTCGGACACATCTGGTGACTTCCGCAAGCTGATGGTTGCCCTGGCAAAGGGTAGAAGAG  120
             ||||||||||||||||||||||||||||||||||||||||||||||||||||||||||||
Sbjct  479   TTTCGGACACATCTGGTGACTTCCGCAAGCTGATGGTTGCCCTGGCAAAGGGTAGAAGAG  538

Query  121   CAGAGGATGGCTCTGTCATTGATTATGAACTGATTGACCAAGATGCTCGGGATCTCTATG  180
             ||||||||||||||||||||||||||||||||||||||||||||||||||||||||||||
Sbjct  539   CAGAGGATGGCTCTGTCATTGATTATGAACTGATTGACCAAGATGCTCGGGATCTCTATG  598

Query  181   ACGCTGGAGTGAAGAGGAAAGGAACTGATGTTCCCAAGTGGATCAGCATCATGACCGAGC  240
             ||||||||||||||||||||||||||||||||||||||||||||||||||||||||||||
Sbjct  599   ACGCTGGAGTGAAGAGGAAAGGAACTGATGTTCCCAAGTGGATCAGCATCATGACCGAGC  658

Query  241   GGAGCGTGCCCCACCTCCAGAAAGTATTTGATAGGTACAAGAGTTACAGCCCTTATGACA  300
             ||||||||||||||||||||||||||||||||||||||||||||||||||||||||||||
Sbjct  659   GGAGCGTGCCCCACCTCCAGAAAGTATTTGATAGGTACAAGAGTTACAGCCCTTATGACA  718

Query  301   TGTTGGAAAGCATCAGGAAAGAGGTTAAAGGAGACCTGGAAAATGCTTTCCTGAACCTGG  360
             ||||||||||||||||||||||||||||||||||||||||||||||||||||||||||||
Sbjct  719   TGTTGGAAAGCATCAGGAAAGAGGTTAAAGGAGACCTGGAAAATGCTTTCCTGAACCTGG  778

Query  361   TTCAGTGCATTCAGAACAAGCCCCTGTATTTTGCTGATCGGCTGTATGACTCCATGAAGG  420
             ||||||||||||||||||||||||||||||||||||||||||||||||||||||||||||
Sbjct  779   TTCAGTGCATTCAGAACAAGCCCCTGTATTTTGCTGATCGGCTGTATGACTCCATGAAGG  838

Query  421   GCAAGGGGACGCGAGATAAGGTCCTGATCAGAATCATGGTCTCCCGCAGTGAAGTGGACA  480
             ||||||||||||||||||||||||||||||||||||||||||||||||||||||||||||
Sbjct  839   GCAAGGGGACGCGAGATAAGGTCCTGATCAGAATCATGGTCTCCCGCAGTGAAGTGGACA  898

Query  481   TGTTGAAAATTAGGTCTGAGTTCAAGAGAAAGTACGGCAAGTCCCTGTACTATTATATCC  540
             |||||||||||||||||| ||||||||||||||||||||||||||||||||||||||||||
Sbjct  899   TGTTGAAAATTAGGTCTGAATTCAAGAGAAAGTACGGCAAGTCCCTGTACTATTATATCC  958

Query  541   AGCAAGACACTAAGGGCGACTACCAGAAAGCGCTGCTGTACCTGTGTGGTGGAGATGACT  600
             ||||||||||||||||||||||||||||||||||||||||||||||||||||||||||||
Sbjct  959   AGCAAGACACTAAGGGCGACTACCAGAAAGCGCTGCTGTACCTGTGTGGTGGAGATGACT  1018

Query  601   GA  602
             ||
Sbjct  1019  GA  1020
```

2. ANXA2 WT 400-1

>52F_002_AnxA2-WT_Anx-A21-400-1_F04 (32 .. 936 = 905_bp)

TGAGAGAGTCCTCGTCGGTTCCCAGCCCCTTCATGGAAGCCTTTAGCTCAGAAGCGT
CATACTGAGCAGGTGTCTTCAATAGGCCCAAAATCACCGTCTCCAGGTGGCCAGATA
AGGCTGACTTCAGTGCTGATGCAAGTTCCTTTTTGGTCCTTCTCTGGTAGGCGAAGG
CAATATCCTGTCTCTGTTCATTGCTGCGGTTGGTCAAAATGTTGACAATGGTGACCTC
ATCCACACCTTTGGTCTTGATGGCTGTTTCAATGTTCAAAGCATCCCGCTCAGCATCA
AAGTTAGTATAGGCTTTGACAGACCCATATGCACTTGGGGGTGTAGAGTGATCACCC
TCCAAGCTGAGCTTGCACAGGATTTCGTGAACAGTAGACATGGTTTATTCCTCCTTA
TTTAATCGATACATTAATATATACCTCTTTAATTTTTAATAATAAAGTTAATCGATAA
TTCCGGTCGAGTGCCCACACAGATTGTCTGATAAATTGTTAAAGAGCAGTGCCGCTT
CGCTTTTTCTCAGCGGCGCTGTTTCCTGTGTGAAATTGTTATCCGCTCACAATTCCAC
ACATTATACGAGCCGGATGATTAATTGTCAACAGCTCATTTCAGAATATTTGCCAGA
ACCGTTATGATGTCGGCGCAAAAAACATTATCCAGAACGGGAGTGCGCCTTGAGCG
ACACGAATTATGCAGTGATTTACGACCTGCACAGCCATACCACAGCTTCCGATGGCT
GCCTGACGCCAGAAGCATTGGTGCACCGTGCAGTCGATGATAAGCTGTCAAACCAG

ATCAATTCGCGCTAACTTACATTAATTGCGTTGCGCTCACTGCCCGCTTTCCAGTCGG
GAAACCTGTCGTGCCAGCTGCATTAATGAATCGGCCAACGCGCGGGG

Download Graphics

Sequence ID: Query_155771 Length: 1020 Number of Matches: 1

Range 1: 1 to 385 Graphics Next Match Previous Match

Score	Expect	Identities	Gaps	Strand
701 bits(379)	0.0	383/385(99%)	0/385(0%)	Plus/Minus

```
Query  1    TGAGAGAGTCCTCGTCGGTTCCCAGCCCCTTCATGGAAGCCTTTAGCTCAGAAGCGTCAT  60
            |||||||||||||||||||||||||||||||||||||||||| ||||||||||||||||||
Sbjct  385  TGAGAGAGTCCTCGTCGGTTCCCAGCCCCTTCATGGAAGCTTTTAGCTCAGAAGCGTCAT  326

Query  61   ACTGAGCAGGTGTCTTCAATAGGCCCAAAATCACCGTCTCCAGGTGGCCAGATAAGGCTG  120
            ||||||||||||||||||||||||||||||||||||||||||||||||||||||||||||
Sbjct  325  ACTGAGCAGGTGTCTTCAATAGGCCCAAAATCACCGTCTCCAGGTGGCCAGATAAGGCTG  266

Query  121  ACTTCAGTGCTGATGCAAGTTCCTTTTTGGTCCTTCTCTGGTAGGCGAAGGCAATATCCT  180
            ||||||||||||||||||||||||||||||||||||||||||||||||||||||||||||
Sbjct  265  ACTTCAGTGCTGATGCAAGTTCCTTTTTGGTCCTTCTCTGGTAGGCGAAGGCAATATCCT  206

Query  181  GTCTCTGTTCATTGCTGCGGTTGGTCAAAATGTTGACAATGGTGACCTCATCCACACCTT  240
            |||||||| ||||||||||||||||||||||||||||||||||||||||||||||||||||
Sbjct  205  GTCTCTGTGCATTGCTGCGGTTGGTCAAAATGTTGACAATGGTGACCTCATCCACACCTT  146

Query  241  TGGTCTTGATGGCTGTTTCAATGTTCAAAGCATCCCGCTCAGCATCAAAGTTAGTATAGG  300
            ||||||||||||||||||||||||||||||||||||||||||||||||||||||||||||
Sbjct  145  TGGTCTTGATGGCTGTTTCAATGTTCAAAGCATCCCGCTCAGCATCAAAGTTAGTATAGG  86

Query  301  CTTTGACAGACCCATATGCACTTGGGGGTGTAGAGTGATCACCCTCCAAGCTGAGCTTGC  360
            ||||||||||||||||||||||||||||||||||||||||||||||||||||||||||||
Sbjct  85   CTTTGACAGACCCATATGCACTTGGGGGTGTAGAGTGATCACCCTCCAAGCTGAGCTTGC  26

Query  361  ACAGGATTTCGTGAACAGTAGACAT  385
            |||||||||||||||||||||||||
Sbjct  25   ACAGGATTTCGTGAACAGTAGACAT  1
```

8.4 Appendix D: Mass Spectrometry Analysis of ANXA2 Gel Band

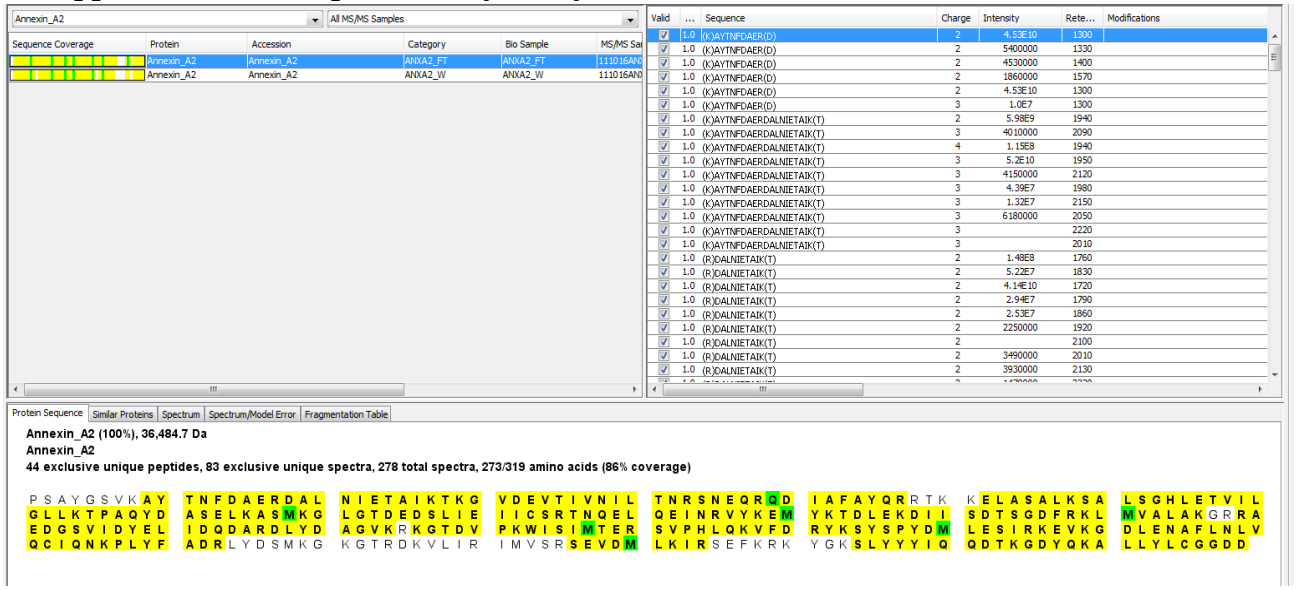

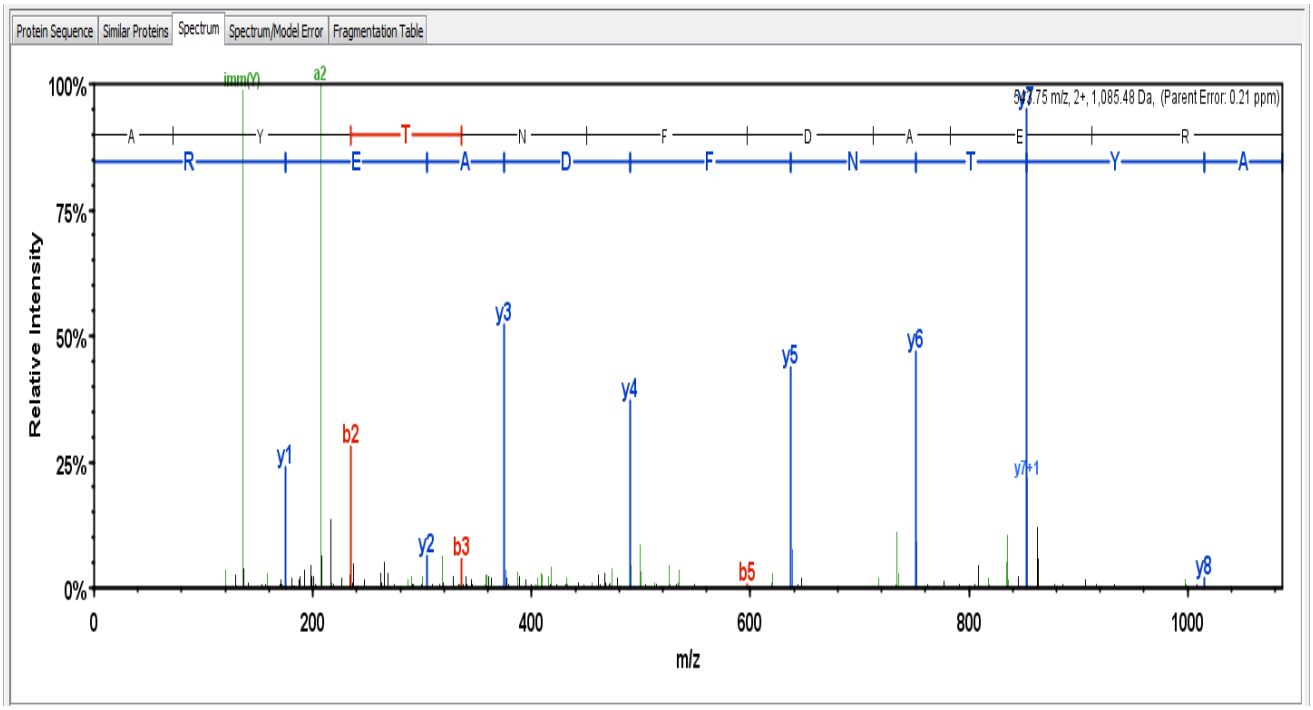

Figure 3: Mass Spectrometry Analysis of ANXA2 Gel Band by Dr. John Leszyk from the University of Massachusetts Medical School

8.5 Appendix E: Preliminary FRET Experiments

In order to see whether removing $PI_{(4,5)}P_2$from the system effects FRET transfer, preliminary experiments were performed with a lipid composition of 70% POPC, 30% POPS and 100% POPC using a 2 to 1 acceptor to donor ratio. The 100% POPC trials were intended to show the degree of light scattering by lipids that does not result from ANXA2-mediated aggregation, because POPC is a neutral lipid that does not bind ANXA2. The 70% POPC 30% POPS trials were meant to see if a FRET transfer occurs in the absence of $PI_{(4,5)}P_2$. In the future, these experiments should be repeated with a higher acceptor to donor ratio in order to better understand the role of the anionic phospholipid POPS in ANXA2 self-association. The 100% POPC experiments should be repeated to better understand the role of light scattering by lipids which does not result from aggregation because POPC is neutral and will not cluster in the presence of calcium or interact with ANXA2.

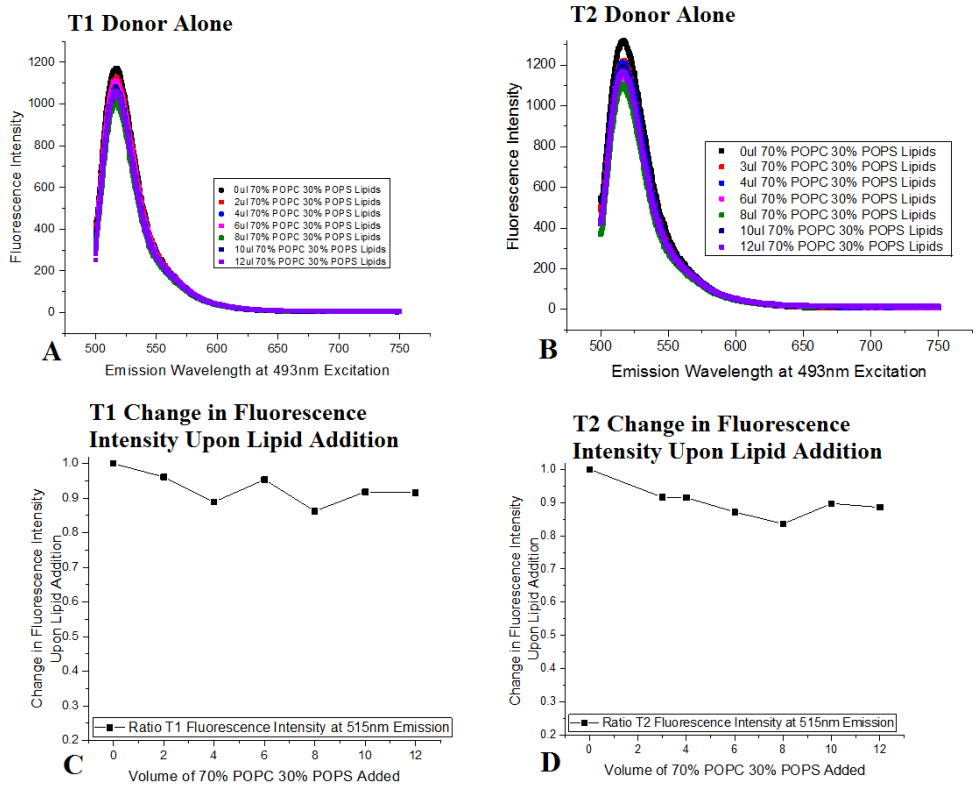

Figure 8.2: *70% POPC 30% POPC 2 to 1 Acceptor to Donor Lipid Titration. Starting concentration 0.5uM donor AlexaFluor 488 and 0.5uM calcium chloride concentration was 0.5mM. The emission spectra were dilution corrected to better display changes in fluorescence intensity upon lipid addition. See Tables 28-29 Appendix G for a summary of the different ratios of lipid to protein and the calcium concentration differences upon lipid addition. (A-B) Change in fluorescence intensity emission spectra upon lipid addition divided by fluorescence intensity prior to lipid addition (C-D) Change in Ratio of Fluorescence Intensity upon Lipid Addition, all values for each trial were divided by the fluorescence intensity when there were no lipids present.*

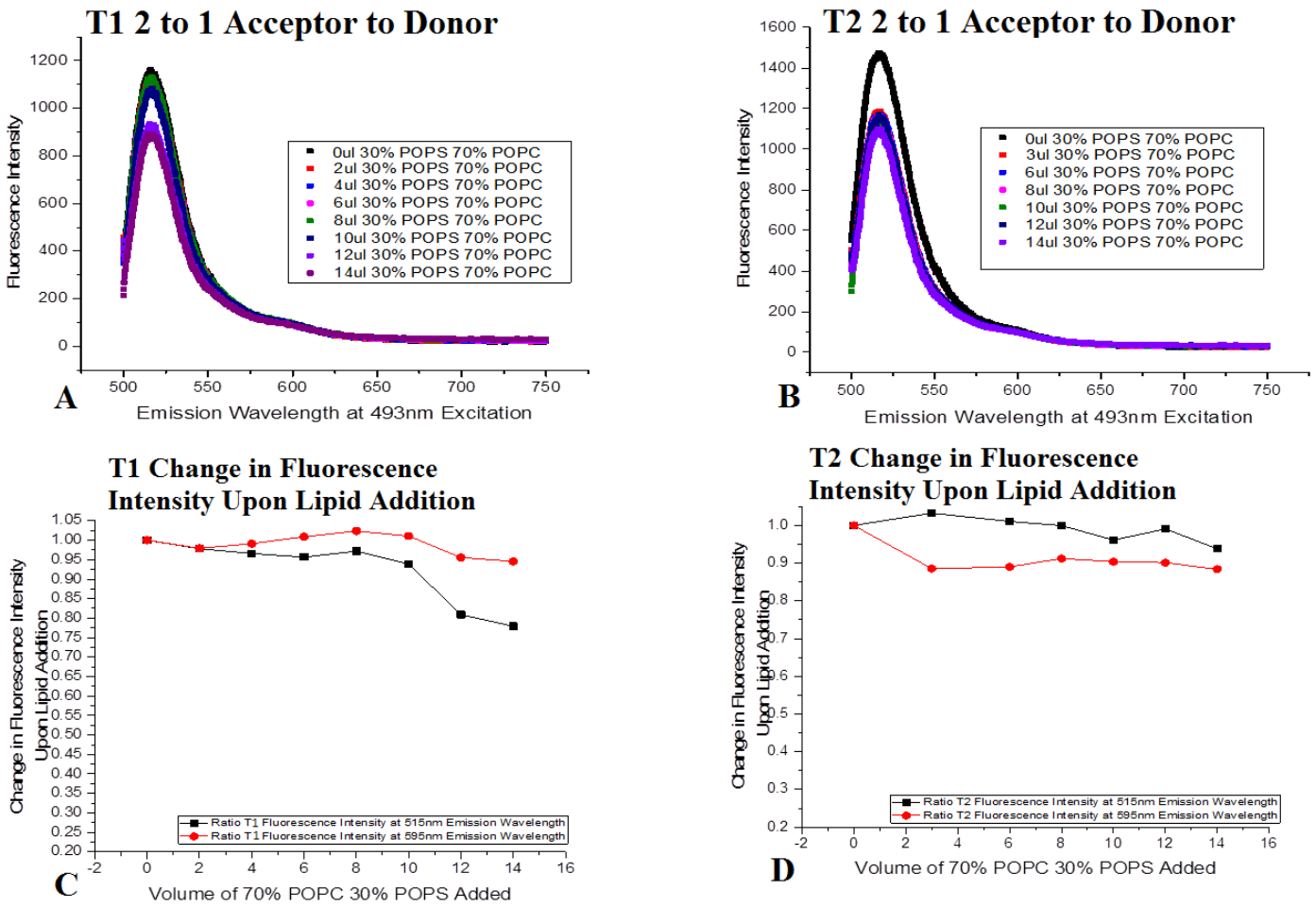

Figure 8.3: *<u>70% POPC 30% POPC 2 to 1 Acceptor to Donor Lipid Titration</u>. Starting concentration 0.5uM donor AlexaFluor 488, 1.0uM acceptor ANXA2 568, 0.5uM calcium chloride concentration was 0.5mM. The emission spectra were dilution corrected to better display changes in fluorescence intensity upon lipid addition. See Tables 30-31 Appendix G for a summary of the different ratios of lipid to protein and the calcium concentration differences upon lipid addition. (A-B) Change in fluorescence intensity emission spectra upon lipid addition divided by fluorescence intensity prior to lipid addition (C-D) Change in Ratio of Fluorescence Intensity upon Lipid Addition, all values for each trial were divided by the fluorescence intensity when there were no lipids present.*

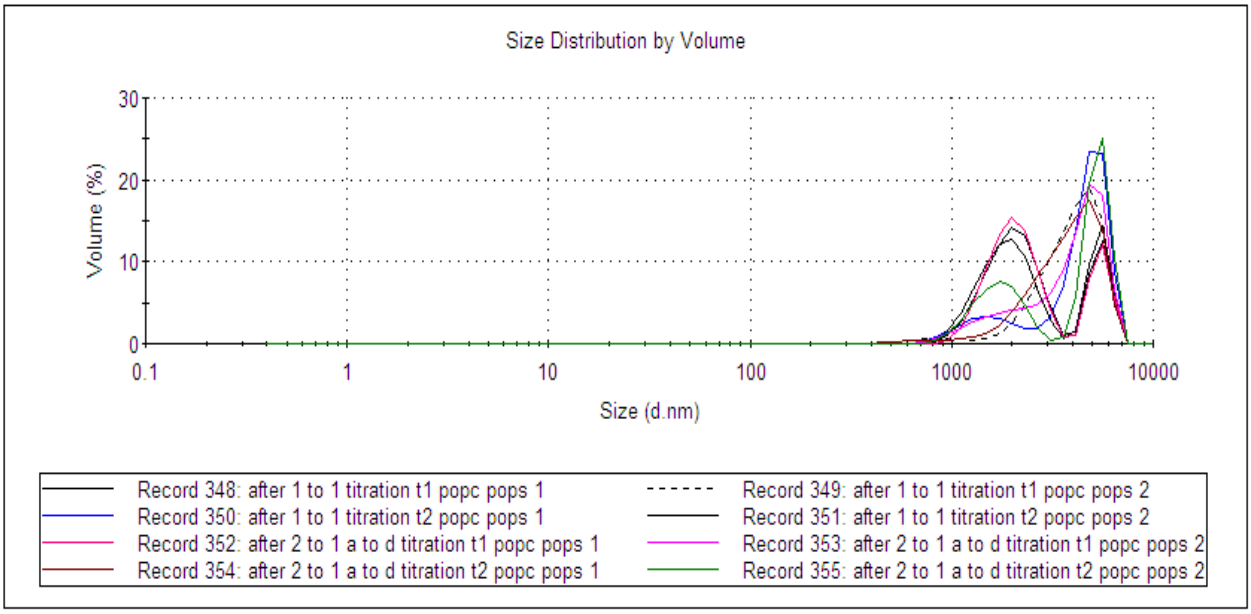

Figure 8.4: *Size Distribution by Volume of the ANXA2 WT AlexaFluor 488 and AlexaFluor 568 after titration with 70% POPC 30% POPS*

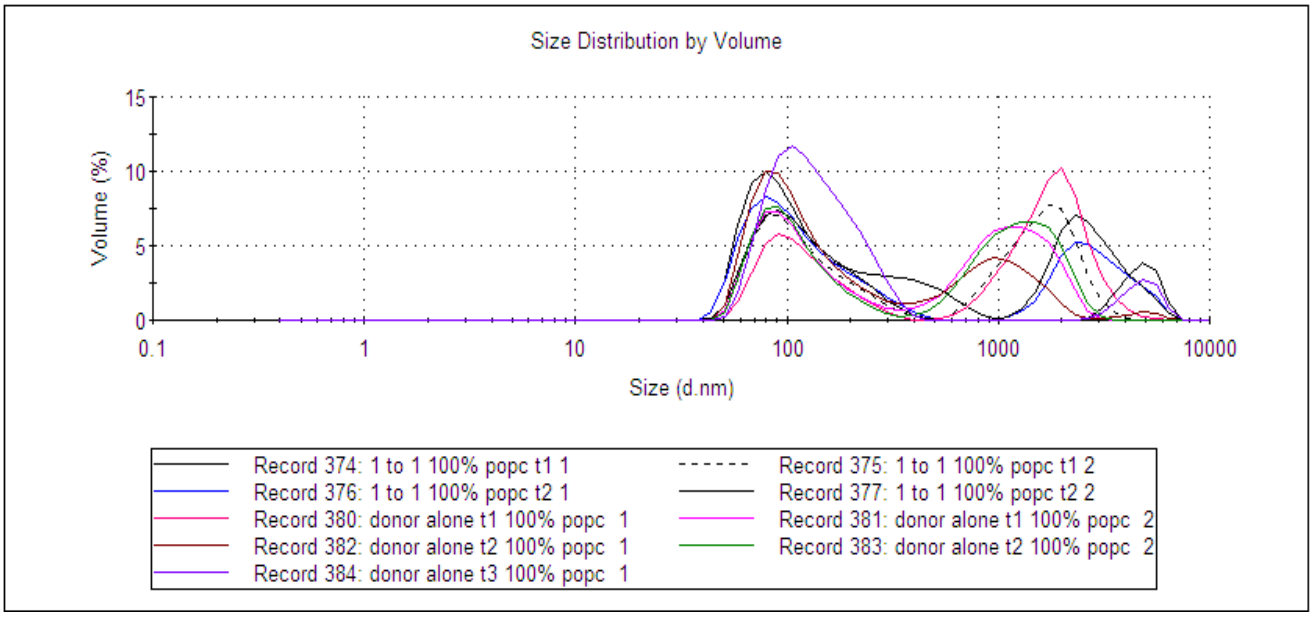

Figure 8.5: *Size Distribution by Volume of the ANXA2 WT AlexaFluor 488 and AlexaFluor 568 after titration with 100% POPC*

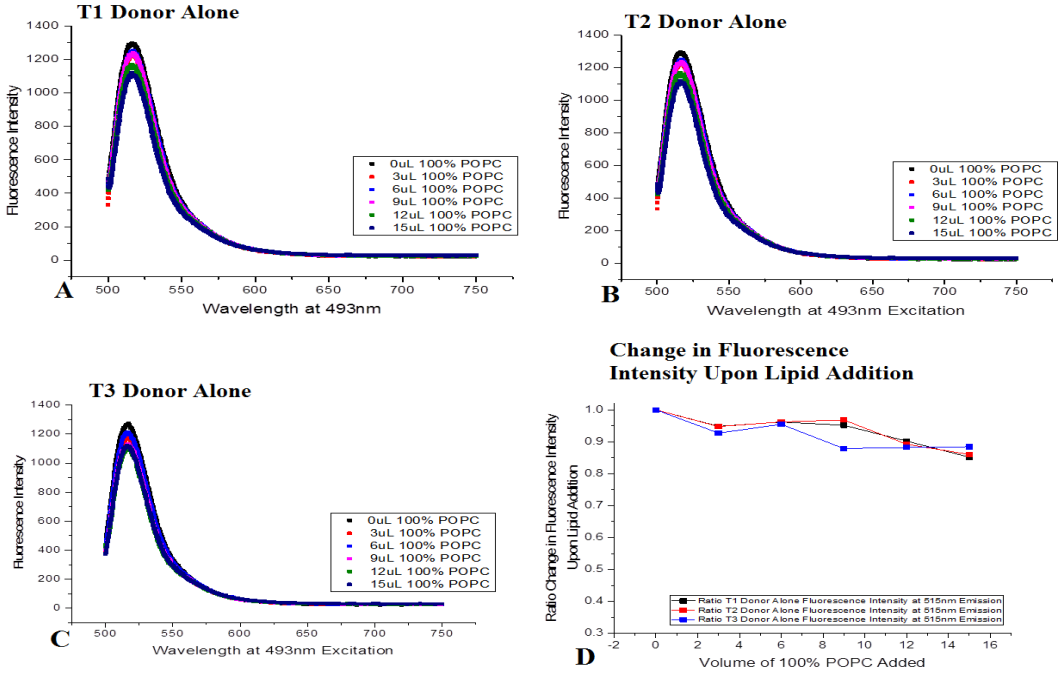

Figure 8.6: *<u>100% POPC Donor Alone Lipid Titration</u>. Starting concentration: 0.5uM donor AlexaFluor 488 and 0.5uM calcium chloride concentration was 0.5mM. The emission spectra were dilution corrected to better display changes in fluorescence intensity upon lipid addition. See Appendix _ for a summary of the different ratios of lipid to protein and the calcium concentration differences upon lipid addition. (A-C) Change in fluorescence intensity emission spectra upon lipid addition divided by fluorescence intensity prior to lipid addition (D) Change in Ratio of Fluorescence Intensity upon Lipid Addition, all values for each trial were divided by the fluorescence intensity when there were no lipids present.*

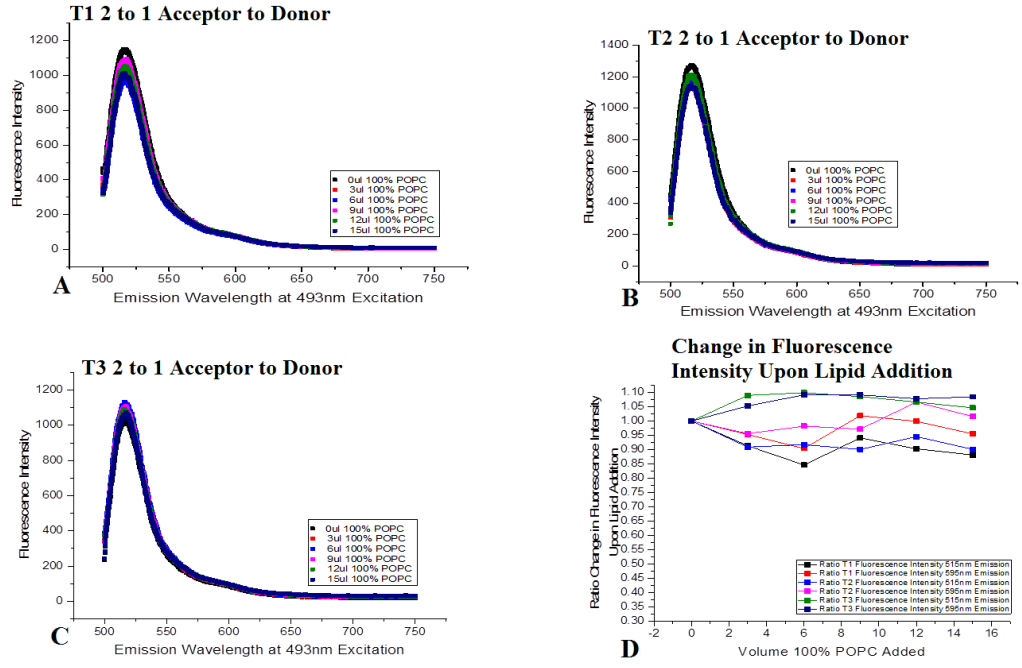

Figure 8.7*: <u>100% POPC 2 to 1 Acceptor to Donor Lipid Titration</u>. I Starting concentration 0.5uM donor AlexaFluor 488, 1.0uM acceptor ANXA2 568, and 0.5uM calcium chloride concentration was 0.5mM. The emission spectra were dilution corrected to better display changes in fluorescence intensity upon lipid addition. See Tables 32-33 Appendix G for a summary of the different ratios of lipid to protein and the calcium concentration differences upon lipid addition. (A-C) Change in fluorescence intensity emission spectra upon lipid addition divided by fluorescence intensity prior to lipid addition (D) Change in Ratio of Fluorescence Intensity upon Lipid Addition, all values for each trial were divided by the fluorescence intensity when there were no lipids present.*

8.6 Appendix F: Tables of Compiled FRET Data for Each Titration

__Table 1__: Change in Donor Emission Fluorescence Intensity Upon 95% POPC 5% $PI_{(4,5)}P_2$ Lipid Addition, Donor Alone

Volume of 95% POPC 5% PI(4,5)P2 Added	T1	T2	T3
0	1	1	1
3	0.9183	0.93239	0.9256
6	0.7636	0.8082	0.9601
9	0.9609	0.8332	0.8958
12	0.8352	0.8790	0.9179
15	0.8854	0.7855	0.9129
18	0.9034	0.8681	0.9371
Average Change	**0.8953**	**0.8723**	**0.9356**

__Table 2__: Change in Fluorescence Intensity Upon 95% POPC 5% $PI_{(4,5)}P_2$ Lipid Addition, 3 to 1 Donor to Acceptor

Volume of 95% POPC 5% PI(4,5)P2 Added	T1 Donor Emission	T1 Acceptor Emission	T2 Donor Emission	T2 Acceptor Emission
0	1	1	1	1
3	1.0245	1.004	0.9127	0.9834
6	0.9376	0.9906	0.9605	1.0284
9	0.9552	1.0142	0.8790	1.0149
12	1.1020	1.1371	0.8836	1.0336
15	0.9211	1.0474	0.9632	1.1179
18	0.8891	1.0923	0.8984	1.0785
Average Change	**0.9756**	**1.0408**	**0.9282**	**1.0367**

__Table 3__: Change in Fluorescence Intensity Upon 95% POPC 5% PI(4,5)P2 Lipid Addition, 4 to 1 Acceptor to Donor

Volume of 95% POPC 5% PI(4,5)P2 Added	T1 Donor Emission	T1 Acceptor Emission
0	1	1
3	0.6102	1.0893
6	0.6392	1.1412
9	0.6710	1.1233
12	0.6406	1.1273
Average Change	**0.7122**	**1.0962**

***Table 4**: Change Fluorescence Intensity Donor Emission Upon 65% POPC 5% PI(4,5)P2 30% POPS Lipid Addition, 4 to 1 Acceptor to Donor*

Volume of 65% POPC 5% PI(4,5)P2 30% POPS Added	T1 Donor Alone	T2 Donor Alone	T1	T2	T3
0	1	1	1	1	1
3	0.9621	0.9315	0.7690	0.9705	0.8146
6	0.9052	1.0245	0.8516	0.8904	0.9329
9	0.8082	0.9874	0.6081	0.8006	0.8436
12	0.8433	0.9078	0.7898	0.9159	0.7480
15	0.8900	-	0.7917	0.8717	0.8312
Average Change	**0.9015**	**0.9702**	**0.8017**	**0.9082**	**0.8617**

***Table 5**: Change Fluorescence Intensity Acceptor Emission Upon 65% POPC 5% PI(4,5)P2 30% POPS Lipid Addition, 4 to 1 Acceptor to Donor*

Volume of 65% POPC 15% PI(4,5)P2 30% POPS Added	T1 Donor Alone	T2 Donor Alone	T1	T2	T3
0	1	1	1	1	1
3	1.0067	1.0102	0.8910	0.9932	0.8915
6	1.0094	1.0182	0.9478	0.9321	0.9645
9	0.9829	1.0488	0.7824	0.8849	0.9512
12	1.0256	1.0762	0.9200	0.9937	0.8758
15	1.1251	-	0.8717	0.9707	0.9909
Average Change	**1.0250**	**1.0307**	**0.9022**	**0.9624**	**0.9457**

***Table 6**: Change in Fluorescence Intensity of the Donor Emission Divided by the T1 Donor Alone Change in Fluorescence Intensity, 4 to 1 Acceptor to Donor, 65% POPC 5% PI(4,5)P2 30% POPS*

Volume of 65% POPC 15% PI(4,5)P2 30% POPS Added	T1	T2	T3
0	0.9312	1.1924	0.723
3	0.7443	1.2028	0.6141
6	0.8761	1.1729	0.7474
9	0.7006	1.1812	0.7570
12	0.8721	1.2951	0.6433
15	0.8288	1.1685	0.9780
Average Change	**0.8255**	**1.2022**	**1.8793**

***Table 7:** Change Fluorescence Intensity Acceptor Emission Upon Calcium Chloride Addition, 4 to 1 Acceptor to Donor, 55% POPC15% PI(4,5)P2 30% POPS*

Volume of 10m CaCl2 Added	Donor Alone	T1	T2	T3	T4
0	1	1	1	1	1
2	1.0664	0.86124	0.99576	1.0508	1.04331
4	1.1322	0.84528	1.04138	0.96472	1.24533
6	1.0881	0.93121	0.97921	0.90536	1.22904
8	1.0955	0.89563	1.0132	0.96115	1.25332
10	1.1177	0.8262	0.96891	1.03763	1.24081
12	1.09073	0.87213	0.9888	1.00941	1.2462
14	1.11172	0.84813	0.99233	0.9428	1.15464
Average Change	**1.0878**	**0.8850**	**0.9974**	**0.9840**	**1.1766**

***Table 8**: Change Fluorescence Intensity Donor Emission Upon Calcium Chloride Lipid Addition, 4 to 1 Acceptor to Donor, 55% POPC 15% PI(4,5)P2 30% POPS*

Volume of 55% POPC 15% PI(4,5)P2 30% POPS Added	Donor Alone	T1	T2	T3	T4
0	1	1	1	1	1
2	1.0294	0.8941	1.0237	1.0437	0.9469
4	1.0925	0.9079	1.0706	0.9517	1.0447
6	1.1194	0.9723	1.0067	0.9718	1.0635
8	1.1110	0.9723	1.0548	0.9977	1.0790
10	1.1844	0.9054	1.0170	1.0702	1.0370
12	1.1478	0.9924	1.0432	1.0449	1.0398
14	1.1936	0.9703	1.0517	1.0207	1.0119

Average Change	**1.1100**	**0.9518**	**1.1013**	**1.0126**	**1.0279**

Table 9: *Change in Donor Emission Fluorescence Intensity Upon Calcium Chloride Addition, 85% POPC 15% PI(4,5)P2, 4 to 1 Acceptor to Donor*

Volume 10mM CaCl2 Added	**Donor Alone**	**T1**	**T2**	**T3**
0	1	1	1	1
2	1.00564	0.97653	0.97358	1.10244
4	0.96807	1.01865	1.05727	1.11293
6	1.00449	0.92757	1.05413	1.1179
8	0.8802	0.76414	1.03399	1.05542
10	0.9204	0.8927	0.99204	1.04982
12	0.93021	0.95459	1.05874	1.11103
14	0.91071	0.92459	1.04037	0.98219
Average Change in Fluorescence Intensity	**0.952465**	**0.93235**	**1.02627**	**1.06647**

Table 10*: Change in Donor Emission Fluorescence Intensity Divided by Donor Alone Titration, 85% POPC 15% PI(4,5)P2, 4 to 1 Acceptor to Donor*

Volume 10mM CaCl2 Added	**T1**	**T2**	**T3**
0	1.0612	0.9732	1.05736
2	1.0305	0.9422	1.15914
4	1.1166	1.0629	1.21558
6	0.9799	1.0213	1.17674
8	0.9215	1.1435	1.26812
10	1.0287	1.0484	1.20534
12	1.0890	1.1077	1.2629
14	1.0774	1.1118	1.1404
Average Change in Fluorescence Intensity	1.0381	1.0514	1.1857

***Table 11**: Change in Donor Emission Fluorescence Intensity Upon 85% POPC 15% PI(4,5)P2 Addition, 4 to 1 Acceptor to Donor*

Volume of 85% POPC 15% PI(4,5)P2 Added	Donor Alone	T1	T2	T3
0	1	1	1	1
3	0.9143	0.9351	0.8741	0.9064
6	0.8033	0.7703	0.8473	0.8793
9	0.8281	0.7939	0.7931	0.7724
12	0.7894	0.7677	0.7239	0.7755
15	0.7535	0.6322	0.7214	0.7567
18	0.6510	0.6562	0.6505	0.7411
Average Change	**0.8199**	**0.7936**	**0.805**	**0.8331**

***Table 12**: Change in Fluorescence Intensity Donor Emission Divided by Donor Alone Fluorescence Intensity, 85% POPC 15% PI(4,5)P2, 4 to 1 Acceptor to Donor*

Volume of 85% POPC 15% PI(4,5)P2 Added	T1	T2	T3
0	0.9046	1.0974	1.0974
3	0.9252	1.0491	1.0879
6	0.8675	1.1576	1.2013
9	0.8672	1.0510	1.0235
12	0.8799	1.0063	1.0781
15	0.7590	1.0507	1.1021
18	0.9119	1.0966	1.2494
Average Change	**0.8736**	**1.0727**	**1.1200**

***Table 13**: Change in Fluorescence Intensity Upon 70% POPC 30% POPS Addition, 2 to 1 Acceptor to Donor*

Volume of 70% POPC 30% POPS Added	T1 Donor Emission	T1 Acceptor Emission	T2 Donor Emission	T2 Acceptor Emission	Donor Alone T1	Donor Alone T2
0	1	1	1	1	1	1
2	0.97825	0.9793	-	-	0.96102	-
3	-	-	1.0326	0.8854	-	0.91594
4	0.9660	0.9911	-	-	0.88894	0.91498
6	0.9566	1.0089	1.0107	0.8904	0.95359	0.87125
8	0.9721	1.0237	0.9997	0.9121	0.86249	0.83609
10	0.9389	1.0109	0.9612	0.9038	0.91815	0.89732
12	.8090	0.9556	0.9909	0.9013	0.91571	0.8855
14	0.7791	0.9457	0.9376	0.8837	-	-
Average Change	**0.9245**	**0.9894**	**0.9904**	**0.9110**	**0.9286**	**0.9030**

***Table 14**: Change in Donor Emission Fluorescence Intensity Upon 100% POPC Addition, Donor Alone*

Volume of 100% POPC Added (uL)	T1	T2	T3
0	1	1	1
3	0.9484	0.9477	0.9273
6	0.9619	0.9624	0.9549
9	0.9518	0.9683	0.8788
12	0.9023	0.8925	0.8824
15	0.8520	0.8603	0.8845
Average Change	0.9361	0.9385	0.9213

***Table 15**: Change in Donor Emission Fluorescence Intensity Upon 100% POPC Addition, 2 to 1 Acceptor to Donor*

Volume of 100% POPC Added (uL)	T1	T2	T3
0	1	1	1
3	0.91346	0.9091	1.0524
6	0.8465	0.9175	1.0989
9	0.9411	0.9007	1.0854
12	0.9031	0.9456	1.0662
15	0.8811	0.9011	1.0461
Average Change	0.9142	0.9290	1.0582

***Table 16**: Change in Acceptor Emission Fluorescence Intensity Upon 100% POPC Addition, 2 to 1 Acceptor to Donor*

Volume of 100% POPC Added (uL)	T1	T2	T3
0	1	1	1
3	0.9532	0.9561	1.0524
6	0.9041	0.9822	1.0916
9	1.0189	0.9717	1.0911
12	0.9990	1.0664	1.0779
15	0.9550	1.0158	1.0847
Average Change	0.9717	0.9987	1.0663

8.7 Appendix G: Tables of Changes in Lipid, ANXA2 & CaCl2 During FRET Experiments

***Table 17**: 95% POPC 5% PI(4,5)P2, Donor Alone Lipid Titration. Calcium, Protein, and Lipid Concentrations and Ratios throughout the Experiment.*

Volume of 95% POPC 5% PI(4,5)P2 Added (uL)	Lipid Volume in L	Lipid Concentration (M)	mM Lipid Concentration	uM Lipid Concentration Dilution Corrected	Starting ANXA2 Acceptor Concentration (uM)	Starting ANXA2 Donor Concentration (uM)	Starting ANXA2 Donor (umoles)	Lipid to Protein Ratio	Starting CaCl2 Concentration (mM)	Starting CaCl2 Conc mmol	Starting CaCl2 Conc uM	CaCl2 umol
0	0	0	0	0	0	0.5	30	0	0.5	0.00003	500	30000
3	0.000003	0.000015	0.015	14.28571	0	0.47619	30	30	0.47619	30	476.1905	30000
6	0.000006	0.00003	0.03	27.27273	0	0.454545	30	60	0.454545	30	454.5455	30000
9	0.000009	0.000045	0.045	39.13043	0	0.434783	30	90	0.434783	30	434.7826	30000
12	0.000012	0.00006	0.06	50	0	0.416667	30	120	0.416667	30	416.6667	30000
15	0.000015	0.000075	0.075	60	0	0.4	30	150	0.4	30	400	30000
18	0.000018	0.00009	0.09	69.23077	0	0.384615	30	180	0.384615	30	384.6154	30000

***Table 18**: 95% POPC 5% PI(4,5)P2 Lipid Titration, 3 to 1 Acceptor to Donor. Calcium, Protein, and Lipid Concentrations and Ratios throughout the Experiment.*

Volume of 95% POPC 5% PI(4,5)P2 Added (uL)	Lipid Volume in L	Lipid Concentration (M)	mM Lipid Concentration	uM Lipid Concentration Dilution Corrected	Starting ANXA2 Acceptor Concentration (uM)	Starting ANXA2 Donor Concentration (uM)	Starting ANXA2 Donor (umoles)	Lipid to Protein Ratio	Starting CaCl2 Concentration (mM)	Starting CaCl2 Conc mmol	Starting CaCl2 Conc uM	CaCl2 umol
0	0	0	0	0	1.5	0.5	30	0	0.5	0.00003	500	30000
3	0.000003	0.000015	0.015	14.28571	1.428571	0.47619	30	7.5	0.47619	30	476.1905	30000
6	0.000006	0.00003	0.03	27.27273	1.363636	0.454545	30	15	0.454545	30	454.5455	30000
9	0.000009	0.000045	0.045	39.13043	1.304348	0.434783	30	22.5	0.434783	30	434.7826	30000
12	0.000012	0.00006	0.06	50	1.25	0.416667	30	30	0.416667	30	416.6667	30000
15	0.000015	0.000075	0.075	60	1.2	0.4	30	37.5	0.4	30	400	30000
18	0.000018	0.00009	0.09	69.23077	1.153846	0.384615	30	45	0.384615	30	384.6154	30000

***Table 19**: 95% POPC 5% PI(4,5)P2 Lipid Titration, 4 to 1 Acceptor to Donor. Calcium, Protein, and Lipid Concentrations and Ratios throughout the Experiment.*

Volume of 95% POPC 5% PI(4,5)P2 Added (uL)	Lipid Volume in L	Lipid Concentration (M)	mM Lipid Concentration	uM Lipid Concentration Dilution Corrected	Starting ANXA2 Acceptor Concentration (uM)	Starting ANXA2 Donor Concentration (uM)	Starting ANXA2 Donor (umoles)	Lipid to Protein Ratio	Starting CaCl2 Concentration (mM)	Starting CaCl2 Conc mmol	Starting CaCl2 Conc uM	CaCl2 umol
0	0	0	0	0	1	0.25	15	0	0.5	0.00003	500	30000
3	0.000003	0.000015	0.015	14.28571	0.952381	0.238095	15	12	0.47619	30	476.1905	30000
6	0.000006	0.00003	0.03	27.27273	0.909091	0.227273	15	24	0.454545	30	454.5455	30000
9	0.000009	0.000045	0.045	39.13043	0.869565	0.217391	15	36	0.434783	30	434.7826	30000
12	0.000012	0.00006	0.06	50	0.833333	0.208333	15	48	0.416667	30	416.6667	30000
15	0.000015	0.000075	0.075	60	0.8	0.2	15	60	0.4	30	400	30000
14	0.000014	0.00007	0.07	56.75676	0.810811	0.202703	15	56	0.405405	30	405.4054	30000
14	0.000014	0.00007	0.07	56.75676	0.810811	0.202703	15	56	0.405405	30	405.4054	30000

***Table 20**: 65% POPC 5% PI(4,5)P2 30% POPS Lipid Titration, 4 to 1 Acceptor to Donor. Calcium, Protein, and Lipid Concentrations and Ratios throughout the Experiment.*

Volume of 65% POPC 5% PI(4,5)P2 30% POPS Added (uL)	Lipid Volume in L	Lipid Concentration (M)	mM Lipid Concentration	uM Lipid Concentration Dilution Corrected	Starting ANXA2 Acceptor Concentration (uM)	Starting ANXA2 Donor Concentration (uM)	Starting ANXA2 Donor (umoles)	Lipid to Protein Ratio	Starting CaCl2 Concentration (mM)	Starting CaCl2 Conc mmol	Starting CaCl2 Conc uM	CaCl2 umol
0	0	0	0	0	2	0.5	30	0	0.5	0.00003	500	30000
3	0.000003	0.000015	0.015	14.28571	1.904762	0.47619	30	6	0.47619	30	476.1905	30000
6	0.000006	0.00003	0.03	27.27273	1.818182	0.454545	30	12	0.454545	30	454.5455	30000
9	0.000009	0.000045	0.045	39.13043	1.73913	0.434783	30	18	0.434783	30	434.7826	30000
12	0.000012	0.00006	0.06	50	1.666667	0.416667	30	24	0.416667	30	416.6667	30000
15	0.000015	0.000075	0.075	60	1.6	0.4	30	30	0.4	30	400	30000

***Table 21**: 65% POPC 5% PI(4,5)P2 30% POPS Lipid Titration, Donor Alone. Calcium, Protein, and Lipid Concentrations and Ratios throughout the Experiment.*

Volume of 65% POPC 5% PI(4,5)P2 30% POPS Added (uL)	Lipid Volume in L	Lipid Concentration (M)	mM Lipid Concentration	uM Lipid Concentration Dilution Corrected	Starting ANXA2 Acceptor Concentration (uM)	Starting ANXA2 Donor Concentration (uM)	Starting ANXA2 Donor (umoles)	Lipid to Protein Ratio	Starting CaCl2 Concentration (mM)	Starting CaCl2 Conc mmol	Starting CaCl2 Conc uM	CaCl2 umol
0	0	0	0	0	0	0.5	30	0	0.5	0.00003	500	30000
3	0.000003	0.000015	0.015	14.28571	0	0.47619	30	30	0.47619	30	476.1905	30000
6	0.000006	0.00003	0.03	27.27273	0	0.454545	30	60	0.454545	30	454.5455	30000
9	0.000009	0.000045	0.045	39.13043	0	0.434783	30	90	0.434783	30	434.7826	30000
12	0.000012	0.00006	0.06	50	0	0.416667	30	120	0.416667	30	416.6667	30000
15	0.000015	0.000075	0.075	60	0	0.4	30	150	0.4	30	400	30000

***Table 22**: 55% POPC 15% PI(4,5)P2 30% POPS 4 to 1 Acceptor to Donor CaCl2 Titration. Calcium, EGTA, Protein, and Lipid Concentrations and Ratios throughout the Experiment*

Volume 10mM CaCl2 Added (uL)	CaCl2 Volume in L	CaCl2 Concentration (M)	mM CaCl2 Concentration	Dilution Corrected uM CaCl2 Concentration	Starting ANXA2 Acceptor Concentration (uM)	Starting ANXA2 Donor Concentration (uM)	Starting ANXA2 Donor Not Dilution Corrected (umoles)	Ratio Lipid to Protein	Starting EGTA Concentration (mM)	Starting EGTA conc uM	EGTA-CaCl2	Starting EGTA Not Dilution Corrected	uM 55% POPC 15% PI(4,5)P2 30% POPS Lipid Concentration
0	0	0	0	0	2	0.5	30	30	0.5	500	500	30000	75
2	0.000002	0.000333	0.333333	322.5806	1.935484	0.483871	30	30	0.483871	483.871	161.2903	30000	72.58065
4	0.000004	0.000667	0.666667	625	1.875	0.46875	30	29.03226	0.46875	468.75	-156.25	30000	68.04435
6	0.000006	0.001	1	909.0909	1.818182	0.454545	30	27.21774	0.454545	454.5455	-454.545	30000	61.8585
8	0.000008	0.001333	1.333333	1176.471	1.764706	0.441176	30	24.7434	0.441176	441.1765	-735.294	30000	54.58103
10	0.00001	0.001667	1.666667	1428.571	1.714286	0.428571	30	21.83241	0.428571	428.5714	-1000	30000	46.78374
12	0.000012	0.002	2	1666.667	1.666667	0.416667	30	18.7135	0.416667	416.6667	-1250	30000	38.98645
14	0.000014	0.002333	2.333333	1891.892	1.621622	0.405405	30	15.59458	0.405405	405.4054	-1486.49	30000	31.61064

***Table 23**: 55% POPC 15% PI(4,5)P2 30% POPS Donor Alone CaCl2 Titration. Calcium, EGTA, Protein, and Lipid Concentrations and Ratios throughout the Experiment.*

Volume 10mM CaCl2 Added (uL)	CaCl2 Volume in L	CaCl2 Concentration (M)	mM CaCl2 Concentration	Dilution Corrected uM CaCl2 Concentration	Starting ANXA2 Acceptor Concentration (uM)	Starting ANXA2 Donor Concentration (uM)	Starting ANXA2 Donor Not Dilution Corrected (umoles)	Ratio Lipid to Protein	Starting EGTA Concentration (mM)	Starting EGTA conc uM	EGTA-CaCl2	Starting EGTA Not Dilution Corrected	uM 55% POPC 15% PI(4,5)P2 30% POPS Lipid Concentration
0	0	0	0	0	0	0.5	30	150	0.5	500	500	30000	75
2	0.000002	0.000333	0.333333	322.5806	0	0.483871	30	150	0.483871	483.871	161.2903	30000	72.58065
4	0.000004	0.000667	0.666667	625	0	0.46875	30	145.1613	0.46875	468.75	-156.25	30000	68.04435
6	0.000006	0.001	1	909.0909	0	0.454545	30	136.0887	0.454545	454.5455	-454.545	30000	61.8585
8	0.000008	0.001333	1.333333	1176.471	0	0.441176	30	123.717	0.441176	441.1765	-735.294	30000	54.58103
10	0.00001	0.001667	1.666667	1428.571	0	0.428571	30	109.1621	0.428571	428.5714	-1000	30000	46.78374
12	0.000012	0.002	2	1666.667	0	0.416667	30	93.56749	0.416667	416.6667	-1250	30000	38.98645
14	0.000014	0.002333	2.333333	1891.892	0	0.405405	30	77.9729	0.405405	405.4054	-1486.49	30000	31.61064

***Table 24**: 85% POPC 15% PI(4,5)P2, 4 to 1 Acceptor to Donor CaCl2 Titration. Calcium, EGTA, Protein, and Lipid Concentrations and Ratios throughout the Experiment.*

Volume 10mM CaCl2 Added (uL)	CaCl2 Volume in L	CaCl2 Concentration (M)	mM CaCl2 Concentration	Dilution Corrected uM CaCl2 Concentration	Starting ANXA2 Acceptor Concentration (uM)	Starting ANXA2 Donor Concentration (uM)	Starting ANXA2 Donor Not Dilution Corrected (umoles)	Ratio Lipid to Protein	Starting EGTA Concentration (mM)	Starting EGTA conc uM	EGTA-CaCl2	Starting EGTA Not Dilution Corrected	uM 85% POPC 15% PI(4,5)P2 Lipid Concentration
0	0	0	0	0	2	0.5	30	30	0.5	500	500	30000	75
2	0.000002	0.000333	0.333333	322.5806	1.935484	0.483871	30	30	0.483871	483.871	161.2903	30000	72.58065
4	0.000004	0.000667	0.666667	625	1.875	0.46875	30	29.03226	0.46875	468.75	-156.25	30000	68.04435
6	0.000006	0.001	1	909.0909	1.818182	0.454545	30	27.21774	0.454545	454.5455	-454.545	30000	61.8585
8	0.000008	0.001333	1.333333	1176.471	1.764706	0.441176	30	24.7434	0.441176	441.1765	-735.294	30000	54.58103
10	0.00001	0.001667	1.666667	1428.571	1.714286	0.428571	30	21.83241	0.428571	428.5714	-1000	30000	46.78374
12	0.000012	0.002	2	1666.667	1.666667	0.416667	30	18.7135	0.416667	416.6667	-1250	30000	38.98645
14	0.000014	0.002333	2.333333	1891.892	1.621622	0.405405	30	15.59458	0.405405	405.4054	-1486.49	30000	31.61064

***Table 25**: 85% POPC 15% PI(4,5)P2, Donor Alone CaCl2 Titration. Calcium, EGTA, Protein, and Lipid Concentrations and Ratios throughout the Experiment.*

Volume 10mM CaCl2 Added (uL)	CaCl2 Volume in L	CaCl2 Concentration (M)	mM CaCl2 Concentration	Dilution Corrected uM CaCl2 Concentration	Starting ANXA2 Acceptor Concentration (uM)	Starting ANXA2 Donor Concentration (uM)	Starting ANXA2 Donor Not Dilution Corrected (umoles)	Ratio Lipid to Protein	Starting EGTA Concentration (mM)	Starting EGTA conc uM	EGTA-CaCl2	Starting EGTA Not Dilution Corrected	uM 85% POPC 15% PI(4,5)P2 Lipid Concentration
0	0	0	0	0	0	0.5	30	150	0.5	500	500	30000	75
2	0.000002	0.000333	0.333333	322.5806	0	0.483871	30	150	0.483871	483.871	161.2903	30000	72.58065
4	0.000004	0.000667	0.666667	625	0	0.46875	30	145.1613	0.46875	468.75	-156.25	30000	68.04435
6	0.000006	0.001	1	909.0909	0	0.454545	30	136.0887	0.454545	454.5455	-454.545	30000	61.8585
8	0.000008	0.001333	1.333333	1176.471	0	0.441176	30	123.717	0.441176	441.1765	-735.294	30000	54.58103
10	0.00001	0.001667	1.666667	1428.571	0	0.428571	30	109.1621	0.428571	428.5714	-1000	30000	46.78374
12	0.000012	0.002	2	1666.667	0	0.416667	30	93.56749	0.416667	416.6667	-1250	30000	38.98645
14	0.000014	0.002333	2.333333	1891.892	0	0.405405	30	77.9729	0.405405	405.4054	-1486.49	30000	31.61064

***Table 26**: 85% POPC 15% PI(4,5)P2 Lipid Titration, Donor Alone. Calcium, Protein, and Lipid Concentrations and Ratios throughout the Experiment.*

Volume of 85% POPC 15% PI(4,5)P2 Added (uL)	Lipid Volume in L	Lipid Concentration (M)	mM Lipid Concentration	uM Lipid Concentration Dilution Corrected	Starting ANXA2 Acceptor Concentration (uM)	Starting ANXA2 Donor Concentration (uM)	Starting ANXA2 Donor (umoles)	Lipid to Protein Ratio	Starting CaCl2 Concentration (mM)	Starting CaCl2 Conc mmol	Starting CaCl2 Conc uM	CaCl2 umol
0	0	0	0	0	0	0.5	30	0	0.5	0.00003	500	30000
3	0.000003	0.000015	0.015	14.28571	0	0.47619	30	30	0.47619	30	476.1905	30000
6	0.000006	0.00003	0.03	27.27273	0	0.454545	30	60	0.454545	30	454.5455	30000
9	0.000009	0.000045	0.045	39.13043	0	0.434783	30	90	0.434783	30	434.7826	30000
12	0.000012	0.00006	0.06	50	0	0.416667	30	120	0.416667	30	416.6667	30000
15	0.000015	0.000075	0.075	60	0	0.4	30	150	0.4	30	400	30000
18	0.000018	0.00009	0.09	69.23077	0	0.384615	30	180	0.384615	30	384.6154	30000

***Table 27**: 85% POPC 15% PI(4,5)P2 Lipid Titration, 4 to 1 Acceptor to Donor. Calcium, Protein, and Lipid Concentrations and Ratios throughout the Experiment.*

Volume of 85% POPC 15% PI(4,5)P2 Added (uL)	Lipid Volume in L	Lipid Concentration (M)	mM Lipid Concentration	uM Lipid Concentration Dilution Corrected	Starting ANXA2 Acceptor Concentration (uM)	Starting ANXA2 Donor Concentration (uM)	Starting ANXA2 Donor (umoles)	Lipid to Protein Ratio	Starting CaCl2 Concentration (mM)	Starting CaCl2 Conc mmol	Starting CaCl2 Conc uM	CaCl2 umol
0	0	0	0	0	2	0.5	30	0	0.5	0.00003	500	30000
3	0.000003	0.000015	0.015	14.28571	1.904762	0.47619	30	6	0.47619	30	476.1905	30000
6	0.000006	0.00003	0.03	27.27273	1.818182	0.454545	30	12	0.454545	30	454.5455	30000
9	0.000009	0.000045	0.045	39.13043	1.73913	0.434783	30	18	0.434783	30	434.7826	30000
12	0.000012	0.00006	0.06	50	1.666667	0.416667	30	24	0.416667	30	416.6667	30000
15	0.000015	0.000075	0.075	60	1.6	0.4	30	30	0.4	30	400	30000
18	0.000018	0.00009	0.09	69.23077	1.538462	0.384615	30	36	0.384615	30	384.6154	30000

***Table 28**: 70% POPC 30% POPS Lipid Titration, Donor Alone T1. Calcium, Protein, and Lipid Concentrations and Ratios throughout the Experiment.*

Volume of 70% POPC 30% POPS Added (uL)	Lipid Volume in L	Lipid Concentration (M)	mM Lipid Concentration	uM Lipid Concentration Dilution Corrected	Starting ANXA2 Acceptor Concentration (uM)	Starting ANXA2 Donor Concentration (uM)	Starting ANXA2 Donor (umoles)	Lipid to Protein Ratio	Starting CaCl2 Concentration (mM)	Starting CaCl2 Conc mmol	Starting CaCl2 Conc uM	CaCl2 umol
0	0	0	0	0	0	0.5	30	0	0.5	0.00003	500	30000
2	0.000002	0.00001	0.01	9.677419	0	0.483871	30	20	0.483871	30	483.871	30000
4	0.000004	0.00002	0.02	18.75	0	0.46875	30	40	0.46875	30	468.75	30000
6	0.000006	0.00003	0.03	27.27273	0	0.454545	30	60	0.454545	30	454.5455	30000
8	0.000008	0.00004	0.04	35.29412	0	0.441176	30	80	0.441176	30	441.1765	30000
10	0.00001	0.00005	0.05	42.85714	0	0.428571	30	100	0.428571	30	428.5714	30000
12	0.000012	0.00006	0.06	50	0	0.416667	30	120	0.416667	30	416.6667	30000

***Table 29**: 70% POPC 30% POPS Lipid Titration, Donor Alone T2. Calcium, Protein, and Lipid Concentrations and Ratios throughout the Experiment.*

Volume of 70% POPC 30% POPS Added (uL)	Lipid Volume in L	Lipid Concentration (M)	mM Lipid Concentration	uM Lipid Concentration Dilution Corrected	Starting ANXA2 Acceptor Concentration (uM)	Starting ANXA2 Donor Concentration (uM)	Starting ANXA2 Donor (umoles)	Lipid to Protein Ratio	Starting CaCl2 Concentration (mM)	Starting CaCl2 Conc mmol	Starting CaCl2 Conc uM	CaCl2 umol
0	0	0	0	0	0	0.5	30	0	0.5	0.00003	500	30000
3	0.000003	0.000015	0.015	14.28571	0	0.47619	30	30	0.47619	30	476.1905	30000
4	0.000004	0.00002	0.02	18.75	0	0.46875	30	40	0.46875	30	468.75	30000
6	0.000006	0.00003	0.03	27.27273	0	0.454545	30	60	0.454545	30	454.5455	30000
8	0.000008	0.00004	0.04	35.29412	0	0.441176	30	80	0.441176	30	441.1765	30000
10	0.00001	0.00005	0.05	42.85714	0	0.428571	30	100	0.428571	30	428.5714	30000
12	0.000012	0.00006	0.06	50	0	0.416667	30	120	0.416667	30	416.6667	30000

***Table 30**: 70% POPC 30% POPS Lipid Titration, 2 to 1 Acceptor to Donor T1. Calcium, Protein, and Lipid Concentrations and Ratios throughout the Experiment.*

Volume of 70% POPC 30% POPS Added (uL)	Lipid Volume in L	Lipid Concentration (M)	mM Lipid Concentration	uM Lipid Concentration Dilution Corrected	Starting ANXA2 Acceptor Concentration (uM)	Starting ANXA2 Donor Concentration (uM)	Starting ANXA2 Donor (umoles)	Lipid to Protein Ratio	Starting CaCl2 Concentration (mM)	Starting CaCl2 Conc mmol	Starting CaCl2 Conc uM	CaCl2 umol
0	0	0	0	0	1	0.5	30	0	0.5	0.00003	500	30000
2	0.000002	0.00001	0.01	9.677419	0.967742	0.483871	30	6.666667	0.483871	30	483.871	30000
4	0.000004	0.00002	0.02	18.75	0.9375	0.46875	30	13.33333	0.46875	30	468.75	30000
6	0.000006	0.00003	0.03	27.27273	0.909091	0.454545	30	20	0.454545	30	454.5455	30000
8	0.000008	0.00004	0.04	35.29412	0.882353	0.441176	30	26.66667	0.441176	30	441.1765	30000
10	0.00001	0.00005	0.05	42.85714	0.857143	0.428571	30	33.33333	0.428571	30	428.5714	30000
12	0.000012	0.00006	0.06	50	0.833333	0.416667	30	40	0.416667	30	416.6667	30000
14	0.000014	0.00007	0.07	56.75676	0.810811	0.405405	30	46.66667	0.405405	30	405.4054	30000

***Table 31**: 70% POPC 30% POPS Lipid Titration, 2 to 1 Acceptor to Donor T2. Calcium, Protein, and Lipid Concentrations and Ratios throughout the Experiment.*

Volume of 70% POPC 30% POPS Added (uL)	Lipid Volume in L	Lipid Concentration (M)	mM Lipid Concentration	uM Lipid Concentration Dilution Corrected	Starting ANXA2 Acceptor Concentration (uM)	Starting ANXA2 Donor Concentration (uM)	Starting ANXA2 Donor (umoles)	Lipid to Protein Ratio	Starting CaCl2 Concentration (mM)	Starting CaCl2 Conc mmol	Starting CaCl2 Conc uM	CaCl2 umol
0	0	0	0	0	1	0.5	30	0	0.5	0.00003	500	30000
3	0.000003	0.000015	0.015	14.28571	0.952381	0.47619	30	10	0.47619	30	476.1905	30000
6	0.000006	0.00003	0.03	27.27273	0.909091	0.454545	30	20	0.454545	30	454.5455	30000
8	0.000008	0.00004	0.04	35.29412	0.882353	0.441176	30	26.66667	0.441176	30	441.1765	30000
10	0.00001	0.00005	0.05	42.85714	0.857143	0.428571	30	33.33333	0.428571	30	428.5714	30000
12	0.000012	0.00006	0.06	50	0.833333	0.416667	30	40	0.416667	30	416.6667	30000
14	0.000014	0.00007	0.07	56.75676	0.810811	0.405405	30	46.66667	0.405405	30	405.4054	30000

***Table 32**: 100% POPC 30% Lipid Titration, Donor Alone. Calcium, Protein, and Lipid Concentrations and Ratios throughout the Experiment.*

Volume of 100% POPC Added (uL)	Lipid Volume in L	Lipid Concentration (M)	mM Lipid Concentration	uM Lipid Concentration Dilution Corrected	Starting ANXA2 Acceptor Concentration (uM)	Starting ANXA2 Donor Concentration (uM)	Starting ANXA2 Donor (umoles)	Lipid to Protein Ratio	Starting CaCl2 Concentration (mM)	Starting CaCl2 Conc mmol	Starting CaCl2 Conc uM	CaCl2 umol
0	0	0	0	0	0	0.5	30	0	0.5	0.00003	500	30000
3	0.000003	0.000015	0.015	14.28571	0	0.47619	30	30	0.47619	30	476.1905	30000
6	0.000006	0.00003	0.03	27.27273	0	0.454545	30	60	0.454545	30	454.5455	30000
9	0.000009	0.000045	0.045	39.13043	0	0.434783	30	90	0.434783	30	434.7826	30000
12	0.000012	0.00006	0.06	50	0	0.416667	30	120	0.416667	30	416.6667	30000
15	0.000015	0.000075	0.075	60	0	0.4	30	150	0.4	30	400	30000

***Table 33**: 100% POPC 30% Lipid Titration, 2 to 1 Acceptor to Donor. Calcium, Protein, and Lipid Concentrations and Ratios throughout the Experiment.*

Volume of 100% POPC Added (uL)	Lipid Volume in L	Lipid Concentration (M)	mM Lipid Concentration	uM Lipid Concentration Dilution Corrected	Starting ANXA2 Acceptor Concentration (uM)	Starting ANXA2 Donor Concentration (uM)	Starting ANXA2 Donor (umoles)	Lipid to Protein Ratio	Starting CaCl2 Concentration (mM)	Starting CaCl2 Conc mmol	Starting CaCl2 Conc uM	CaCl2 umol
0	0	0	0	0	1	0.5	30	0	0.5	0.00003	500	30000
3	0.000003	0.000015	0.015	14.28571	0.952381	0.47619	30	10	0.47619	30	476.1905	30000
6	0.000006	0.00003	0.03	27.27273	0.909091	0.454545	30	20	0.454545	30	454.5455	30000
9	0.000009	0.000045	0.045	39.13043	0.869565	0.434783	30	30	0.434783	30	434.7826	30000
12	0.000012	0.00006	0.06	50	0.833333	0.416667	30	40	0.416667	30	416.6667	30000
15	0.000015	0.000075	0.075	60	0.8	0.4	30	50	0.4	30	400	30000